THE DEVELOPMENT OF ENZYME ELECTRODES

by

Derek Harry Craston B.Sc.

A thesis submitted for the degree of Doctor of Philosophy of the University of London and for the Diploma of Membership of Imperial College.

Department of Chemistry

Imperial College

London SW7 2AY

October 1986

ABSTRACT

The work described in this thesis involves the use of organic conducting salts as electrode materials for use in enzyme electrodes. It has been found that these electrodes can be used to effect the oxidation of some flavoenzyme oxidases which are reduced during the catalytic oxidation of their substrate. This has provided the basis for the development of sensors comprising a layer of the enzyme trapped by a membrane next to the surface of a conducting salt electrode.

Sensors of this type have been made for the enzymes glucose oxidase, L-amino acid oxidase, D-amino acid oxidase and xanthine oxidase using TTF TCNQ as the electrode material. All of these give current responses, at an electrode potential of +50 mV (w.r.t. SCE), when the appropriate substrate is added. Analysis of the current versus concentration profiles thus obtained, according to the theoretical model which is presented, allows the rate limiting steps controlling the response of the device to be identified. These are the diffusion of substrate through the membrane, and the electrode kinetics, under conditions of unsaturated and saturated enzyme respectively. Similar results are obtained using glucose oxidase with electrodes made from NMP TCNQ or Quinolinium TCNQ. All of these enzymes adsorb strongly onto the conducting salt electrodes, which allows the development of sensors without a membrane.

The oxidation of the reduced form of glucose oxidase on electrodes made from TTF TCNQ has been investigated. The results show that the rate constant for the enzyme oxidation is sensitive to changes in the electrode area and the applied potential. The mechanism of the electron transfer between the enzyme and the electrodes is not entirely understood. The most likely explanation is that it occurs via a heterogeneous reaction between the enzyme and species from the salt adsorbed on the electrode surface.

ACKNOWLEDGEMENTS

I would like to thank:-

John Albery for his supervision.

The SERC for financial support.

Philip Bartlett for his supervision in the first year of my project, and K. W. Sim for his guidance over this same period.

Bryan Driscoll, Bruce Lennox, Paul Wilde, Sally Durrant and Lindy Murphy for proof-reading sections of this thesis.

Michael Pritchard for making the cavity and press pellet electrodes, and John Hooper for his technical assistance.

Everybody in the Albery research group for their friendship over the last three years. In particular, as well as those mentioned above, Andy, Keith, Chris P., Mark and Colin.

To my parents

CONTENTS

LIST OF FIGURES

LIST OF TABLES

CHAPTER 1

INTRODUCTION

An enzyme electrode is a device which interfaces an enzymatic system to an electrochemical detector. The enzymatic system consists of one or more enzymes and is entrapped or immobilized near the surface of the detector. When enzyme substrate is introduced into the locality of one of these devices a catalytic reaction occurs producing a particular product. The build up of this product can then be monitored electrochemically, where the signal thus obtained is related to the concentration of the enzyme substrate present.

The most important use of enzyme electrodes is in the area of analytical chemistry, and in particular bioanalytical chemistry, where it is often important to be able to obtain a rapid or a continuous measurement of the concentration of a single species in a medium containing many different compounds. Electrochemical techniques such as amperometry and potentiometry lend themselves to this purpose, but unfortunately the species of interest often exhibits poor (irreversible) electrochemical behaviour on conventional electrode materials. We try to get round this problem by combining the electrochemical detector with an enzymatic system, which catalyses a reaction involving the compound of interest, producing a species

which can easily be measured electrochemically. Also because enzymes are highly specific towards their substrates the resulting response of the device is highly selective to that species, and hence it can be used as an effective sensor in complex solutions.

Here a brief description is given of the types of enzymatic and electrode systems that are commonly used in enzyme electrodes. This is followed by a more detailed description of the enzymatic systems, the flavoenzymes, and the electrochemical systems, conducting organic salt electrodes, which have provided the basis for this study. For a fuller overview of the area of enzyme electrochemistry the interested reader is referred to a number of good review articles. [1,2,3,4,5]

1.1 Enzyme Electrodes

As described above, enzyme electrodes consist of an enzyme layer immobilised near an electrochemical detector. Numerous methods of enzyme immobilisation have been reported in the literature [6,7]. These include entrap ment between two membranes [8] or in a hydrophilic gel [9], chemical or physical attachment onto surfaces [10], and copolymerisation into membranes [11]. The method of immobilisation employed is important as it can affect such properties of the enzyme as the Michaelis constant (K_M) [12], the maximum velocity (V_{max}) [12], and the pH and temperature profiles [13]. Optimisation of the method of immobilisation can result in

an increase in both the selectivity and life time of the enzyme leading to an improved performance in the enzyme electrode sensor.

The electrochemical detector employed can be either potentiometric, measuring a Nernstian change in potential with concentration, or amperometric, measuring the current obtained on oxidising or reducing one of the products of the enzymatic reaction on the surface of an electrode.

Potentiometric sensors are often used when one of the products of the enzyme reaction is an ionic species. They are based on the use of ion selective electrodes [14], such as those selective for ammonium [15], protons [16] and cyanide [17]. Ammonium ion selective electrodes [18] have been used in conjunction with the enzyme urease to produce a sensor for urea. Here the enzyme catalyses the hydrolysis of urea producing ammonia, and the increase in ammonium ion concentration is monitored using the ammonium ion selective electrode. Similar systems have been developed for the detection of penicillin using the enzyme penicillinase in conjunction with a pH electrode [19], and for the detection of amygdalin using the enzyme β-glucosidase in conjunction with a cyanide selective electrode [20].

In the case where the product of the enzymic reaction is electroactive an amperometric method of detection can be employed [21]. There are many examples of amperometric enzyme electrodes in the literature some of which are described later in this chapter. The one which has received the most attention however is that which detects glucose

using the enzyme glucose oxidase. Here the product of the enzyme reaction, hydrogen peroxide, is detected by oxidation on a platinum electrode [22].

1.2 Flavoproteins

The flavoenzymes are a class of respiratory enzymes which contain the redox active prosthetic group flavinadenine dinucleotide (FAD) or flavin mononucleotide (FMN). There are two groups of flavoproteins one which contain iron or iron and molybdenum centers ,eg. xanthine oxidase, and the other which contain no metals ,eg. glucose oxidase. The flavin groups (figure 1.2.1) consist of a redox active isoalloxazine moiety onto which the adenosyl diphosphoribityl (FAD) or phosphoribityl (FMN) are attached at the N-10 position. The specific modes of attachment of the flavin group to the enzyme varies from enzyme to enzyme, but is in all cases ionic with the equilibrium constant for the dissociation of bound complex in most cases being of the order of 10^{-8}-10^{-9} mol dm^{-3}.

Many flavoproteins perform a two electron transfer directly on a substrate, with a resulting reduction in the flavin group of the enzyme. On reduction, the isoalloxazine moiety changes shape from a planar to a bent configuration [23]. The reoxidation of the enzyme to its active form normally involves reaction with molecular oxygen leading to the production of hydrogen peroxide. Some of these oxygen dependent flavoenzymes are described at the end of this

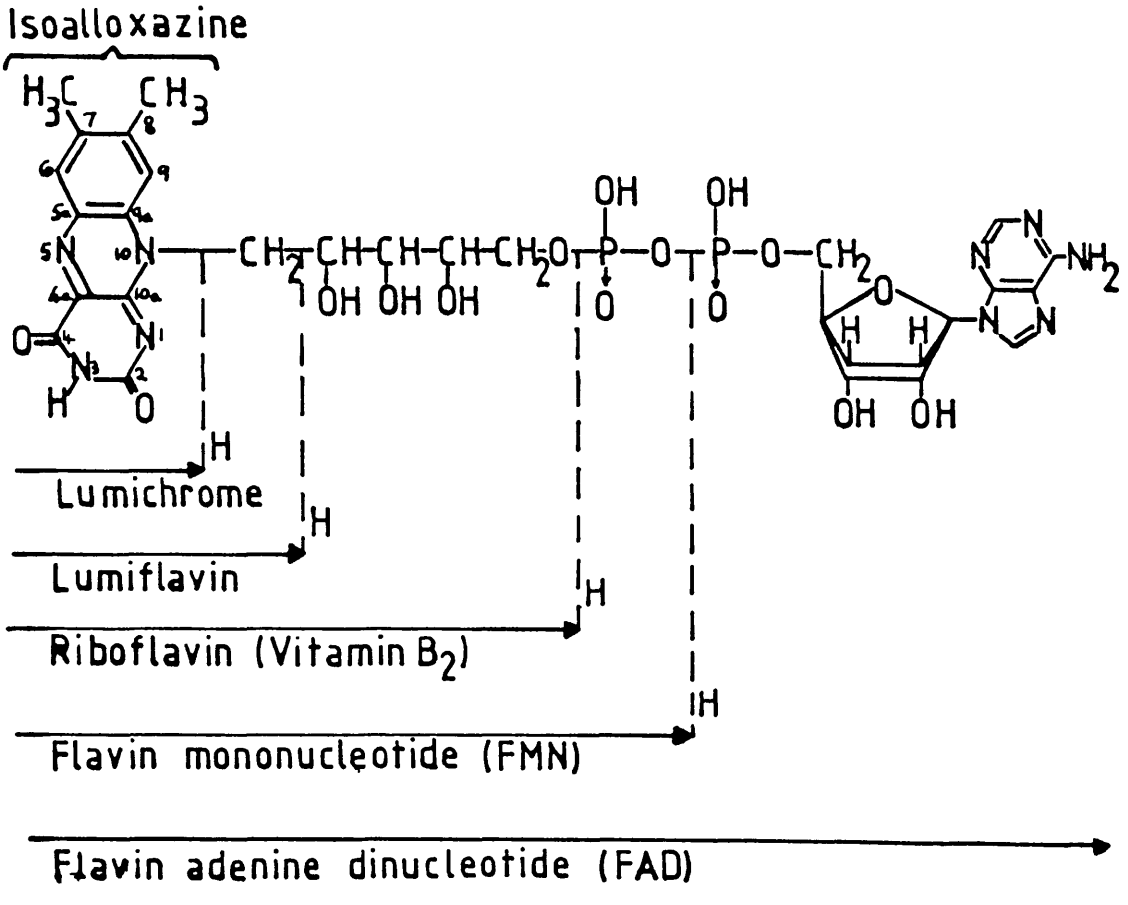

Figure 1.2.1: Formulae for the flavin nucleotide sequence.

section.

$$\text{substrate} + \text{protein(flavin}_{ox}\text{)} \longrightarrow \text{product} + \text{protein(flavin}_{red}\text{)}$$

$$\text{protein(flavin}_{red}\text{)} + O_2 \longrightarrow \text{protein(flavin}_{ox}\text{)} + H_2O_2$$

Another class of flavoproteins are those which are intermediates in the respiratory chain. These act as bridging species for the transfer of electrons from the pyridine nucleotides, such as NADPH, to the cytochromes. The reduced form of these electron transferring flavoproteins do not rapidly react with oxygen.

The electrochemical behaviour of free FMN and FAD is characterised by strong adsorption on the electrode and two superposed reversible one electron steps [24]. The reduction potentials of these steps show a fairly complex pH dependence [25] arising from the fact that there are at least nine distinguishable different flavin species .ie. one cationic, one neutral and one anionic species in each redox state (figure 1.2.2). The binding interaction between the protein and the flavin generally results in a change in the redox potentials of the flavin.

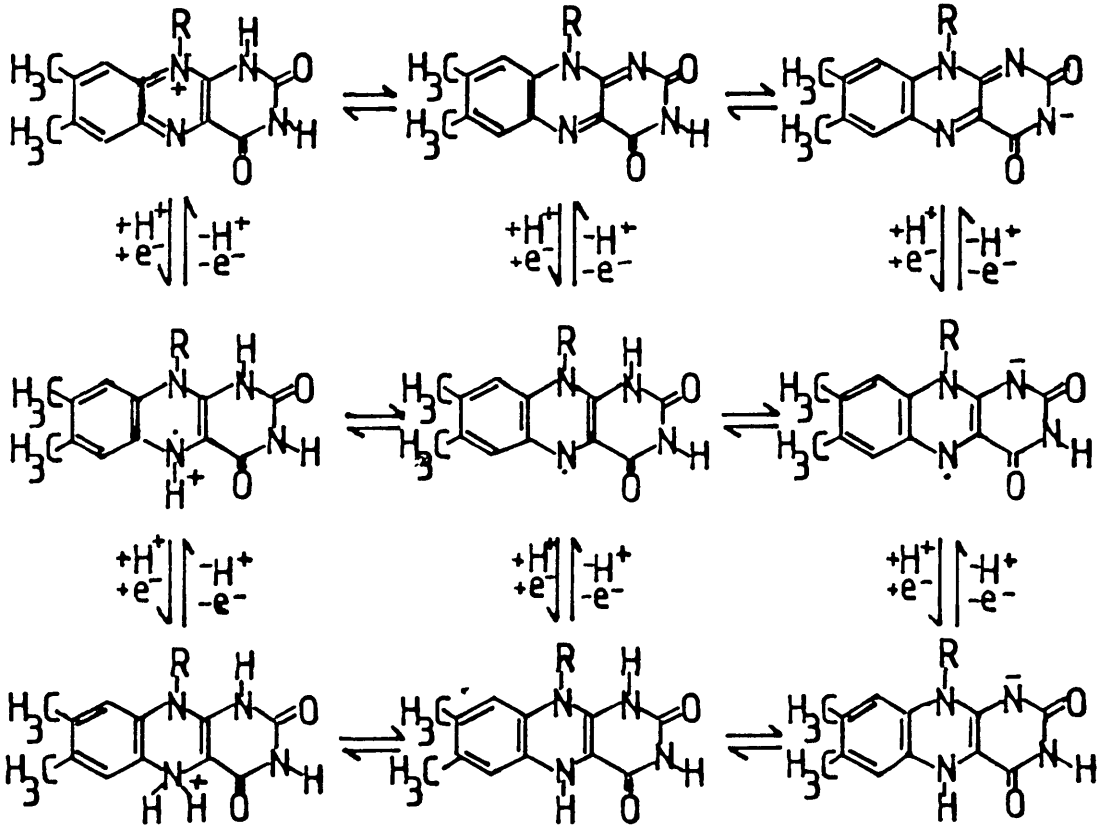

Figure 1.2.2: The different redox states of the isoalloxazine group of the flavins.

1.2.1 Glucose Oxidase

Glucose oxidase catalyses the oxidation of β-D-glucose by molecular oxygen to give gluconolactone, which is subsequently hydrolysed to gluconic acid, and hydrogen peroxide.

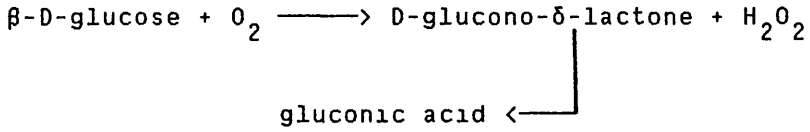

The two most common sources of the enzyme are from Aspergillus Niger and from some species of Penicillium. In both cases it consists of a dimer with two tightly bound FAD molecules. The molecular weight of the enzyme is approximately 186,000 as obtained from Aspergillus Niger and 160,000 as obtained from Penicillium [26]. The FAD prosthetic groups are very tightly bound and have been shown to stabilise the apoenzyme, changing its conformation from a loose flexible coil to a tight spherical form [27]. The enzyme is highly specific to β-D-glucose though it does show slight activity to a small number of other sugars. It is inhibited by D-arabinose and by halides [28]. The kinetics of the enzyme including the pH and temperature dependence have been described [28,29,30,31] and are well characterised.

1.2.2 D-Amino Acid Oxidase

D-amino acid oxidase catalyses the oxidation of D-amino acids by oxygen to give 2-oxoacids, ammonia and hydrogen peroxide.

$$\text{a D-amino acid} + O_2 \longrightarrow \text{a 2-oxo-acid} + NH_3 + H_2O_2$$

The enzyme can be extracted from hog kidney [32] and exists in both a monomeric, and at high concentrations, a dimeric form. The molecular weight of the dimer is approximately 100,000, with two FAD prosthetic groups per molecule of the apoenzyme [33]. The monomeric form of the enzyme has been found to be more active than the dimer. Reversible binding of the FAD prosthetic groups to the apoenzyme means that they can easily be removed from the protein by dialysis. Again the kinetics of the enzymatic reaction have been studied [34,35], and as one might expect both the V_{max} and the K_M vary depending on which D-amino acid is present. Enzyme inhibitors include some straight chain fatty acids and 2-hydroxyacids.

1.2.3 L-Amino Acid Oxidase

L-amino acid oxidase catalyses the oxidation of L-amino acids with the products of the reaction being a 2-oxo-acid, ammonia and hydrogen peroxide.

$$\text{a L-amino acid} + O_2 \longrightarrow \text{a 2-oxo-acid} + NH_3 + H_2O_2$$

The enzyme occurs fairly widespread in nature, with the main sources being from the snake vennom of Crotulus Adamanteus (diamond rattlesnake) and Agkistrodon Piscivorces (Cottonmouth moccasin) [36]. The enzyme has a molecular weight of approximately 130,000 and is composed of two FAD units per molecule of the enzyme [37]. The kinetics of the enzyme have been described [38], with a feature being enzyme inhibition at high concentrations of the substrate. Again both the V_{max} and K_M of the enzyme depend on which L-amino acid is present.

1.2.4 Xanthine Oxidase

Xanthine oxidase is a metal containing flavoprotein containing 2 FAD, 2 molybdenum and 4 iron sulphur centers per molecule. The enzyme catalyses the oxidation of xanthine to urate, but shows poor specificity oxidising a number of aldehydes, purines, pteridines, pyrimidines and other heterocyclic compounds [39].

$$\text{xanthine} + H_2O + O_2 \longrightarrow \text{urate} + H_2O_2$$

The enzyme is extracted from bovine milk or porcine liver with a molecular weight of 285,000 and 385,000 respectively. The kinetics have been investigated [40], and it appears that the FAD prosthetic group does not need to be present in order for the oxidation of the substrate to be observed. The enzyme is inhibited by excess substrate.

1.3 Enzyme Electrodes Based on Flavoenzymes

The use of flavoenzymes has received much attention with respect to their application in enzyme electrochemistry. There are two main reasons for this. Firstly one of the products (hydrogen peroxide) and one of the reactants (oxygen) of the enzymatic reaction can easily be measured electrochemically. Secondly the substrates of these enzymes are of considerable interest clinically and/or industrially. For example the use of glucose oxidase has allowed the development of systems for the electrochemical detection of glucose, which itself exhibits poor electrochemical behaviour [41,42,43]. The use of glucose sensors has obvious applications in the monitoring of blood glucose levels (particularly in diabetics) and also in the fermentation industry.

a) Sensors based on the electrochemical monitoring of oxygen or hydrogen peroxide

The first enzyme electrode was described by Clarke in 1962 [8], and involved the use of glucose oxidase (GOD) in conjunction with an oxygen electrode. This device relied on the amperometric monitoring of the depletion of oxygen, which is consumed during the enzymatic reaction. This was followed in 1970 by a similar device which this time monitored the accumulation of hydrogen peroxide [22].

$$2H^+ + GOD(FAD) + glucose \longrightarrow GOD(FADH_2) + gluconolactone$$

$$gluconolactone \longrightarrow gluconic\ acid$$

$$GOD(FADH_2) + O_2 \longrightarrow GOD(FAD) + H_2O_2$$

$$H_2O_2 \xrightarrow{electrode} O_2 + 2H^+$$

Most of the subsequently developed systems based on the flavoenzymes [44,45,46,47] employ the same electrochemical method of detection with new improved methods for enzyme immobilisation. Immobilisation can confer greater stability to the enzyme and hence increases the life time of the sensor.

b) Systems based on the use of mediators

The problem with all of the systems mentioned above is that when the ambient oxygen concentration is low the response of the device will depend not only on the concentration of substrate, but will also be sensitive to fluctuations in the local oxygen tension. To overcome this problem redox mediators (M) have been used to replace oxygen in the reoxidation of the enzyme.

$$2H^+ + flavoenz(FAD) + substrate \longrightarrow flavoenz(FADH_2) + product$$

$$2M_{ox} + flavoenz(FADH_2) \longrightarrow flavoenz(FAD) + 2M_{red}$$

$$2M_{red} \xrightarrow{electrode} 2M_{ox}$$

Many different biological mediators are known [48], most of which undergo single electron transfer with the enzyme. In choosing a suitable mediator for use in a particular amperometric sensor the following must be taken into consideration:-

(a) The mediator must show good reversible electrochemistry with a well defined reduction potential sufficiently different from that of the enzyme that the desired reaction goes to completion.

(b) The mediator must be soluble enough, and the rate of the mediator enzyme reaction rapid enough, that the kinetics of this reaction do not control the response of the sensor over the substrate concentration range of interest.

(c) Both reduced and oxidised forms of the mediator must be stable, not reacting with any other species present or inhibiting the enzyme.

Some examples of known mediators include quinone [49], ferrocyanide [50], ferrocene [51] and phenazine methosulphate [52].

c) Direct electron transfer between the enzyme and the electrode

An even simpler system than those previously described involves the direct oxidation of the enzyme on the surface of an electrode.

$$2H^+ + \text{flavoenz(FAD)} + \text{substrate} \longrightarrow \text{flavoenz}(FADH_2) + \text{product}$$

$$\text{flavoenz}(FADH_2) \xrightarrow{\text{electrode}} \text{flavoenz(FAD)} + 2H^+$$

Scheller and co-workers observed direct electron transfer between glucose oxidase and mercury electrodes [53]. Durliat and Comtat [54] found that suitably pretreated platinum electrodes could be used to oxidise the reduced form of the enzyme glucose oxidase, though Duke and co-workers were previously unable to observe this [55]. Glucose oxidase, L-amino acid oxidase and xanthine oxidase have been covalently linked to glassy carbon electrodes by cyanuric chloride linkages, and in each case direct electron transfer with the electrode surface was observed [56,57]. Bourdillon [58], however, found that direct electron transfer is not possible when glucose oxidase is attached onto glassy carbon electrodes by carbodiimide linkages.

In 1980 Kulys and co-workers [59,60] showed that the conducting organic salts N-methylphenazinium (NMP) 7,7,8,8-tetracyano-p-quinodimethan (TCNQ) and

N-methylacridinium (NMA) TCNQ [61] could be used as electrode materials to bring about the oxidation of both glucose and xanthine oxidases. The mechanism they proposed [62] was that dissolved species from the salt act as homogeneous mediators for the enzyme oxidation. In this thesis it will be shown that this process can also be performed using a number of different conducting salts as electrode materials, and that the likely mechanism for the electrode process involves electron transfer between the enzyme and species adsorbed on the electrode surface.

1.4 Conducting Organic Salts

The first molecular crystal exhibiting highly conducting properties was reported in 1954 [63], but interest in the field really began with the discovery of TCNQ (figure 1.4.1) by Melby and co-workers [64] in 1960. TCNQ is a planar molecule which is unusual in that it is electron poor and readily accepts an electron to form a stable radical anion. In the presence of a donor molecule (D) TCNQ was found to act as an electron acceptor (A) resulting in the formation of an organic salt [62,65,66]. Some of these salts were found to exhibit high electrical conductivity along one of the crystal axes, these materials often being referred to as 1-dimensional organic conductors, organic metals or conducting organic salts.

There are two types of conducting organic salts, the first of these are the simple radical anion salts which have

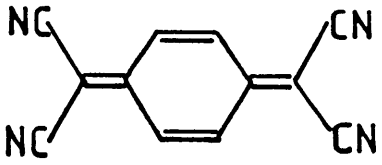

TCNQ

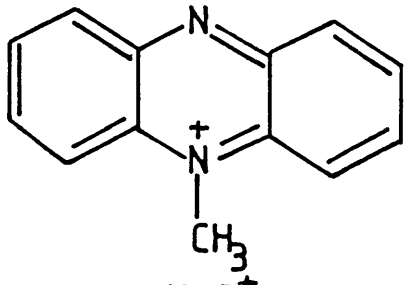

NMP^+

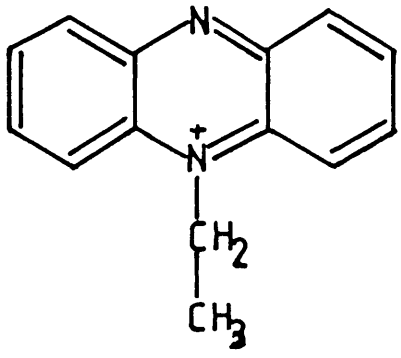

NEP^+

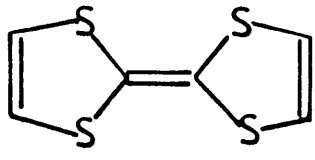

TTF

Figure 1.4.1: Chemical structures of TCNQ, NMP^+, NEP^+ and TTF.

the form $D_n^{a+}A_m^{b-}$. Examples of these are the TCNQ salts of tetrathiafulvalene (TTF) and NMP (figure 1.4.1). The second type are the complex salts which have the form $D_n^{a+}A_m^{b-}A_p^0$ or $D_n^{a+}D_p^0A_m^{b-}$. Examples of these complex salts are the TCNQ salt of triethylammonium (TEA), $TEA(TCNQ)_2^-$ [65] and $TTF\ Cl_{0.7}$ [67].

There has been much work carried out over the last twenty years by both chemists and physicists to try to find out why these materials conduct [68,69,70]. What has been concluded is that the following two conditions must be present. Firstly the crystal structure must be such that the donor and acceptor molecules are arranged into separate stacks. An example of the importance of this can be seen in the difference between the TCNQ salts of N-ethylphenazine (NEP) and NMP where the donor species have similar chemical structures (figure 1.4.1). NEP TCNQ forms stacks of alternate donor and acceptor molecules and as a result this material is an insulator; in the case of NMP TCNQ, which is a good conductor, the donors and acceptors arrange themselves into separate stacks (figure 1.4.2). The second condition concerns the degree of charge transfer that occurs between the donor and acceptor molecules, which is described by the equation:-

$$D + A \longrightarrow D^{\sigma+}A^{\sigma-}$$

If σ is less than 1 as is in the case of TTF TCNQ

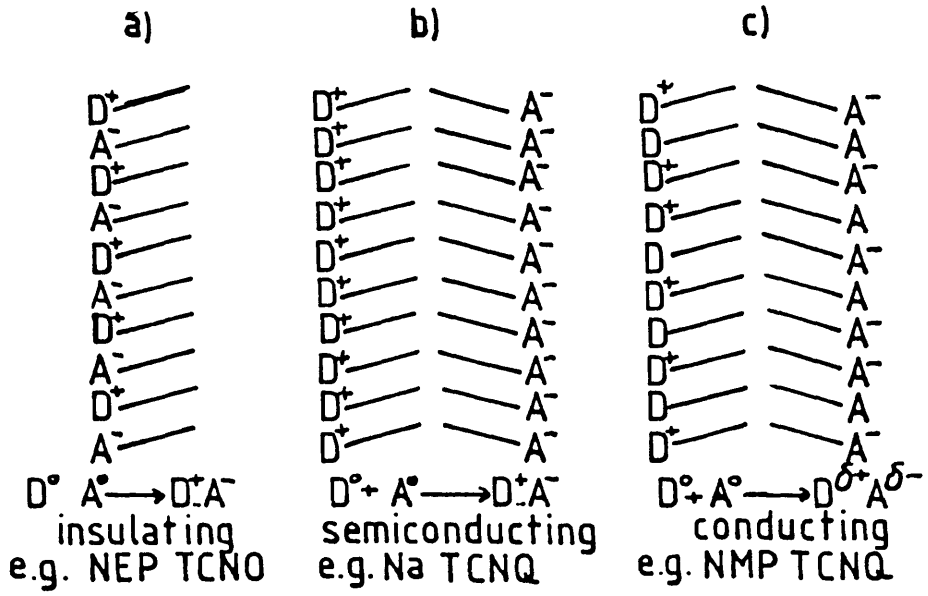

Figure 1.4.2: Schematic view of the packing in organic charge transfer crystals.

a) insulating

b) semiconducting

c) conducting

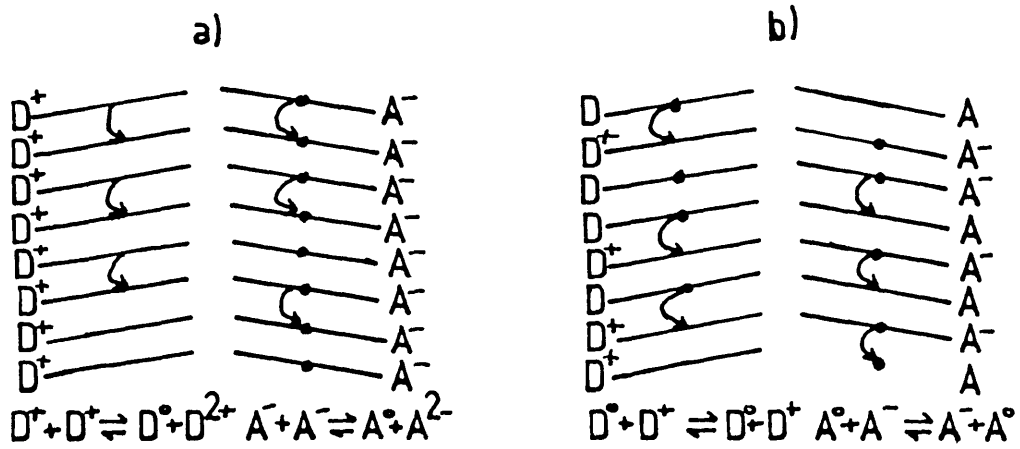

Figure 1.4.3: Model of charge transfer in organic salts.

a) complete charge transfer

b) incomplete charge transfer

(σ=0.59 at room temperature [71]) and NMP TCNQ (σ=0.91 at room temperature [72]) then conductivity will be observed. If σ is equal to 1 as in alkali metal TCNQ complexes then the resulting material is a semiconductor (figure 1.4.2).

1.4.1 Crystal Structure

The crystal structures of a large number of 1-dimensional organic metals are known [73,74,75] and in every case the donors and acceptors form segregated stacks. In the individual stacks π orbital overlap between adjacent molecules results in energy band formation. These partially filled bands lead to metallic like conductivity, provided the intramolecular electron repulsion is not too strong compared to the bandwidth [67]. The π orbitals of the molecules are strongly directional interacting along the stacks, with only weak interactions in the perpendicular directions. Hence, the conductors exhibit very anisotropic conduction.

Answering the question as to why segregated stacks are formed rather than the more conventional mixed stack is not a trivial matter as it involves a large number of interactions between both molecules in the same stack, and acceptors and donors in different stacks. The importance of high polarizability and small molecular size of the donor and acceptor have been emphasized [69] as both of these lead to an increase in the band width. An example of the importance of interactions between molecules in different

stacks is seen in TTF TCNQ where the intermolecular sulphur-nitrogen interaction plays a part in determining the crystal structure [76]. The situation is further complicated in the case of NMP TCNQ where it is believed that the presence of trace impurities is important for the formation of segregated stacks [77].

1.4.2 Incomplete Charge Transfer

The importance of incomplete charge transfer can be described by treating the electron transfer as an electron exchange between adjacent molecular species in a stack (figure 1.4.3). In the case where there is complete charge transfer then electron hopping in the stack requires an energetically unfavourable disproportionation process [77]; whereas when there is incomplete charge transfer electrons can jump between ionic and neutral species in the stack. A more rigorous description involves use of band structure where the difference between semiconductors and metals is the difference between filled and partially filled bands [78]. In the complex salts the conductivity along the stacks is again due to unfilled bands, but these bands are unfilled not because of incomplete charge transfer but rather because of mixed valence.

Again the answer to the question of what determines the degree of charge transfer (σ) in these materials is complex but the most important effect involves the ionic binding. If we imagine that the electrons in the crystal of D-A are

in thermodynamic equilibrium between a neutral and a fully ionic electronic structure,

$$D^0 + A^0 \underset{I - E}{\overset{E_m}{\rightleftharpoons}} D^+ + A^-$$

then the degree of charge transfer will be determined by an interplay between the Madelung binding energy (E_m) and the difference between the ionisation energy of the donor (I), and the electron affinity of the acceptor (E).

Taking examples of salts with TCNQ as the acceptor, an approximate estimate of the relative ionisation potentials of possible donors can be obtained by looking at their electrochemical reduction potentials in solution (figure 1.4.4). Conducting TCNQ salts are obtained with donors whose reduction potentials are in a particular narrow potential range. Below and above this range semiconductors or insulators and neutral species are formed respectively. Obviously treatment in this manner is not rigorous as we require knowledge of the Madelung energy which depends on such factors as the charge on the ions and the ionic separation [69]. Wheland and Gillison [79] have reported a study of a large number of charge transfer salts, and they concluded that conductivity tends to be observed in salts which are composed of a moderately good donor species combined with a moderately good acceptor species.

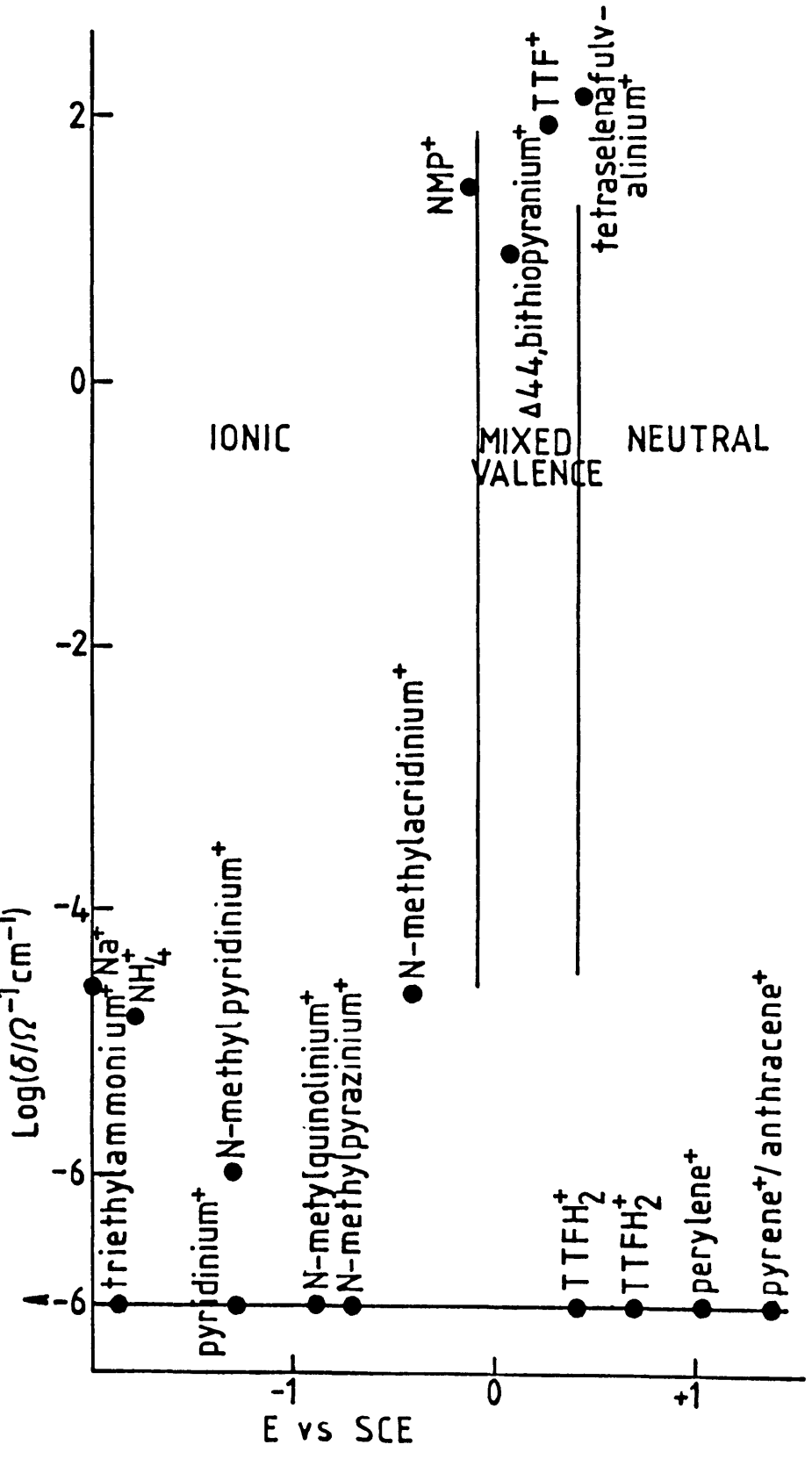

Figure 1.4.4: Plot of the conductivity at 300 K of the TCNQ salts of a variety of cations versus the reduction potential of the cation.

1.4.3 Conductivity

The room temperature conductivity of conducting organic salts based on TCNQ varies between 1 and 10^3 Ω^{-1} cm^{-1} which is slightly less than that of graphite and mercury but greater than that of semiconductors such as n-type silicon (table 1.1). The conductivity of these salts is affected by both temperature and pressure [67]. The effect of temperature on the conductivity of some conducting salts can be seen in figure 1.4.5. In most cases a maximum is reached at low temperatures before dropping off sharply as the temperature approaches absolute zero. The poor conductivity at very low temperatures arrises from the dimerisation of pairs of molecules in the stacks which is referred to as Peierls distortion [80].

In general it is found that the complex organic salts exhibit higher conductivity than the simple salts [81].

1.4.4 Electrochemistry

The electrochemical behaviour of some conducting organic salts of TCNQ have been reported by Jaeger and Bard [82,83]. In these cyclic voltammetry was used to investigate the electrochemical behaviour of electrodes made from different donor-TCNQ salts and in particular TTF TCNQ, in different background electrolytes. It was found that in every case the electrodes were only stable over a certain potential range. Upon sweeping the potential outside of this range the electrode is oxidised or reduced. Subsequent

TABLE 1.1

Conductivity of a variety of materials

material	conductivity $(\sigma)/\Omega^{-1}$ cm^{-1}
Cu	6.4×10^{5}
Au	4.1×10^{5}
Hg	4.4×10^{4}
TTF TCNQ	7.0×10^{2}
NMP TCNQ	1.0×10^{2}
n-type Si	4.0×10^{1}

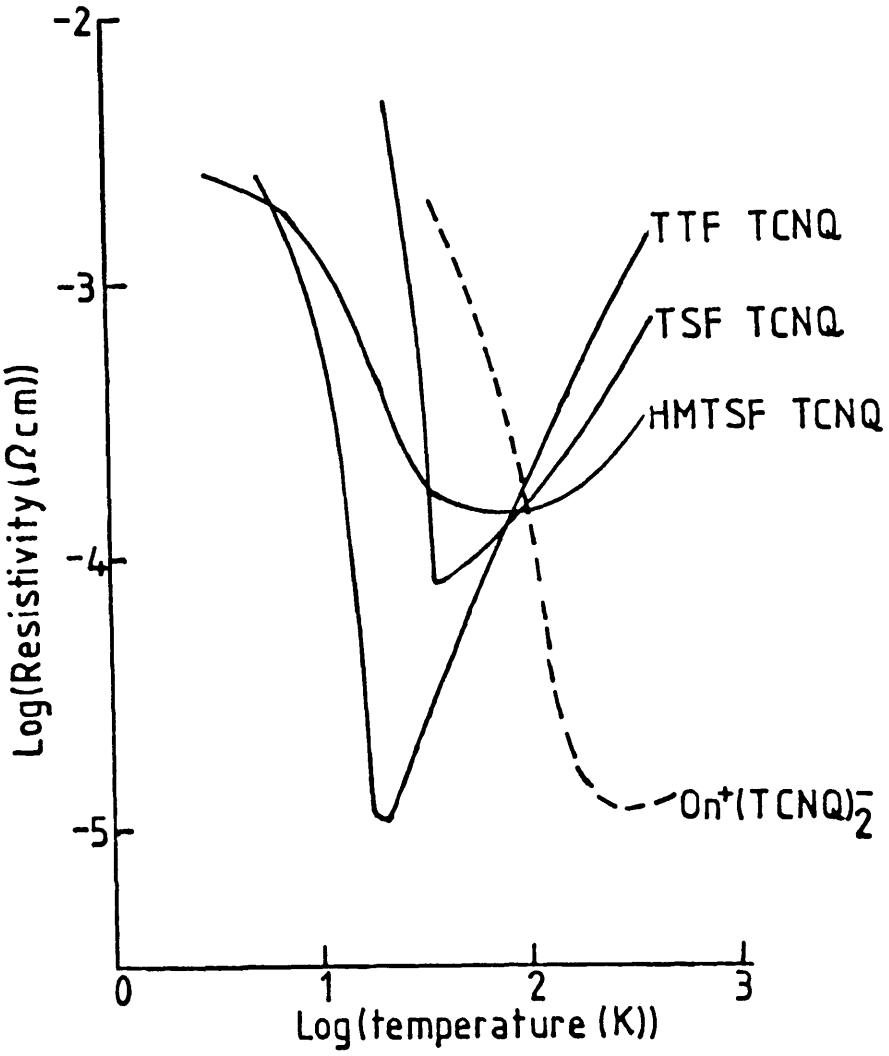

Figure 1.4.5: Temperature dependence of the resistivity of some conducting organic salts.

Qn ≡ Quinolinium

TSF ≡ Tetraselenafulvalinium

HMTSF ≡ Hexamethylenetetraselenafulvalinium

sweeps show peaks attributable to insoluble compounds formed on the electrode surface. Cyclic voltammetry has also been used to synthesise and investigate the properties of mixed valence TTF halide salts [84,85,86]. Other electrochemical studies to have been carried out are those by Wheland [79], who electrochemically grew crystals of TTF TCNQ, and by Sharp, who described the use of semiconducting organic radical salts of TCNQ as ion selective electrodes [87,88].

CHAPTER 2

EXPERIMENTAL

In this chapter a description is given of the materials, equipment and experimental procedures used in this study.

2.1 Chemicals, Solutions and membranes

Details of enzymes and substrates used are given in table 2.1. All other chemicals were commercially obtained and of AnalaR grade, with both these and the enzymes being used without any further purification. Details of the conducting salts used during this investigation and their syntheses are given in table 2.2.

All solutions were made up using doubly deionised water (DDW) which had been purified by first passing through an ion exchange resin (Houseman), and then further by circulating in a Milli Q system (Millipore). The resistance of the water thus obtained was greater than 10 MΩ cm^{-2}. Phosphate buffers were made using 0.1 mol dm^{-3} sodium chloride and 0.15 mol dm^{-3} sodium hydrogen orthophosphate which were titrated with hydrochloric acid to obtain the desired pH. Tris buffers were made using 0.1 mol dm^{-3} Tris and 0.1 mol dm^{-3} lithium sulphate titrated with sulphuric acid to obtain the desired pH. The enzymes were either used

TABLE 2.1

Enzyme Substrate Systems

Enzyme	Xanthine Oxidase	D-Amino acid Oxidase	L-Amino acid Oxidase	Glucose Oxidase
Activity (u/mg)	1.25	14	0.44	254
Substrate	Xanthine	D-Alanine	Phenylalanine	Glucose
pH	7.4	8.0	6.5	7.4
Buffer	Phosphate	Tris	Phosphate	Phosphate
Supplier	Sigma	Sigma	Sigma	Boeringer

TABLE 2.2

The Conducting salts

Material	Preparation of salt and supply of Donor	Microanalysis					
		Calculated %			Found %		
		C	N	H	C	N	H
TTF TCNQ	Ref. 66 Aldrich	52.94	13.72	1.90	52.87	13.61	1.86
NMP TCNQ	Ref. 61 Aldrich	75.30	21.10	3.80	75.17	21.20	3.71
$Fc^+ (TCNQ)_2^-$	Ref. 65 Aldrich	68.70	18.90	3.00	68.69	18.89	2.96
$Cu(DPA) (TCNQ)_2$	Ref. 65 *	63.50	23.97	2.64	60.83	22.37	2.76
$Q^+ (TCNQ)_2^-$	† Aldrich	73.60	23.42	2.97	69.50	21.87	2.67
$TEA^+ (TCNQ)_2^-$	Ref. 65 BDH	70.59	24.70	4.70	70.63	25.09	4.48
$Pb (DTF)_2$	Ref. 89 BDH	insufficient obtained					
$TEA^+ TCNQ^-$	Ref. 65 BDH	70.59	22.88	6.54	69.94	22.72	6.13

* $Cu(DPA) (TCNQ)_2$ was prepared by addition of 2,2'-dipyridylamine (Aldrich) to a aqueous solution of copper(II)chloride (Hopkins & Williams).

† Prepared by mixing a solution of quinoline (0.14 cm^3) in 50 cm^3 pH=4 HCl with a solution of 0.5g of LiTCNQ (prepared as in Ref. 61) in 10 cm^3 of MilliQ water . The product was collected and washed thoroughly using first a solution of HCl (pH=4) and then ether.

as supplied, if in solution, or dissolved using a known amount of enzyme per cm^{-3} of the appropriate buffer. Solutions of the enzyme substrates were made up in the appropriate buffer, with the glucose solutions being made twenty four hours before use so as to allow equilibration of the anomers [90]. In the case of xanthine a saturated solution was made. The concentration of this was found to be 0.55 mmol dm^{-3} by measuring the absorption at λ= 277 nm (using a Unicam SP 1800 uv spectrophotometer) and taking the extinction coefficient (ε) to be 9300 mol^{-1} cm^{2} [91].

Non aqueous electrochemistry was carried out in acetonitrile (Fisons dried distilled) which was further purified by first refluxing for ninety minutes over calcium hydride (1% weight/volume), and then fractionally distilled at high reflux ratio under argon. This was then stored under argon prior to use.

Dialysis tubing was obtained from Gallenkamp (PJC-400-090W) and from Cole-Palmer (Spectrapor 2). These were pretreated to soften and remove impurities by boiling in a 1% weight/volume sodium carbonate solution for ten minutes. Membranes were prepared by cutting the tubing into strips of about three centimetres; and were stored in a solution of 10 mmol dm^{-3} Tris & 1 mmol dm^{-3} EDTA at 4°C.

All glassware was cleaned regularly by soaking in a dilute solution of Decon 90 (BDH), and then rinsing thoroughly with DDW.

2.2 Electrodes

The following different types of conducting organic salt electrodes have been used.

a) Pressed Pellet Electrodes:- Pellets 1-2 mm thick, and 7 or 3mm in diameter of the conducting salt were pressed at a pressure of 8×10^{8} N m^{-2} using a Specac handpress and die. These were then mounted on a brass rod using silver loaded araldite and sealed in epoxy resin to make rotating disc electrodes. To make rotating ring disc electrodes the pressed pellet was again mounted on a brass rod, and this then surrounded by a insulating gap of epoxy resin and a thin platinum ring before sealing in epoxy resin.

b) Drop Coated Electrodes:- A mixture of the conducting salt and polyvinyl chloride (9:1 w/w) was made up into a thick slurry by addition of a small amount of tetrahydrofuran (THF). The resulting slurry was drop coated onto a glassy carbon disc electrode (radius 3.5 mm). The coat was built up with successive additions of the slurry until the electrode was completely covered; between each addition the surface was dried by gentle air blowing.

c) Cavity Electrodes:- A platinum disc (radius 1 mm or 3.5 mm) was press fitted into teflon with a recess (depth~ 1 mm). The cavity was then filled with the same conducting salt, PVC and THF slurry as in 2) (figure 2.2.1). The solvent was allowed to evaporate for at least 1 hour. The electrode was then trimmed with a scalpel and polished

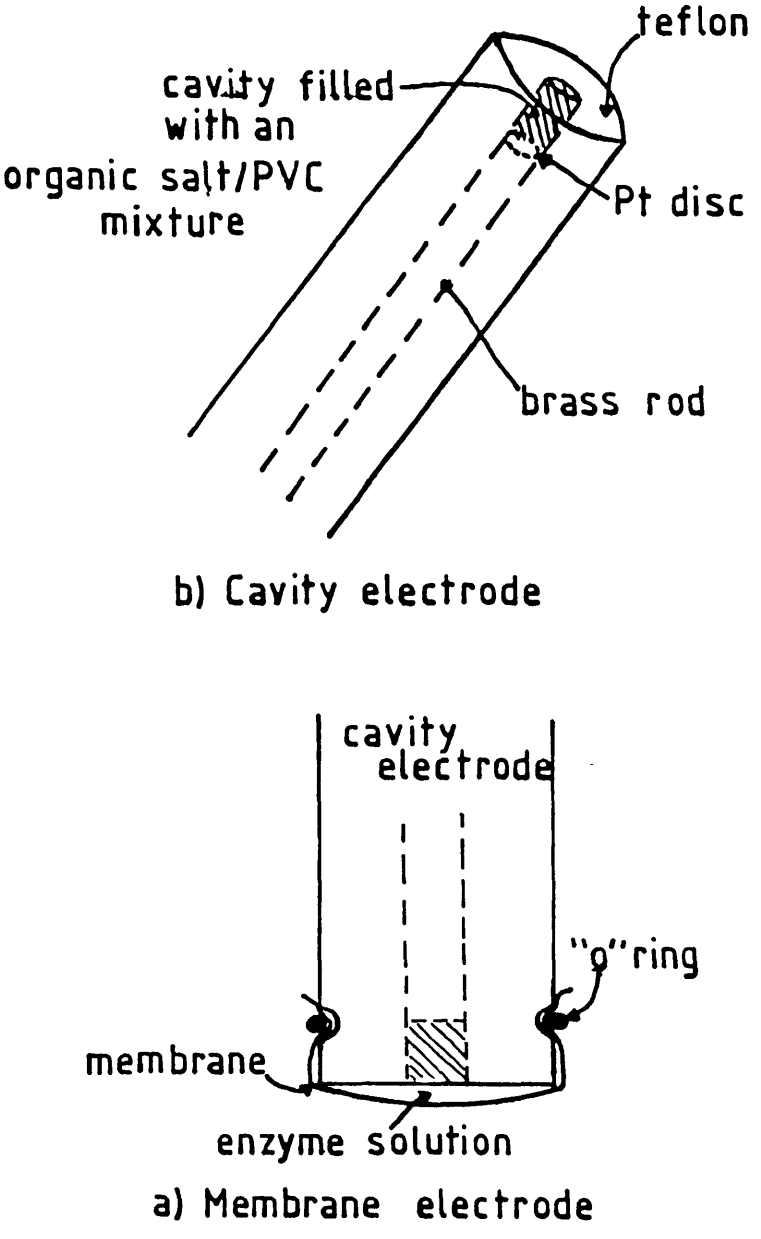

Figure 2.2.1: Schematic representation of a membrane electrode (a) and a cavity electrode (b).

using 0.3 μm alumina in DDW. The cavity electrode was always repolished before use.

Membrane enzyme electrodes were made from these cavity electrodes by trapping a drop of an enzyme electrolyte solution between the electrode and the membrane, with the latter being secured with an "o" ring (figure 2.2.1). Excess enzyme solution was removed by copious washing with DDW.

d) Single Crystal Electrodes:- Single crystals of ferrocinium (Fc) TCNQ ($Fc^{+}(TCNQ)^{-}_{2}$) and triethylammonium (TEA) TCNQ ($TEA^{+}(TCNQ)^{-}_{2}$) were made into electrodes by first attaching a fine copper wire to one end of the crystal (~0.1 mm x 0.1 mm x 3mm) using silver loaded epoxy resin, and then sealing with epoxy resin into the end of a melting point tube, leaving about half of the crystal exposed to the electrolyte (figure 2.2.2).

All other electrochemical studies were carried out using standard platinum and glassy carbon rotating disc electrodes [92], made by Michael Pritchard.

Standard calomel electrodes were used as reference electrodes for aqueous electrochemistry, and all quoted potentials are with respect to this. The calomel electrodes used were made at our laboratories and were tested regularly against a commercial electrode (Radiometer), only being used when the difference between the two was less than ± 2 mV. For non aqueous electrochemistry a Ag/Ag^{+} reference

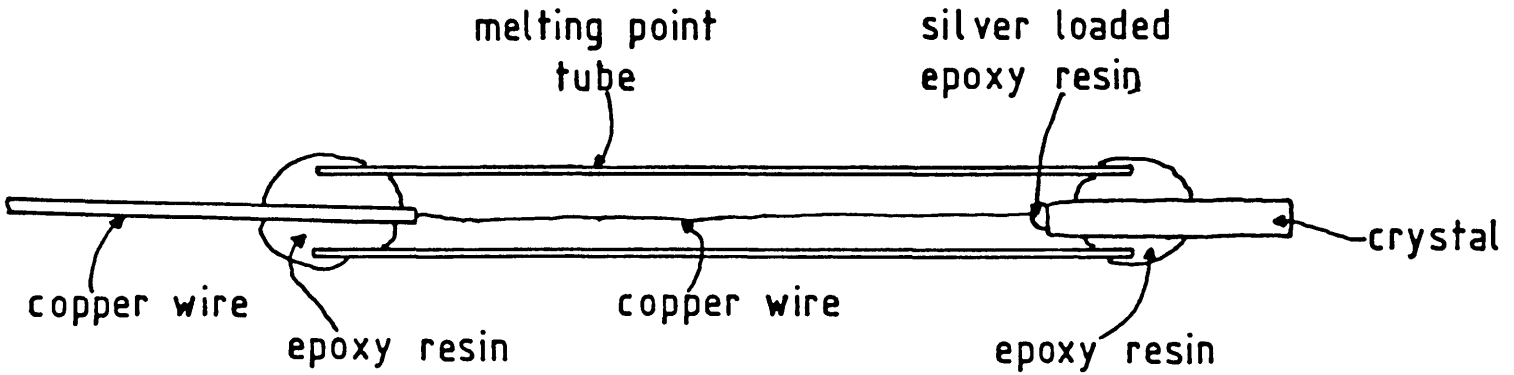

Figure 2.2.2: Cross section of a single crystal electrode.

electrode was used consisting of a silver wire immersed in a solution of 10 mmol dm^{-3} silver perchlorate, 0.1 mol dm^{-3} lithium perchlorate in acetonitrile.

Pieces of platinum gauze were employed as counter electrodes. These were washed regularly before use by soaking in a concentrated nitric acid solution.

2.3 Apparatus

Electrochemical experiments were carried out using a modular arrangement of voltage followers, potentiostats, triangular wave generators, voltage sources, subtractors and galvanostats [93] which were connected together as appropriate to the experimental requirement.

Experimental readouts were taken using a Bryans series 60000 or 29000 chart recorder.

For rotating disc work the electrodes were mounted on an Oxford Electrodes bearing block with sealed mercury contacts. This block was supported on two vertical poles attached to a solid base. The rotation speed was controlled by an Oxford Electrodes motor controller combined with a printed armature d.c. servo motor (Printed Motors Company). Speeds from 0.5 to 50 Hz were available and were stable to $\pm$ 0.01 Hz.

2.4 Experimental Cells

Most of the experiments were carried out in the glass cell shown in figure 2.4.1. The solution in the cell is kept at a constant temperature of 25 ± 0.2 °C by pumping water from an external source through the water jacket.

Experiments carried out with enzyme in the bulk solution were performed using a two compartment cell as described by Cass et al. [51].

2.5 Experimental Procedures

Unless otherwise stated all solutions were deoxygenated prior to electrochemical measurement by bubbling nitrogen (B.O.C. "white spot" , pretreated by passing through reduced anthraquinone-2-sulphonate) through them for about half an hour. During the experiments nitrogen was passed over the surface of the solution to ensure that it remained deoxygenated.

2.5.1 Current Time Transients

By far the most common experiment carried out involved placing a solution of an enzyme, either behind a membrane or in the bulk, in contact with a conducting salt electrode. The electrode was then poised at a potential, which unless otherwise stated was +50 mV with respect to SCE. The current was then monitored as a function of time with

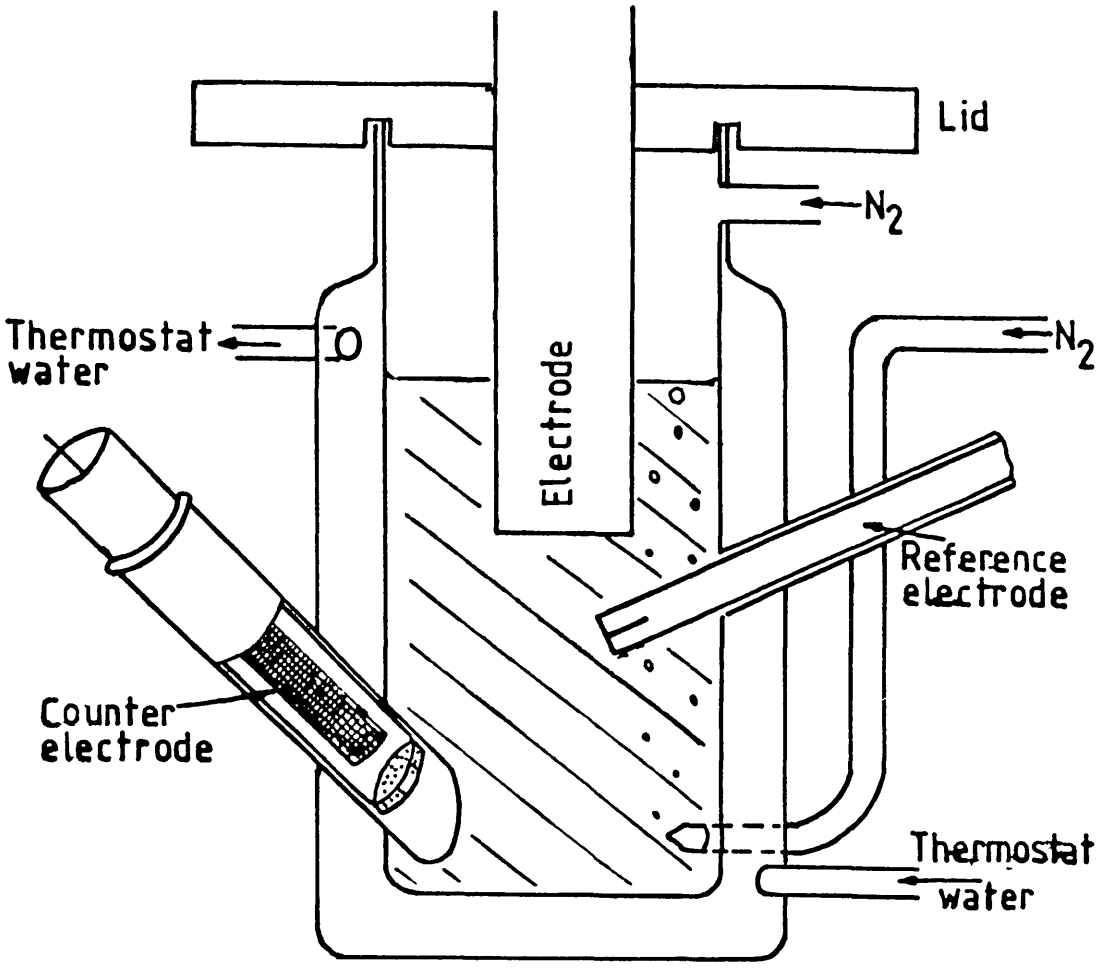

Figure 2.4.1: The electrochemical cell.

additions of small aliquots of a stock solution of the substrate.

CHAPTER 3

THEORY

In this chapter a theoretical treatment is developed for the enzyme electrodes applicable to this study. It considers the response obtained at a conducting salt electrode in the presence of enzyme substrate, when the enzyme is either in the bulk solution or behind a membrane.

3.1 Enzyme in the Bulk Solution

Considering the case where there is enzyme and substrate in the bulk solution then the reaction sequence can be written as follows:-

Solution

$$2H^+ + Enz(FAD) + substrate \longrightarrow Enz(FADH_2) + product$$

Electrode

$$Enz(FADH_2) \longrightarrow Enz(FAD) + 2H^+ + 2e^-$$

This system can be simplified to:-

Solution

$$A \xrightarrow{k} B$$

Electrode

$$B \xrightarrow{k'} A$$

Where A and B represent the oxidised and the reduced forms of the enzyme which are at concentrations of a and b respectively. Since the concentration of enzyme is very much less than that of the substrate , it can be assumed that there is no concentration polarisation of the substrate in the solution, and hence we can express the homogeneous rate, k, by

$$(k)^{-1} = (k_{cat})^{-1} + K_M(k_{cat}[S])^{-1} \qquad (3.1)$$

where [S] is the concentration of substrate, K_M is the Michaelis constant for the enzyme, and k_{cat} is the rate constant for the enzyme reaction under saturated conditions.

The heterogeneous rate constant k' represents the rate of the electrochemical oxidation of the reduced form of the enzyme.

The transport and kinetics of A in the diffusion layer are given by

$$D\partial^2 a/\partial x^2 = ka \qquad (3.2)$$

where D is the diffusion coefficient of the oxidised form of the enzyme.

Assuming that the diffusion coefficients of A and B are the same and noting that the total concentration of the

enzyme e_Σ can be given by

$$a + b = e_\Sigma \qquad (3.3)$$

the following boundary condition is applicable:-

$$\text{at } x=0 \quad D\partial a/\partial x = -D\partial b/\partial x = -k'b = -k(e_\Sigma - a)$$

Also in the bulk of the solution we assume that all of the enzyme is in the B form; this assumption holds for glucose oxidase in the absence of oxygen. Hence at the boundary of the diffusion layer ($x = x_D$) $a = 0$. The current is given by

$$i = nFAk'b_0 \qquad (3.4)$$

where n is the number of electrons, A is the area of the electrode, F is Faraday's constant (96487 C mol^{-1}) and b_0 is the concentration of B at the electrode surface. Solution of equation (3.2) subject to the boundary conditions leads to:-

$$i = \frac{nFAk'e_\Sigma}{1 + k'\tanh(x_D k^{1/2}/D^{1/2})/(kD)^{1/2}} \qquad (3.5)$$

Depending on the relative thickness of the diffusion layer, x_D, and the reaction layer for converting A to B,

$(D/k)^{1/2}$, equation (3.5) gives two different cases. When $x_D << (D/k)^{1/2}$, there is very little regeneration of B in the diffusion layer and equation (3.5) reduces to the same form as that for a normal current voltage curve [94].

$$\frac{nFAe_\Sigma}{i} = \frac{1}{k'} + \frac{x_D}{D}$$

In this case the current does not depend on the concentration of the substrate, S. On the other hand, when $x_D >> (D/k)^{1/2}$, then equation (3.5) can be written:-

$$\frac{nFAe_\Sigma}{i} = \frac{1}{k'} + \frac{1}{(Dk)^{1/2}} \qquad (3.6)$$

In this expression the two terms on the right hand side describe rate limiting electrode and enzyme kinetics. When the enzyme is unsaturated, k will depend on the concentration of S. If this term is dominant then from equations (3.1) and (3.6)

$$i = nFA(Dk_{cat}[S]/K_M)^{1/2}e_\Sigma \qquad (3.7)$$

and the current will have a half order dependence on the substrate concentration. If the enzyme is saturated then from equations (3.1) and (3.6) we find:-

$$i = nFA(k_{cat}D)^{1/2}e_\Sigma \qquad (3.8)$$

3.2 Membrane Electrodes

The situation will now be considered where a layer of enzyme is trapped on the surface of a conducting organic salt electrode using a membrane, illustrated schematically in figure 3.2.1. Here enzyme substrate, S, in the bulk solution diffuses through the membrane where it undergoes an enzymatic reaction with the oxidised form of the enzyme, E, producing reduced enzyme, E', and product P. The reduced enzyme is subsequently converted back to its active form on the electrode surface with the product diffusing out through the membrane into the bulk solution. Under steady state conditions the rate of all of these processes will be the same, and the observable flux can therefore be defined in terms of each of these individual steps.

Starting first with the enzyme kinetics, a simple one substrate one product reaction is assumed, described as follows.

$$S + E \underset{k_{-1}}{\overset{k_1}{\rightleftharpoons}} ES \underset{k_{-2}}{\overset{k_2}{\rightleftharpoons}} E'P \underset{k_{-3}}{\overset{k_3}{\rightleftharpoons}} E' + P \qquad (3.9)$$

The equilibrium constant for each step in the above scheme can be given by

$$K_n = k_n / k_{-n}$$

with the overall equilibrium constant, K_{TD}, for converting reactants S + E to products P + E' equal to:-

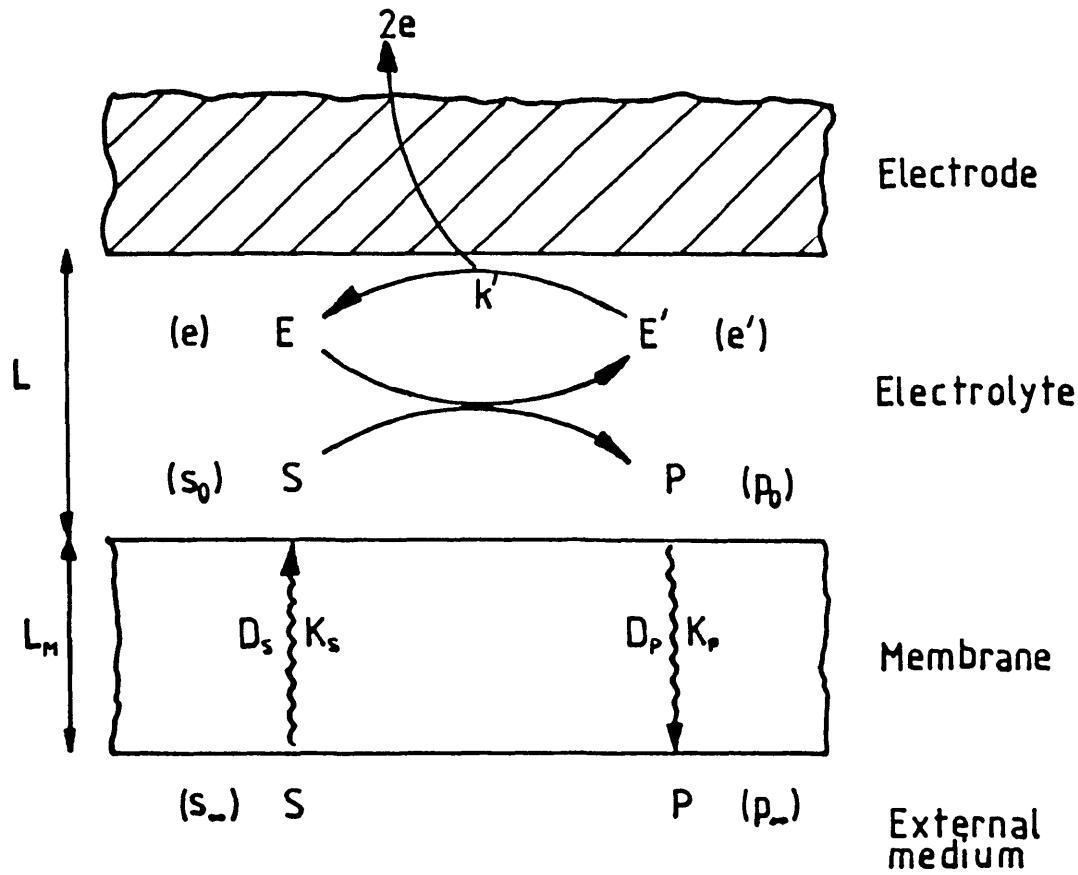

Figure 3.2.1: The membrane electrode.

$$K_{TD} = K_1 K_2 K_3$$

It is assumed that the thickness of the enzyme substrate reaction layer is not smaller than the thickness of the electrolyte layer behind the membrane, and hence there is no concentration polarisation of species in this layer. Situations where this is not the case are dealt with elsewhere [95].

Using lower case letters to denote the concentration of the different species, and for s and p the subscripts ∞ and o to indicate the concentrations outside and inside the membrane respectively the flux, j, can be written as follows:

$$j = L[k_1 s_o . e - k_{-1} es] \qquad (3.10)$$

$$= L[k_2 es - k_{-2} e' p] \qquad (3.11)$$

$$= L[k_3 e' p - k_{-3} e' . p_o] \qquad (3.12)$$

Turning to the transport of S and P through the membrane, these can be described by the mass transfer rate constants k'_s and k'_p where

$$k'_x = D_x K_x / L_m$$

X is either S or P, D_x is the diffusion coefficient and K_x the partition coefficient of X in the membrane and L_m is the thickness of the membrane. This leads to two further

expressions for the flux:-

$$j = k'_s(s_\infty - s_0) \qquad (3.13)$$

$$= k'_p(p_0 - p_\infty) \qquad (3.14)$$

Finally the flux can be equated with the rate of the enzyme turnover on the electrode, which is assumed to be irreversible, and is described by the heterogenous rate constant k'.

$$j = k'e' \qquad (3.15)$$

The total concentration of enzyme, e_Σ, can be given by the sum of the concentration of all of the different enzyme forms.

$$e_\Sigma = e + es + e'p + e' \qquad (3.16)$$

Hence there are seven unknowns j, s_0, p_0, e, es, e'p and e' and seven equations, (3.10) to (3.16), which can be solved by elimination of the six unknown concentrations to give:-

$$\frac{e_\Sigma}{j} = \left\{ 1 - \frac{j}{k'_s s_\infty} \right\} \left\{ \frac{1}{Lk_{cat}} + \frac{1}{k'} + \frac{K_3^{-1}(1 + K_2^{-1})}{k'} \left[p_\infty + \frac{J}{k'_p} \right] \right\}$$

$$+ \frac{1}{s_\infty} \left\{ \frac{K_M}{Lk_{cat}} + \frac{K_1^{-1}K_2^{-1}K_3^{-1}}{k'} \left[p_\infty + \frac{J}{k'_p} \right] \right\} + \frac{e_\Sigma}{k'_s s_\infty} \quad (3.17)$$

where

$$1/k_{cat} = 1/k_2 + 1/K_2k_3 + 1/k_3$$

and

$$K_M/k_{cat} = 1/k_1 + 1/K_1k_2 + 1/K_1K_2k_3$$

These expressions for k_{cat} and K_M/k_{cat} have been discussed by Albery and Knowles [96].

At first sight equation (3.17) looks very complicated, but it is unlikely that all the terms on the right hand side contribute equally to the overall expression. What is more likely is that one of the terms is dominant and hence controls the electrode response. The various terms in equation (3.17) are now discussed.

Firstly, if the final term is dominant then $J \approx k'_s s_\infty$, which means that from equation (3.12) the concentration of substrate behind the membrane is very small. Under these conditions the response is controlled by the rate of transport of S through the membrane, with the enzyme and

electrode kinetics being sufficiently rapid so that S is consumed as soon as it passes through the membrane.

Secondly there are two terms which include L. These terms are dominant when the enzyme kinetics are rate limiting with the K_M/k_{cat} and $1/k_{cat}$ terms describing unsaturated and saturated conditions respectively.

Two of the terms involve $p_\infty + j/k'_p$, which from equation (3.14) is equal to the concentration of product behind the membrane. If this is large and the value of k' is low then build up of E' and P behind the membrane will tend to push the equilibria in (3.9) to the left resulting in the predominant enzyme form being either E'P, ES or E. The first of these two product inhibition terms (in the second bracket) applies when most of the enzyme is present as either ES or E'P, while the term in the third bracket applies when most of the enzyme is present as E and therefore requires S to be converted to E'. When E' is the predominant form then the simple $(k')^{-1}$ term is dominant and hence the electrode kinetics are rate limiting.

The expression in the first bracket comes out because when $j \approx k'_s s_\infty$ then the flux is limited by mass transport of S through the membrane, hence the concentration of substrate in the electrolyte layer is much less than it is in the bulk. When this is the case the contributions from all of the saturated rate constants becomes less.

3.2.1 No Product Inhibition

The system can now be simplified by assuming that the product inhibition terms are negligible and we can therefore ignore all the terms in p_0 in equation (3.17). The case where product inhibition is important has been discussed by Albery and Bartlett [95]. Equation (3.17) now becomes:-

$$\frac{e_\Sigma}{j} = \left\{1 - \frac{j}{k'_s s_\infty}\right\}\left\{\frac{1}{Lk_{cat}} + \frac{1}{k'}\right\} + \frac{K_M}{Lk_{cat}s_\infty} + \frac{e_\Sigma}{k's_\infty} \qquad (3.18)$$

Rearrangement of this into a form similar to a Hanes plot [98] for the analysis of Michaelis-Menten kinetics gives:-

$$\frac{s_\infty}{j} = \frac{1}{k'_{ME}}\left\{1 + \frac{s_\infty}{K_{ME}}\left[1 - \frac{j}{k'_s s_\infty}\right]\right\} \qquad (3.19)$$

where

$$\frac{1}{k'_{ME}} = \frac{K_M}{e_\Sigma Lk_{cat}} + \frac{1}{k'_s} \qquad (3.20)$$

and

$$K_{ME} = \frac{K_M(Lk_{cat})^{-1} + e_\Sigma(k'_s)^{-1}}{(Lk_{cat})^{-1} + (k')^{-1}} \qquad (3.21)$$

Since the response obtained for the electrode at low substrate concentrations is equal to $k'_{ME}s_\infty$, k'_{ME} can be thought of as the effective electrochemical rate constant for the enzyme electrode under unsaturated conditions.

The saturated rate constant, $k'_{cat,E}$, can be defined as

$$(k'_{cat,E})^{-1} = (Lk_{cat})^{-1} + (k')^{-1} = e_\Sigma/J_{MAX} \qquad (3.22)$$

where J_{MAX} is the maximum obtainable flux for the electrode. Rearranging equations (3.20) to (3.22) gives:-

$$K_{ME} = \frac{k'_{cat,E}e_\Sigma}{k'_{ME}} \qquad (3.23)$$

Hence K_{ME} has a similar form to the expression for the Michaelis constant for an enzyme, i.e. saturated rate divided by unsaturated rate constant, and can therefore be thought of as the Michaelis constant for the enzyme electrode.

From equation (3.19) it can be seen that as $s_\infty \longrightarrow 0$ then $s_\infty/J = (k'_{ME})^{-1}$. The parameter, ϱ, is now defined as:-

$$\varrho = (J/s_\infty)(k'_{ME})^{-1} \qquad (3.24)$$

Substitution into equation (3.19) gives:-

$$y = \frac{\varrho^{-1} - 1}{s_\infty} = \frac{1}{K_{ME}} \left[1 - \frac{\varrho k'_{ME}}{k'_s} \right] \qquad (3.25)$$

Therefore from a plot of y versus ϱ, the value of K_{ME} can be obtained from the intercept on the y-axis, and from the intercept on the x-axis the ratio k'_{ME}/k'_s can be obtained. If this ratio is equal to unity then $k'_{ME} \approx k'_s$ and hence under unsaturated conditions the diffusion of substrate through the membrane is rate limiting. If this ratio is very much less than one then $k'_{ME} \approx K_M/Lk_{cat}e_\Sigma$ and the unsaturated enzyme kinetics are rate limiting. Figure 3.2.2 shows theoretical current versus concentration, Hanes and y versus ϱ (equation (3.25)) plots for different ratios of k'_{ME}/k'_s.

It can be concluded therefore that treatment of data first by Hanes plots followed by y versus ϱ plots (equation (3.25)) allows the determination of the current controlling step at a particular concentration of substrate, and the value of this rate constant.

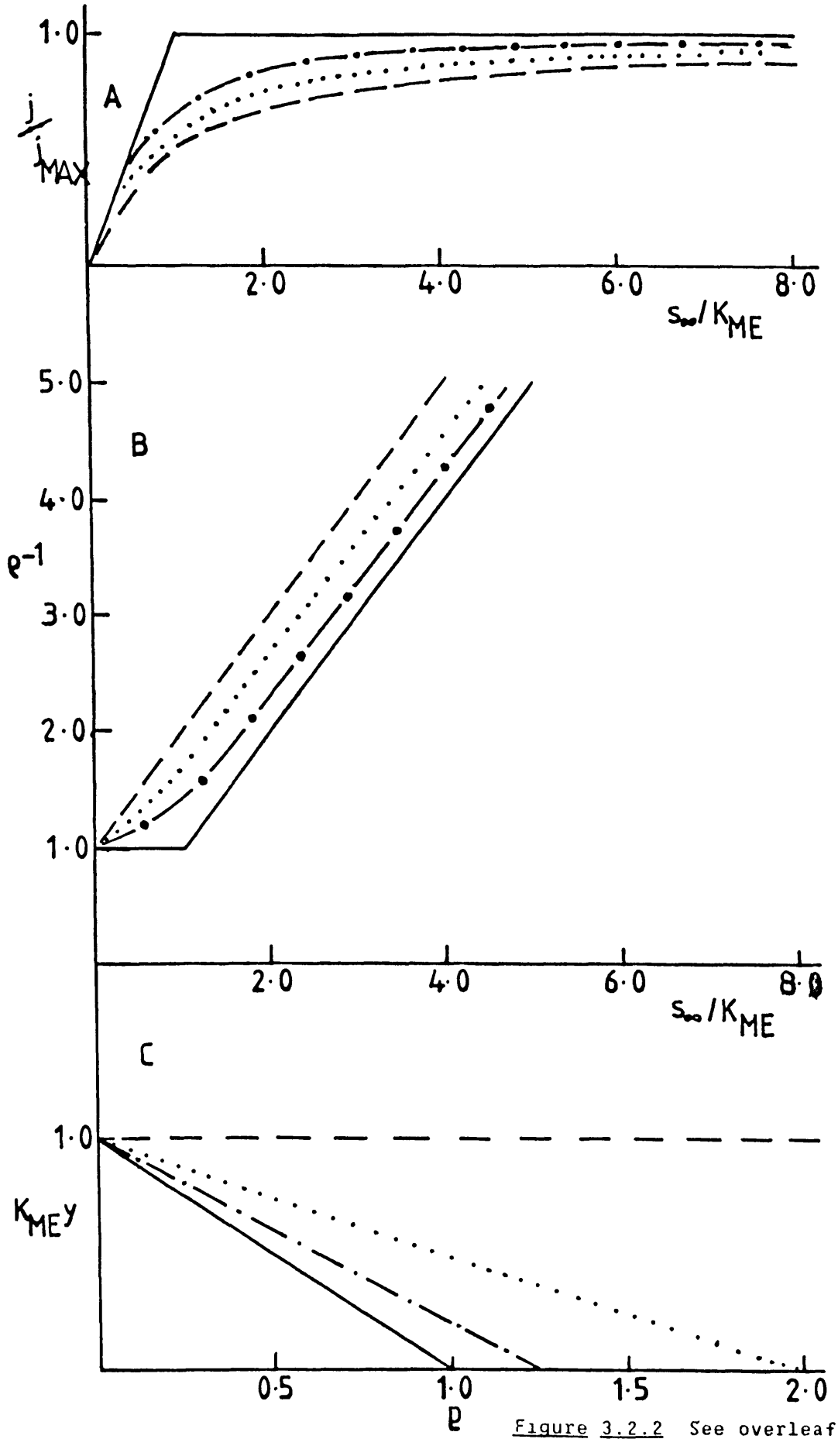

Figure 3.2.2 See overleaf

Figure 3.2.2: A shows plots of flux against substrate concentration for different values of k'_{ME}/k'_s. For these curves B and C show the corresponding Hanes plots and y versus ϱ plots respectively. The values of k'_{ME}/k'_s are as follows:- ———— , 1.0, —·—, 0.8, ..., 0.5, — — —, 0.0.

CHAPTER 4

THE USE OF CONDUCTING ORGANIC SALTS AS ELECTRODE MATERIALS IN ENZYME ELECTRODES

This chapter deals with the utilisation of a number of conducting organic salts as electrode materials. The electrochemical behaviour of these electrodes and their use in carrying out the oxidation of some flavoenzymes is described.

4.1 The Electrochemistry of Conducting Organic Salts

The TCNQ salts of the donors in Figure 4.1.1 and the lead(II) salt of 9-Dicyanomethylene-2,4,7-trinitrofluorene (DTF) have been used as electrode materials in this investigation. These were synthesised and made into electrodes as described in chapter 2. Their electrochemical behaviour was investigated by cyclic voltammetry [98] carried out in pH = 7.4 phosphate buffer at a sweep rate of 5 mV s^{-1}.

a) TCNQ salts of quinolinium, copper dipyridylamine, TTF and NMP

The cyclic voltammograms (cv's) of the electrodes made from the TCNQ salts of Quinolinium ($Q^{+}(TCNQ)_2^{-}$), copper dipyridylamine ($Cu(DPA)(TCNQ)_2$), NMP and TTF are shown in figure 4.1.2. These were obtained using packed cavity electrodes, though drop coated and pressed pellet (for TTF

Donors

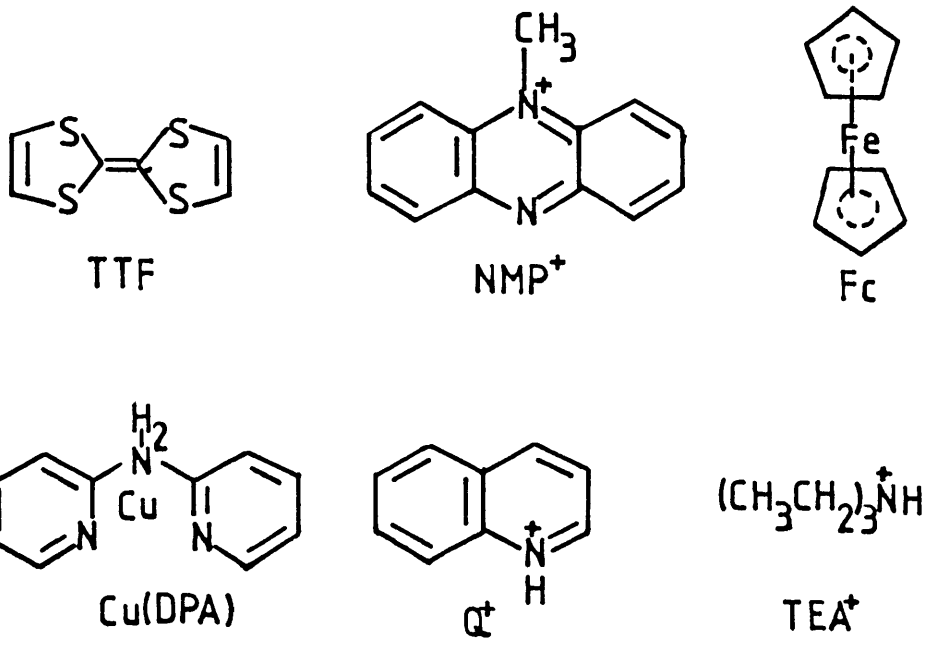

Acceptors

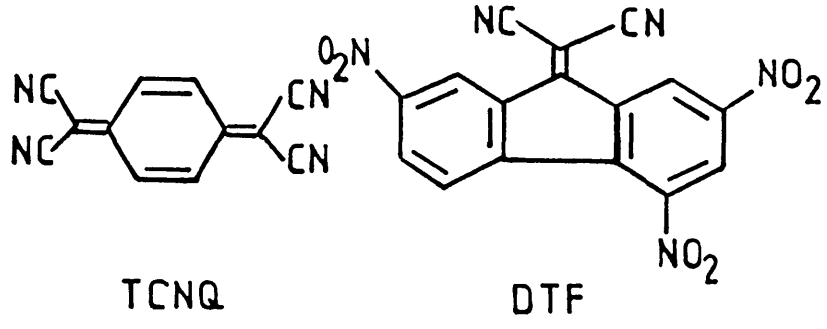

Figure 4.1.1: Structures of the donors and acceptors used in this study.

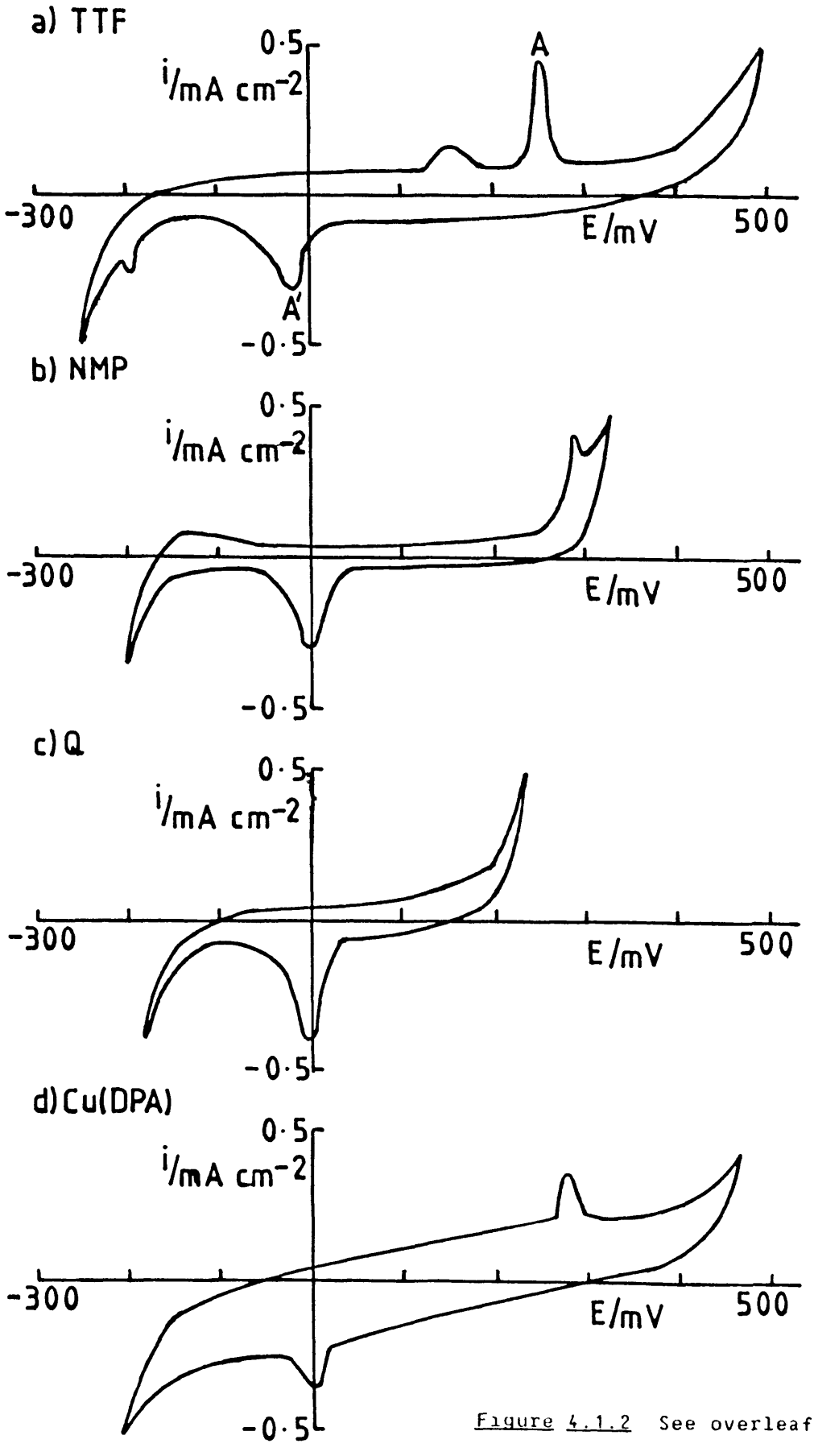

Figure 4.1.2 See overleaf

Figure 4.1.2: Cyclic voltammograms at TTF TCNQ (a), NMP TCNQ (b), $Q^{+}(TCNQ)_2^{-}$ (c) and $Cu(DPA)(TCNQ)_2$ (d) drop coated electrodes in pH = 7.4 phosphate buffer versus SCE. The sweep rate was 5 mV/s.

TCNQ and NMP TCNQ) electrodes showed identical electrochemical behaviour. These salts all show similar properties to those previously described by Jaeger and Bard [82,83]. In each case the material is only stable over a certain potential range. When the potential is swept outside this range in a positive direction then the material is oxidised. For example in the case of TTF TCNQ the electrode oxidation process is as follows:-

$$TTF\ TCNQ \longrightarrow TCNQ^{0} + TTF^{2+} + 2e$$

Likewise if the potential is swept outside the negative limit the salt is reduced.

$$TTF\ TCNQ \longrightarrow TCNQ^{2-} + TTF^{0} - 2e$$

The stable ranges of these salts are given in table 4.1.

The peaks on the cv's, shown in figure 4.1.2a as A and A', are only observed after a potential outside the stable potential range of the material has been applied to the electrode. In all four cases peaks were observed at about zero and +280 mV, and can be explained by the formation of the insoluble species $TCNQ^{0}$ and sodium TCNQ on the electrode surface on oxidation and reduction of the salt respectively. The two peaks therefore represent the following electrochemical processes:-

TABLE 4.1

Approximate Stable Potential Ranges of the Conducting Organic Salt Electrodes

Salt	Positive Limit/mV	Negative Limit/mV
TTF TCNQ	+500	-250
NMP TCNQ	+400	-150
$Cu(DPA)(TCNQ)_2$	+500	-200
$Q^+(TCNQ)_2^{-1}$	+300	-200
$Fc^+(TCNQ)_2^{-1}$ (a)	+300	-500
$Fc^+(TCNQ)_2^{-1}$ (b)	+300	-400
$TEA^+(TCNQ)_2^{-1}$ (b)	+200	-100
$Pb(DTF)_2$	+600	-300

(a) Packed cavity electrode.

(b) Single crystal electrode.

280 mV $Na^+TCNQ^- - e \longrightarrow TCNQ^0 + Na^+$ A

0 mV $TCNQ^0 + Na^+ + e \longrightarrow Na^+TCNQ^-$ A'

The area under these two peaks is the same, and is determined by the number of coulombs passed on taking the electrode outside its stable potential range.

In addition, electrodes made from TTF TCNQ sometimes show two other peaks at -180 and +150 mV. Again these are only observed after the electrode has been oxidised or reduced by applying a potential outside the stable range of the material. They probably occur as a result of the formation of the insoluble species TTF^0 and TTF^+Cl^- on the electrode surface.

b) TCNQ salts of triethylammonium and ferrocinium

Turning now to the TCNQ salts of ferrocinium ($Fc^+(TCNQ)_2^-$) and triethylammonium ($TEA^+(TCNQ)_2^-$), the cv's obtained are shown in figure 4.1.3. Drop coated electrodes of these two materials show somewhat different behaviour from that of the other salts (figure 4.1.3(a and b)). The $TEA^+(TCNQ)_2^-$ electrode appears to be unstable at all potentials other than at its open circuit potential, which is about +165 mV. A peak is observed at 0 mV, superimposed on the reduction current, which could again be due to the reduction of surface $TCNQ^0$. The stable range of drop coated $Fc^+(TCNQ)_2^-$ electrodes is given in table 4.1. When the potential is taken outside of either these limits subsequent sweeps show peaks at 0 and -400 mV.

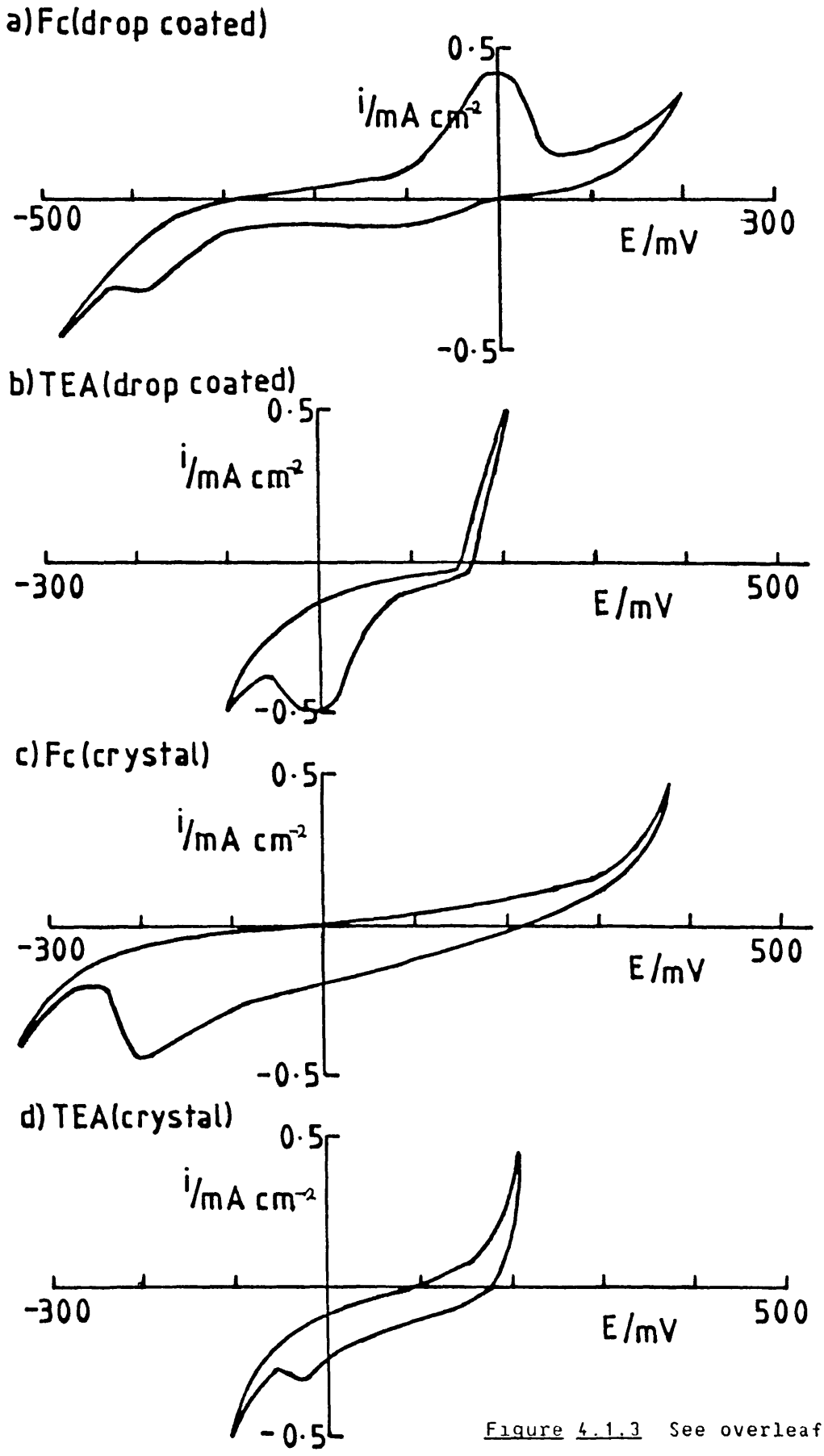

Figure 4.1.3 See overleaf

Figure 4.1.3: Cyclic voltammograms at $Fc^{+}(TCNQ)_2^{-}$ ((a) drop coated (c) single crystal) and $TEA^{+}(TCNQ)_2^{-}$ ((b) drop coated and (d) single crystal) electrodes in pH = 7.4 phosphate buffer versus SCE. The sweep rate was 5 mV/s.

Single crystal electrodes of these two materials gave different cv's (figure 4.1.3(c and d)) to those obtained using drop coated electrodes. In the case of $TEA^{+}(TCNQ)_2^{-}$ the behaviour was similar to that of the four materials described earlier. The stable potential range of the electrodes are given in table 4.1. A peak, probably due to the surface reduction of $TCNQ^{0}$, is observed at about 0 mV after the potential has been swept outside this stable range. Single crystals of $Fc^{+}(TCNQ)_2^{-}$ appear to have a stable potential range between -400 and +300 mV. A very broad peak centred at -300 mV is observed after the potential is taken outside the stable range of the material. On cycling between the limits, the shape of the crystal changes as illustrated schematically in figure 4.1.4.

The fabrication of the drop coated electrodes (see 2.2) involves adding THF to the conducting salts. All of the materials are sparingly soluble in this liquid and hence on solvent evaporation the dissolved salt must precipitate out onto the electrode surface. Decomposition of dissolved species from the salt, or a change in crystal structure on solvent evaporation, may therefore be the cause of the difference in the observed electrochemistry between the single crystal and drop coated electrodes.

c) Lead DTF

A cv of a drop coated $Pb(DTF)_2$ electrode is shown in figure 4.1.5. The stable range of this material is between +600 and -300 mV with small peaks being observed at

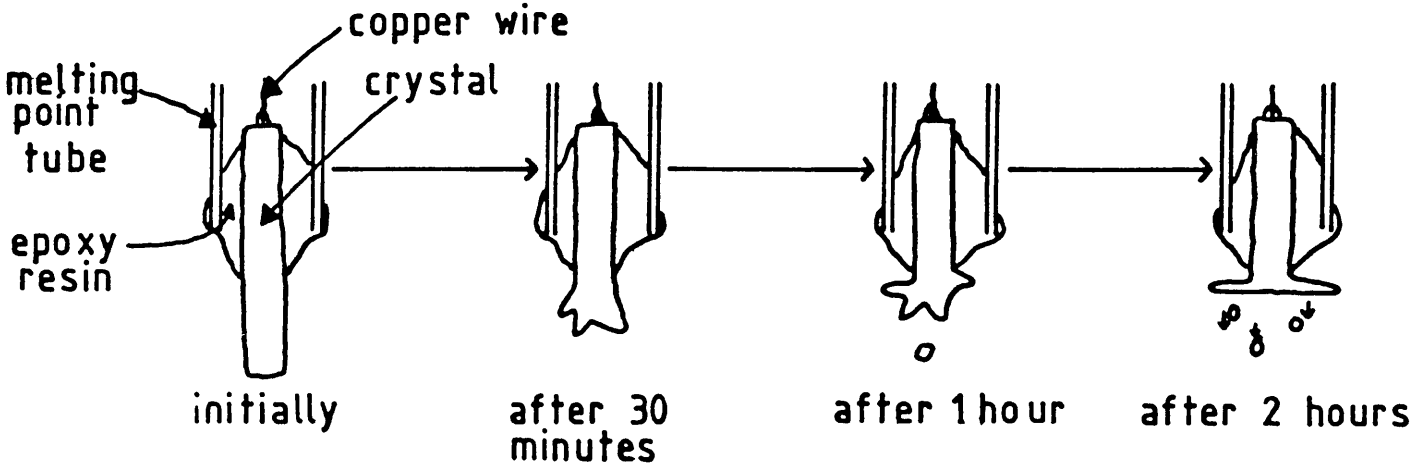

Figure 4.1.4: Schematic representation of the change in shape of a $Fc^{+}(TCNQ)_2^{-}$ single crystal electrode on continuously sweeping the applied potential between the stable potential limits of the salt.

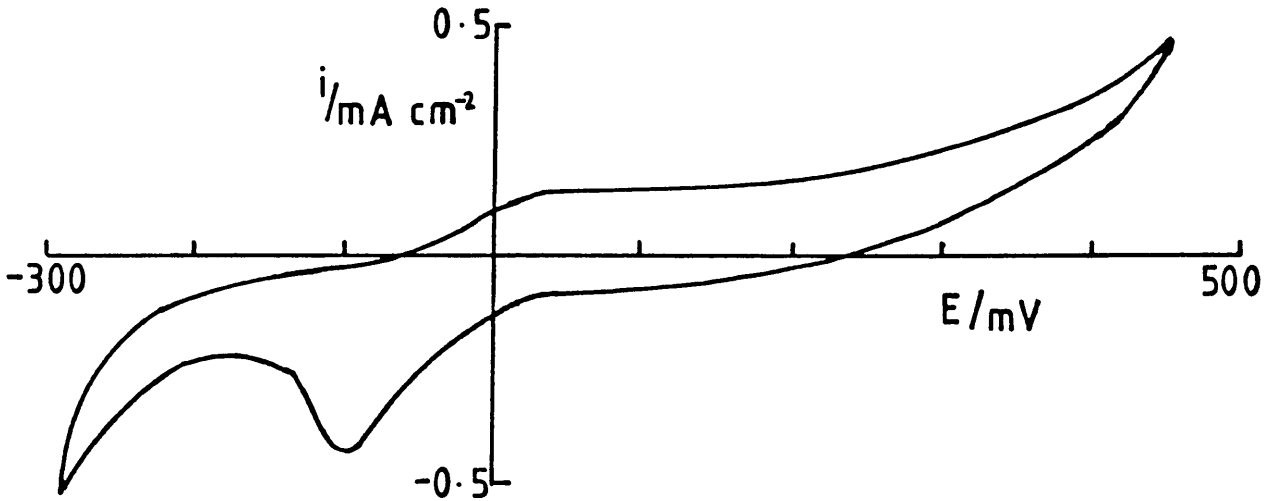

Figure 4.1.5: Cyclic voltammogram at a Pb $(DTF)_2$ drop coated electrode in pH = 7.4 phosphate buffer versus SCE. The sweep rate was 5 mV/s.

-150 and 0 mV when the potential is taken outside this range. These are probably due to the formation of the insoluble species DTF^0 and sodium DTF on the electrode surface.

4.2 Oxidation of Glucose Oxidase on Conducting Salt Electrodes

Preliminary experiments were performed to find out whether the conducting organic salt electrodes, described in 4.1, could be used to reoxidise the reduced form of glucose oxidase. In these either a drop coated electrode (TCNQ salts of TTF, NMP, Q or Cu(DPA), or lead DTF) or a single crystal electrode ($TEA^+(TCNQ)_2^-$ or $Fc^+(TCNQ)_2^-$), was placed in a solution of phosphate buffer containing glucose oxidase, and a potential of +50 mV then applied. For all of the electrode materials a current was observed which decayed, gradually reaching a steady state value after a period of about half an hour. The magnitude, direction and stability of this steady state current (background current) varied depending on the electrode material and the potential applied. In each case, after allowing the background current to settle addition of glucose resulted in an increase in current. No such increase in current was observed when glucose was added in the absence of glucose oxidase, and hence it can be concluded that the current obtained corresponds to the oxidation of the enzyme, rather than the oxidation of glucose, on the electrode surface.

a) TCNQ salts of Q, NMP and TTF

Electrodes made from the TCNQ salts of TTF, NMP, and Q gave very stable background currents in the absence of glucose. At a potential of +50 mV these were of the order of +2μA, +0.2μA and +0.1μA for 3.5 mm radius drop coated electrodes of Q, NMP and TTF respectively. Use of these materials in membrane electrodes is described in more detail later in this chapter.

b) Lead DTF

The background currents of Pb $(DTF)_2$ drop coated electrodes drifted with time and therefore it is impossible to determine accurately the current response to injected glucose. There is no doubt, however, that an increase in current is observed in the presence of glucose and glucose oxidase. This shows the enzyme can be oxidised on organic conductors where TCNQ is not a constituent of the salt.

c) Copper dipyridylamine TCNQ

A large steady state reduction current (-20 μA cm^{-2}) is observed using drop coated electrodes of $Cu(DPA)(TCNQ)_2$ at +50 mV in the absence of glucose and glucose oxidase. This background current is highly potential dependent and further experiments using this material were performed at +150 mV in order to minimise its value. When one of these electrodes is held at +150 mV in a solution of 198 Units cm^{-3} of glucose oxidase (1 Unit is the amount of enzyme that will oxidise 1 μ mol of substrate in 1 minute), addition of

sufficient glucose to saturate the enzyme results in an increase in current of 0.91 μA. From equation (3.8) the saturated response is given by:-

$$\frac{nFAe_{\Gamma}}{i} = \frac{1}{(Dk_{cat})^{1/2}} + \frac{1}{k'} = \frac{1}{k_{sat}}$$

The literature value for the k_{cat} of the enzyme is 800 s^{-1}[28]. This value, combined with the number of Units of enzyme per cm^{-3} of buffer solution, can be used to estimate the concentration of the enzyme, which works out to be approximately 4.1×10^{-9} mol cm^{-3}. Using this, a value for n of 2, and an electrode area of 0.38 cm^2, we get that $(k_{sat})^{-1} \approx 300$ cm^{-1} s. Taking the diffusion coefficient of the enzyme, D, to be approximately 10^{-6} cm^2 s^{-1} a value for $(Dk_{cat})^{-1/2}$ of about 40 cm^{-1} s is obtained. This value is within a factor of ten of the experimental value of $(k_{sat})^{-1}$, and so because of the errors involved in the approximation of D and the electrode area, it is impossible to tell which of the two terms in equation (3.8), $(Dk_{cat})^{-1/2}$ or $(k')^{-1}$, is dominant. It is therefore uncertain whether the saturated response of the electrode is controlled by the electrode kinetics or by the enzyme kinetics, or by a mixture of both of these processes.

d) Ferrocinium TCNQ

Single crystal electrodes of $Fc^{+}(TCNQ)_2^{-}$, of ~ 0.41 mm^2 area, gave stable background currents of the order of -30 nA at a potential of +50 mV. For these electrodes in a solution of 254 Units cm^{-3} glucose oxidase, injection of a sufficient quantity of glucose to saturate the enzyme gave an increase in current of 0.11 μA. This gives a value for $(k_{sat})^{-1}$ of approximately 40 cm^{-1} s which agrees well with the theoretical value for $(Dk_{cat})^{-1/2}$ given above. Hence it is likely that the saturated response of the electrode is controlled by the enzyme kinetics.

The unsaturated behaviour of the electrode can be described by equation (3.7).

$$i = nAF(Dk_{cat}[S]/K_M)^{1/2}e_{\Sigma}$$

A plot of current versus concentration of glucose to the power 1/2 is shown in figure 4.2.1 for the same electrode and solution as above. A reasonable straight line is obtained (the small intercept may be caused by interference from a small amount of residual dissolved oxygen), with a gradient of 44.8 nA $mmol^{1/2}$ $dm^{-3/2}$. This gives a value of K_M of approximately 0.6 mmol dm^{-3} which is somewhat different from the literature value of 7 mmol dm^{-3} [99]. This difference may be due to errors in the approximation of the electrode area and the diffusion coefficient of the enzyme.

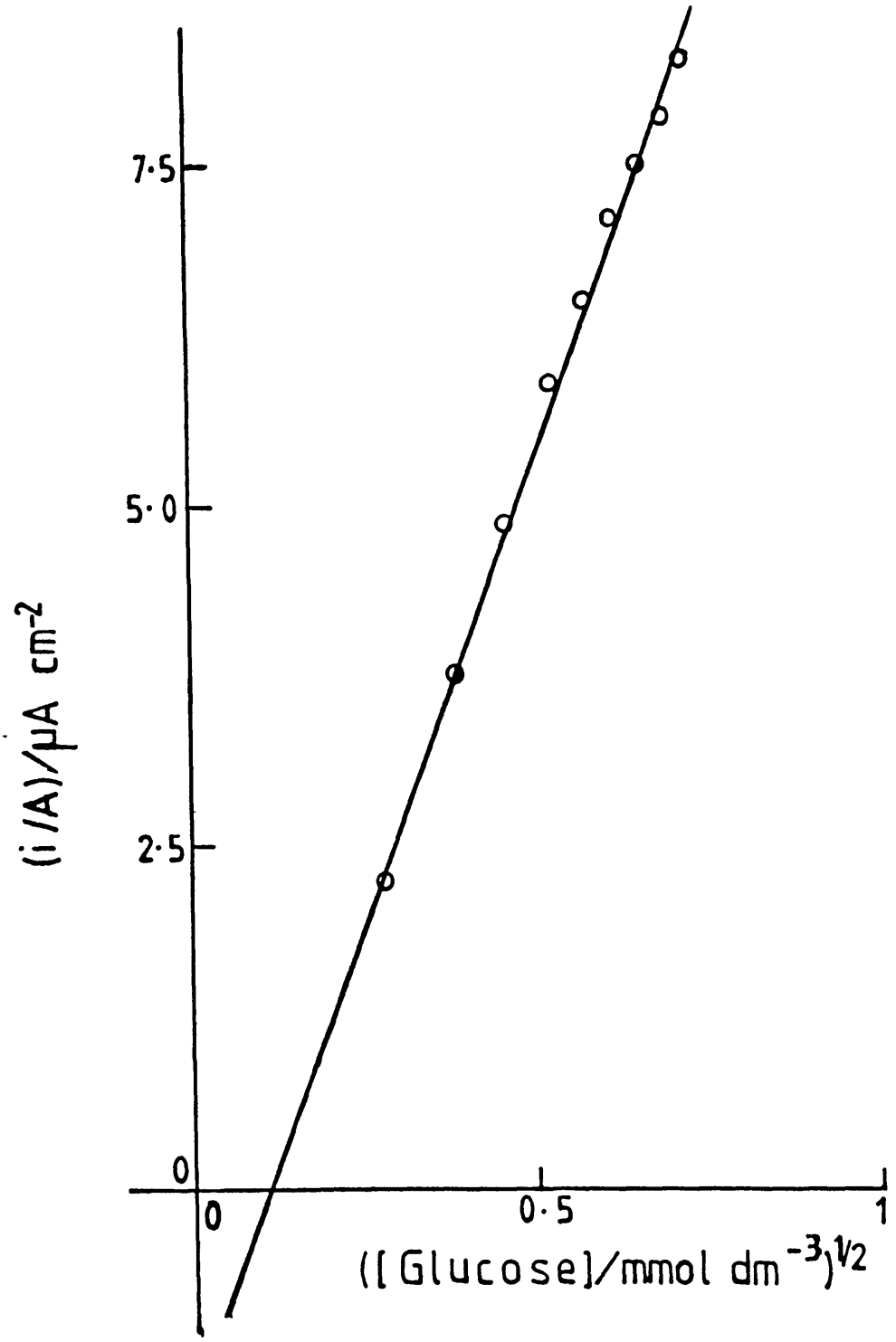

Figure 4.2.1: Plot of current density from a $Fc^{+}(TCNQ)_2^{-}$ single crystal electrode against the square root of the glucose concentration according to equation (3.7).

e) Triethylammonium TCNQ

Single crystal $TEA^{+}(TCNQ)_2^{-}$ electrodes (area ~ 0.2 mm^2) gave large background currents at +50 mV, -40 nA, and therefore, as in the case of $Cu(DPA)(TCNQ)_2$ electrodes, further experiments on this material were carried out at +150 mV (background current = 2 nA). When one of these electrodes was placed in a solution of glucose oxidase (982 Units cm^{-3}) addition of enough glucose to saturate the enzyme gave an increase in current of 66 nA. From equation (3.8) this gives a value for $(k_{sat})^{-1}$ of approximately 120 cm^{-1} s which is within a factor of three of the theoretical value for $(k_{cat}D)^{-1/2}$. It is concluded therefore, that under saturated conditions the kinetics of the enzyme substrate reaction are rate limiting.

Under unsaturated conditions the theory (chapter 3.1) predicts that the response should follow equation (3.7), being proportional to the square root of the substrate concentration. Instead, a linear relationship between the flux and substrate concentration is observed (figure 4.2.2). A possible explanation of this could be that the electrode response is due to the oxidation of enzyme adsorbed on the electrode surface, and not enzyme in the bulk solution. The kinetics of this case are described later in this chapter (4.4). No response to glucose was observed, however, when one of these electrodes was pretreated by soaking in a solution of glucose oxidase. It is therefore likely that this linear relationship is obtained because the response of the device is controlled by the rate of supply of glucose to

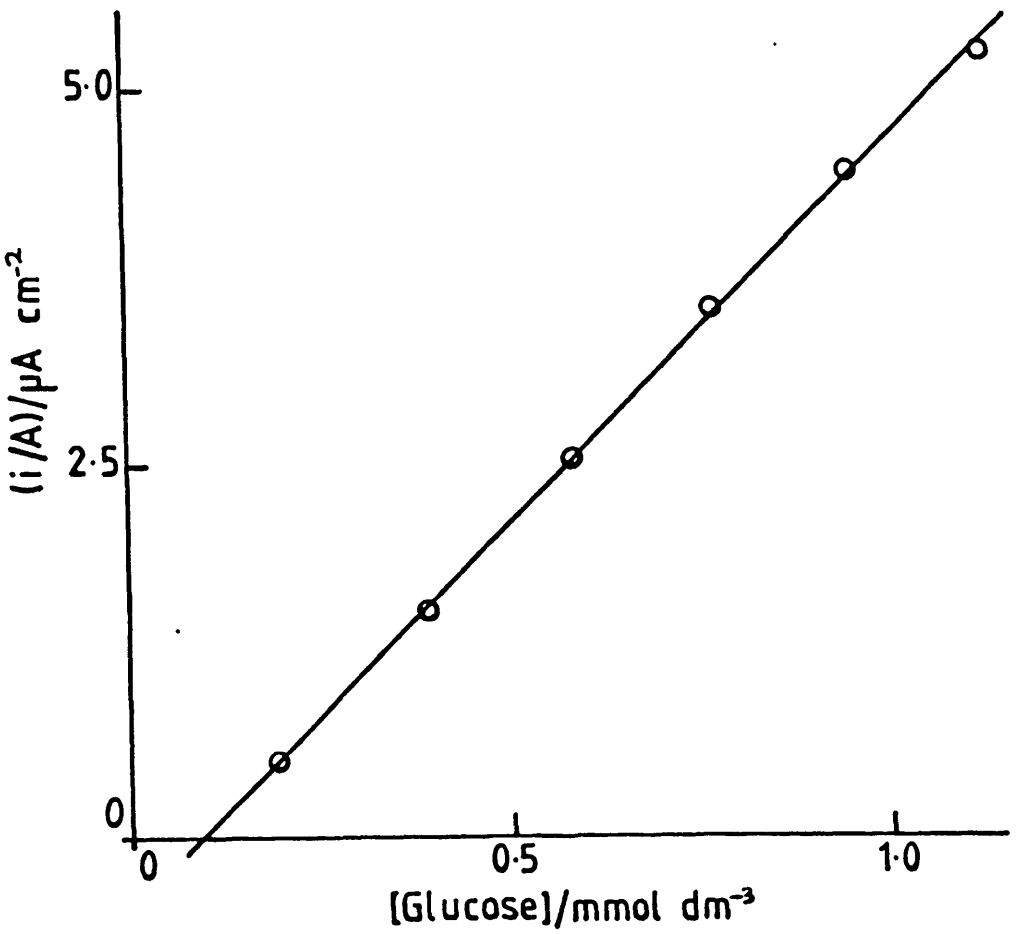

Figure 4.2.2: Plot of the current density from a $TEA^{+}(TCNQ)_{2}^{-}$ single crystal electrode against the concentration of glucose.

the electrode. If this is the case, then the current response will be given by

$$i = nFAD_G[glucose]/X_D \qquad (4.1)$$

where D_G is the diffusion coefficient of glucose and X_D is the thickness of the diffusion layer on the electrode surface. At a concentration of glucose of 1.98 mmol dm^{-3} the current obtained was 18 nA. Taking D_G to be 5×10^{-6} cm^2 s^{-1} gives an X_D of about 0.2 cm. Since nitrogen is constantly bubbled through the solution to ensure that no oxygen is present, the solution is kept well mixed, and therefore this value of X_D is not unreasonable.

4.3 Membrane Electrodes

4.3.1 The Current Response of Membrane Electrodes

Membrane electrodes of the TCNQ salts of Q, NMP and TTF were prepared as described in chapter 2 (Gallenkamp membranes). These were then poised at a potential of +50 mV, and the current monitored as a function of glucose concentration after the background current had reached a steady state value. The current versus concentration plots of typical data are shown in figure 4.3.1.

In chapter 3 a theoretical description of this system was developed, leading to a method for data analysis which can be used to determine the rate limiting step for these

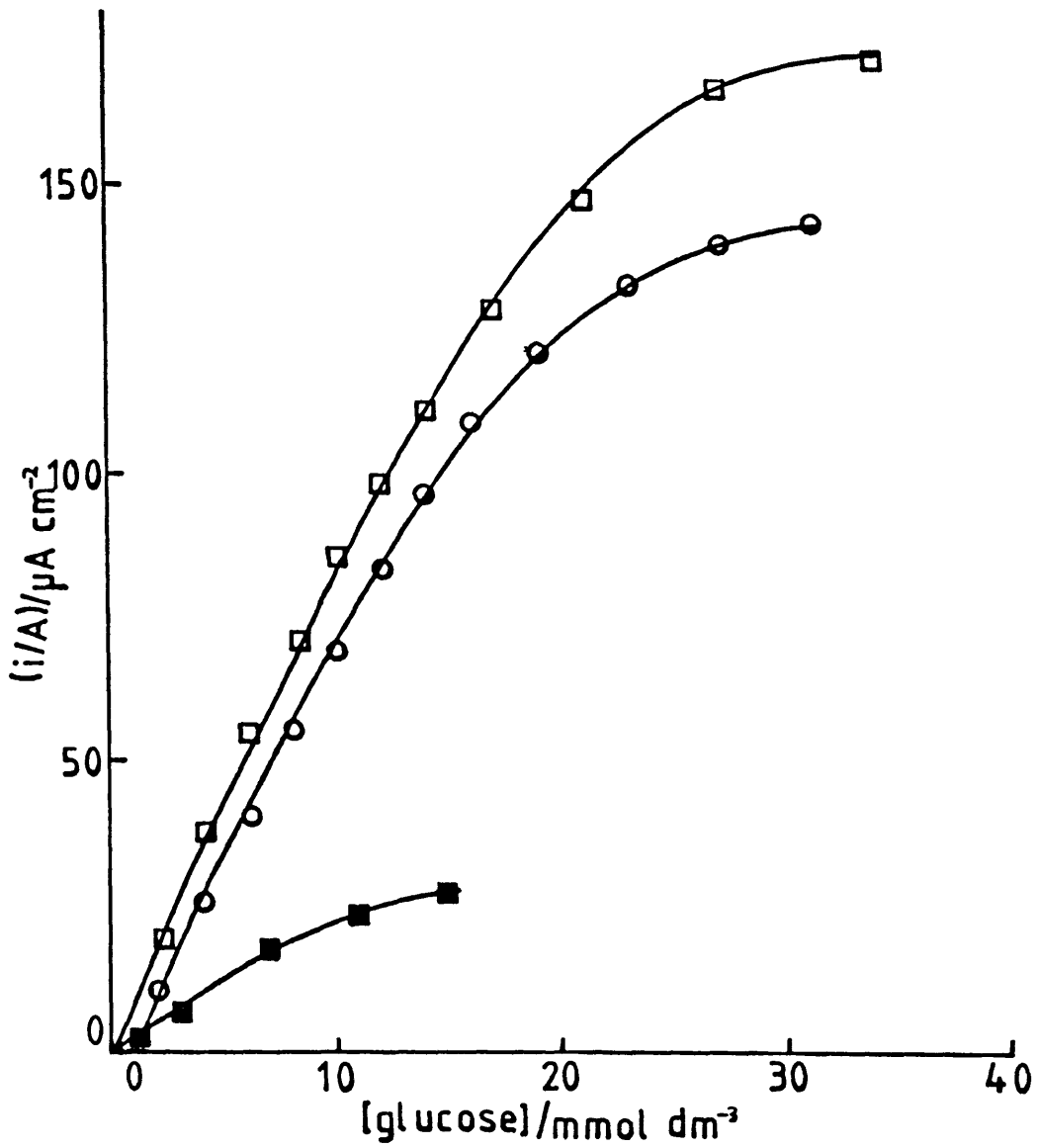

Figure 4.3.1: Typical results for current from membrane electrodes with increasing glucose concentration. The three electrode materials were TTF TCNQ (□), NMP TCNQ (○) and $Q^{+}(TCNQ)_{2}^{-}$ (■).

enzyme electrodes at different concentrations of substrate. The first stage of the analysis is to make a Hanes plot [97] of nFA[glucose]/i against [glucose] according to equation (3.19).

$$\frac{s_\infty}{J} = \frac{1}{k'_{ME}}\left\{1 + \frac{s_\infty}{K_{ME}}\left[1 - \frac{J}{k'_s s_\infty}\right]\right\}$$

The Hanes plots of the data in figure 4.3.1 are shown in 4.3.2. For all three of the electrode materials a horizontal section is observed at low concentrations of glucose. From equation (3.19) the intercept on the y axis of this plot is equal to $(k'_{ME})^{-1}$, which is defined in equation (3.20) as,

$$\frac{1}{k'_{ME}} = \frac{K_M}{Lk_{cat}e_\Gamma} + \frac{1}{k'_s}$$

where the various rate constants in these two expressions are discussed in chapter 3.

Values of k'_{ME} for each of the different conducting salt membrane electrodes are collected in table 4.2. Knowing k'_{ME} the parameter ϱ (which is given by equation (3.24)) can be calculated.

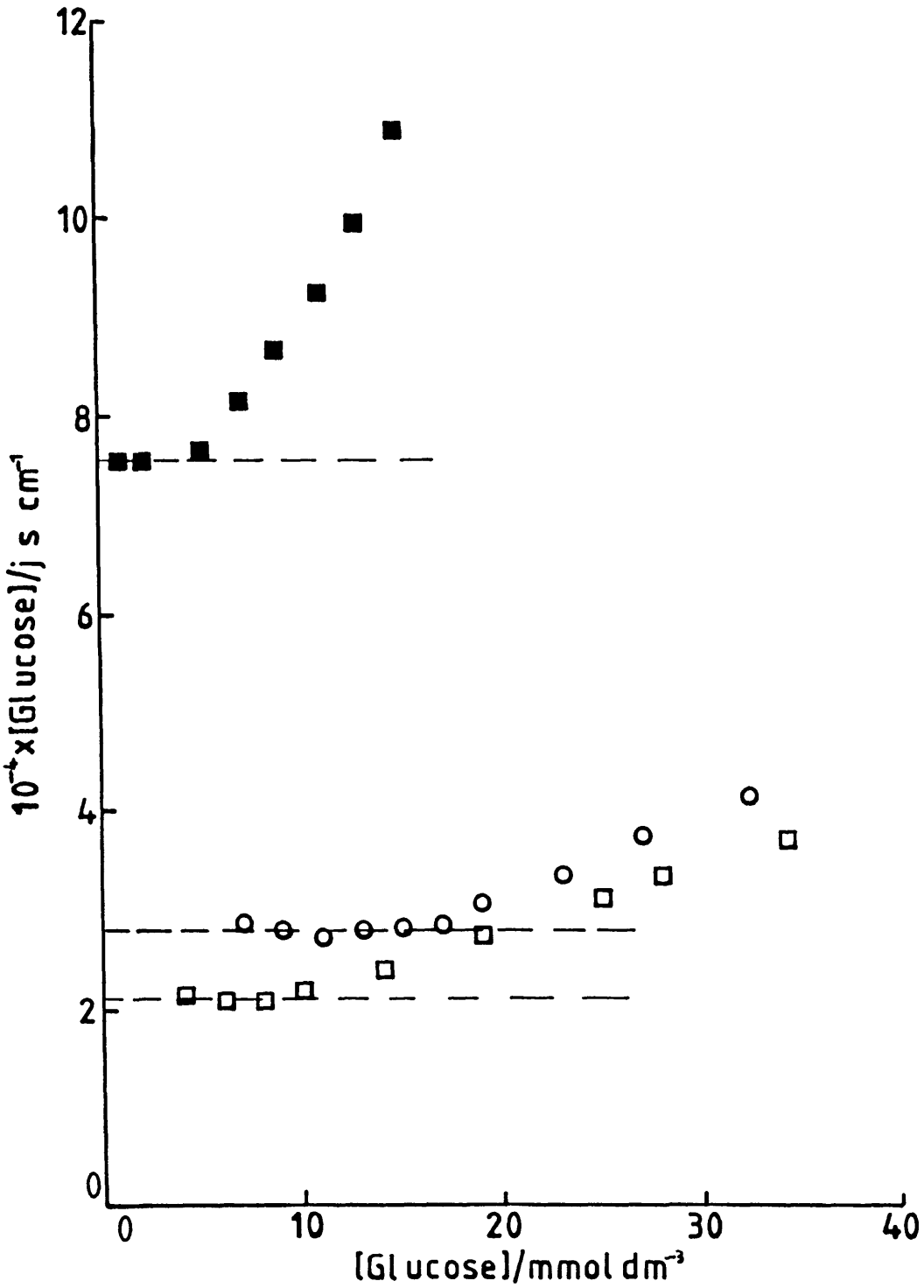

Figure 4.3.2: Hanes plots of the data in figure 4.3.1. The three electrode materials were TTF TCNQ (□), NMP TCNQ (O) and $Q^{+}(TCNQ)_2^{-}$ (■).

TABLE 4.2

Results for Glucose Oxidase Membrane Electrodes

Electrode Material	k'_{ME} / cm s^{-1}	K_{ME} / mmol dm^{-3}	$k'_{cat,E}$ / cm s^{-1}
TTF TCNQ	4.7×10^{-5}	20	9.0×10^{-2}
NMP TCNQ	3.0×10^{-5}	22	8.0×10^{-2}
$Q^{+}(TCNQ)_2^{-}$	1.3×10^{-5}	11	1.4×10^{-2}

$$\varrho = (j/s_\infty)(k'_{ME})^{-1}$$

The next step in the analysis is to plot y versus ϱ according to equation (3.25):-

$$y = \frac{\varrho^{-1} - 1}{s_\infty} = \frac{1}{K_{ME}}\left[1 - \frac{\varrho k'_{ME}}{k'_s}\right]$$

The y versus ϱ plots are shown in figure 4.3.3. In each case the intercept on the x-axis is approximately equal to 1 and hence (from equation (3.25)) $k'_{ME} \approx k'_s$. From equation (3.20) it can therefore be concluded that $(Lk_{cat}e_\Gamma)/K_M >> k'_s$. Thus at low substrate concentrations the rate limiting step is the diffusion of glucose through the membrane. The subsequent enzyme and electrode steps are so fast that they are not rate limiting. The fact that the transport of the glucose through the membrane is rate limiting explains why the values of k'_{ME} for the different conducting salt electrodes are all so similar. The thickness of the membrane, L_m, is about 0.3 mm; k'_s is given by

$$k'_s = \frac{K_s D_s}{L_m}$$

which gives a value for $K_s D_s$ of the order of 10^{-6} cm^2 s^{-1}. This value is in good agreement with that found by Leypolt

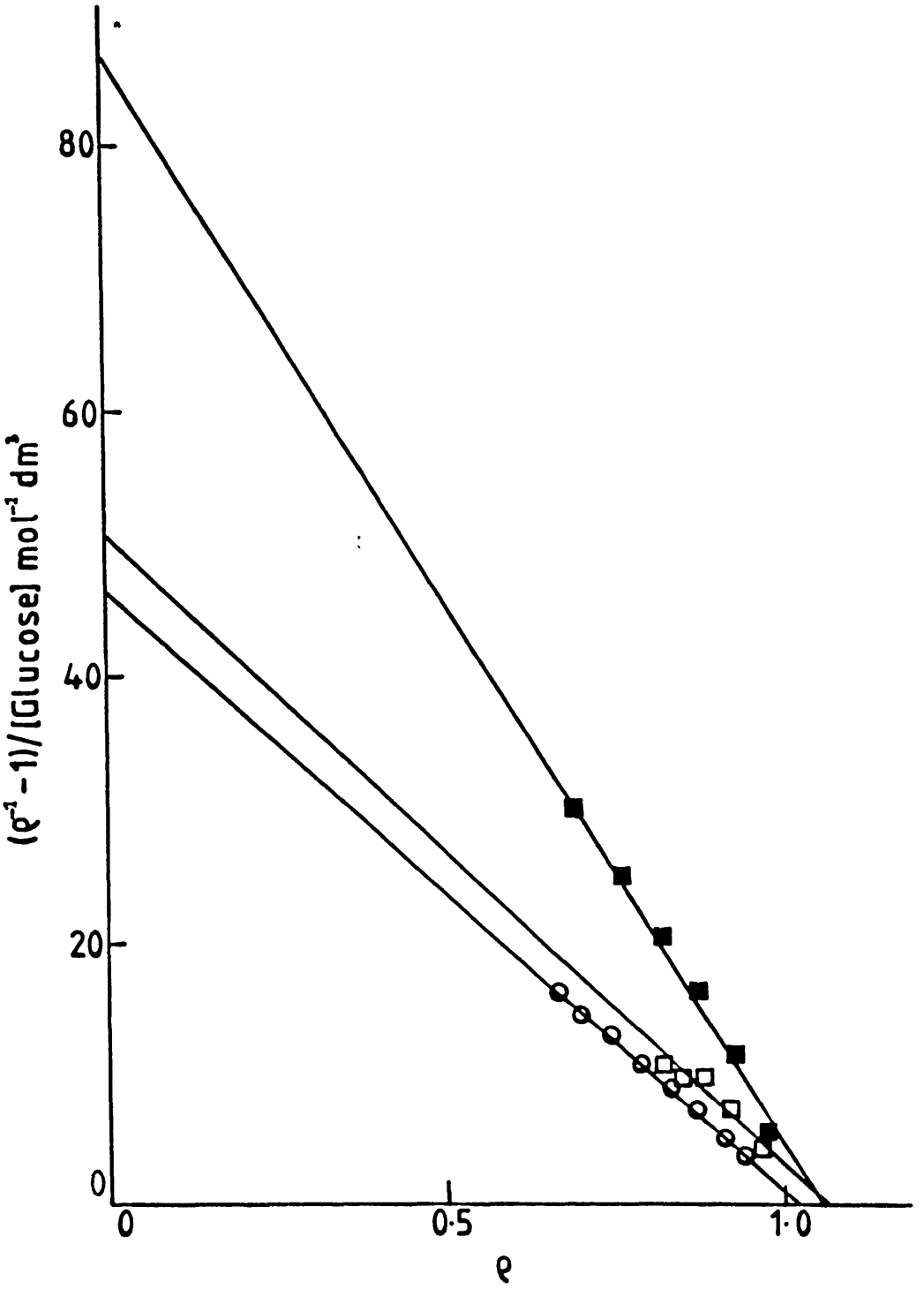

Figure 4.3.3: y versus ϱ plots from the data in figure 4.3.2. The three electrode materials were TTF TCNQ (□), NMP TCNQ (○) and $Q^+(TCNQ)_2^-$ (■).

and Gough [100], who used a rotating disc electrode method to measure the transport properties of a similar membrane.

Returning to figure 4.3.3, from the intercept on the y-axis K_{ME}, the Michaelis constant for the enzyme electrode, can be calculated. Values of K_{ME} for each of the enzyme electrodes are collected in table 4.2. From equation (3.23) $k'_{cat,E}$ is given as

$$k'_{cat,E} = \frac{K_{ME}k'_{ME}}{e_{\Sigma}}$$

where from equation (3.22)

$$(k'_{cat,E})^{-1} = (Lk_{cat})^{-1} + (k')^{-1}$$

Using the values of k'_{ME} and K_{ME} obtained from the Hanes and y versus ϱ plots, and a value of e_{Σ} calculated from the number of units of the enzyme used assuming a value of k_{cat} of 800 s^{-1} [28], $k'_{cat,E}$, the rate constant for the saturated electrode, is obtained. Values of this rate constant for the various enzyme electrodes are collected in table 4.2. The two terms in equation (3.22) describe saturated enzyme and electrode kinetics. The ratio of these two terms can be found from a knowledge of K_{ME}, K_M and the ratio k'_s/k'_{ME} as determined from the y versus ϱ plots. Equations (3.20), (3.22) and (3.23) can be rearranged to give:-

$$\frac{k_{cat}L}{k'} = \frac{K_M}{K_{ME}(1 - k'_{ME}/k'_s)} - 1 \qquad (4.2)$$

The literature value of K_M is 7 mmol dm^{-3} [99]. The values of K_{ME} in table 4.2 are about 20 mmol dm^{-3}. Within experimental error it is found that for all three materials k'_{ME} is equal to k'_s. It can therefore be concluded that the bracket in the denominator of equation (4.2) is smaller than 0.1 mmol dm^{-3}. Therefore $k_{cat}L/k' > 10$ and hence the rate limiting process in the saturated region is the electrode kinetics and not the enzyme kinetics. The electrochemical rate constants, k', for the three materials are given by the values of $k'_{cat,E}$ in table 4.2. Taking k_{cat} to be 800 s^{-1} and a value for L of several tens of microns, it is found that in accord with the analysis, the inequality $k_{cat}L/k' > 10$ is satisfied. Finally it is satisfactory that all of the values of k' in table 4.2 are larger than 10^{-2} cm s^{-1}, thus showing that these three conducting salts are good electrocatalysts for the oxidation of glucose oxidase.

4.3.2 Electrode Stability

The membrane electrodes described above can only be used as reliable sensors for the detection of glucose, if they are robust. To test the stability of these electrodes,

a TTF TCNQ membrane electrode was made using a solution of 725 Units cm^{-3} of glucose oxidase. Experiments as described above, in which the electrode is held at a potential of +50 mV in a solution of buffer and the current monitored as a function of glucose concentration, were carried out each day for two weeks, and then again at the end of the third and fourth weeks. In between experiments the electrode was kept in continuous operation (i.e. poised at a potential of +50 mV) in a buffer solution containing sufficient glucose to saturate the enzyme.

The current versus concentration, Hanes and y versus ϱ plots of the data obtained on days 1, 9, 14 and 28 are shown in figures 4.3.4, 4.3.5 and 4.3.6. From the intercept on the y axis of the Hanes plots the values of k'_{ME} for the electrode on the different days were calculated, and are given in table 4.3. These decrease with time dropping to 42% of the original value after 28 days. The intercepts on the x-axis of the y versus ϱ plots are all close to unity, which shows that throughout the 28 day period the unsaturated response of the electrode was controlled by the rate of diffusion of substrate through the membrane, and hence $k'_{ME} \approx k'_s$. The decrease in the response of the electrode under unsaturated conditions is therefore caused by a deterioration in the transport properties of glucose in the membrane.

The intercepts on the y-axis of the y versus ϱ plots can be used to obtain values of K_{ME} for the electrode on the different days. These are collected in table 4.3 as are the

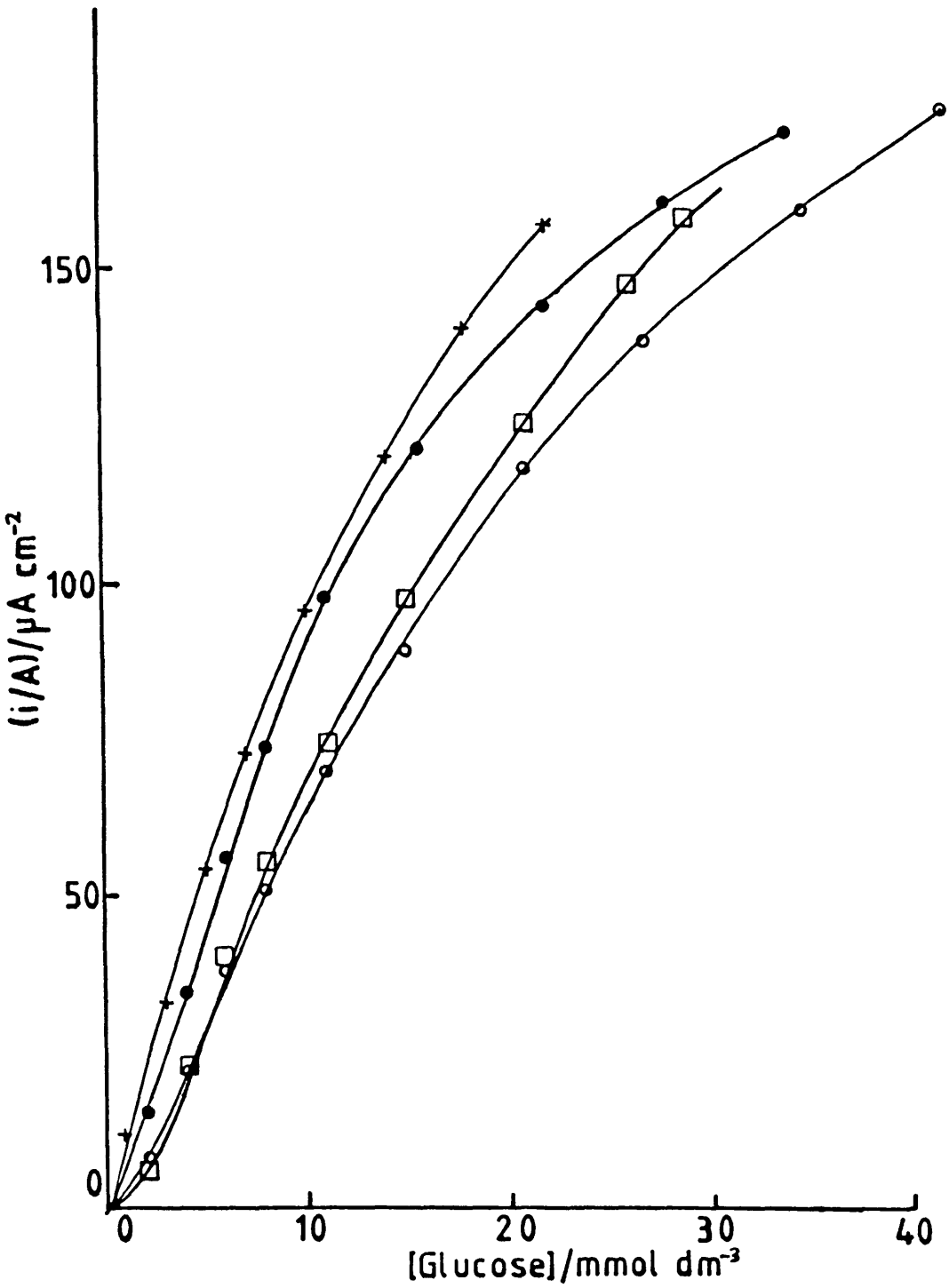

Figure 4.3.4: Response of a TTF TCNQ/glucose oxidase membrane electrode to increasing concentrations of glucose after 1 (+), 9 (●), 14 (□) and 28 (○) days of continuous operation.

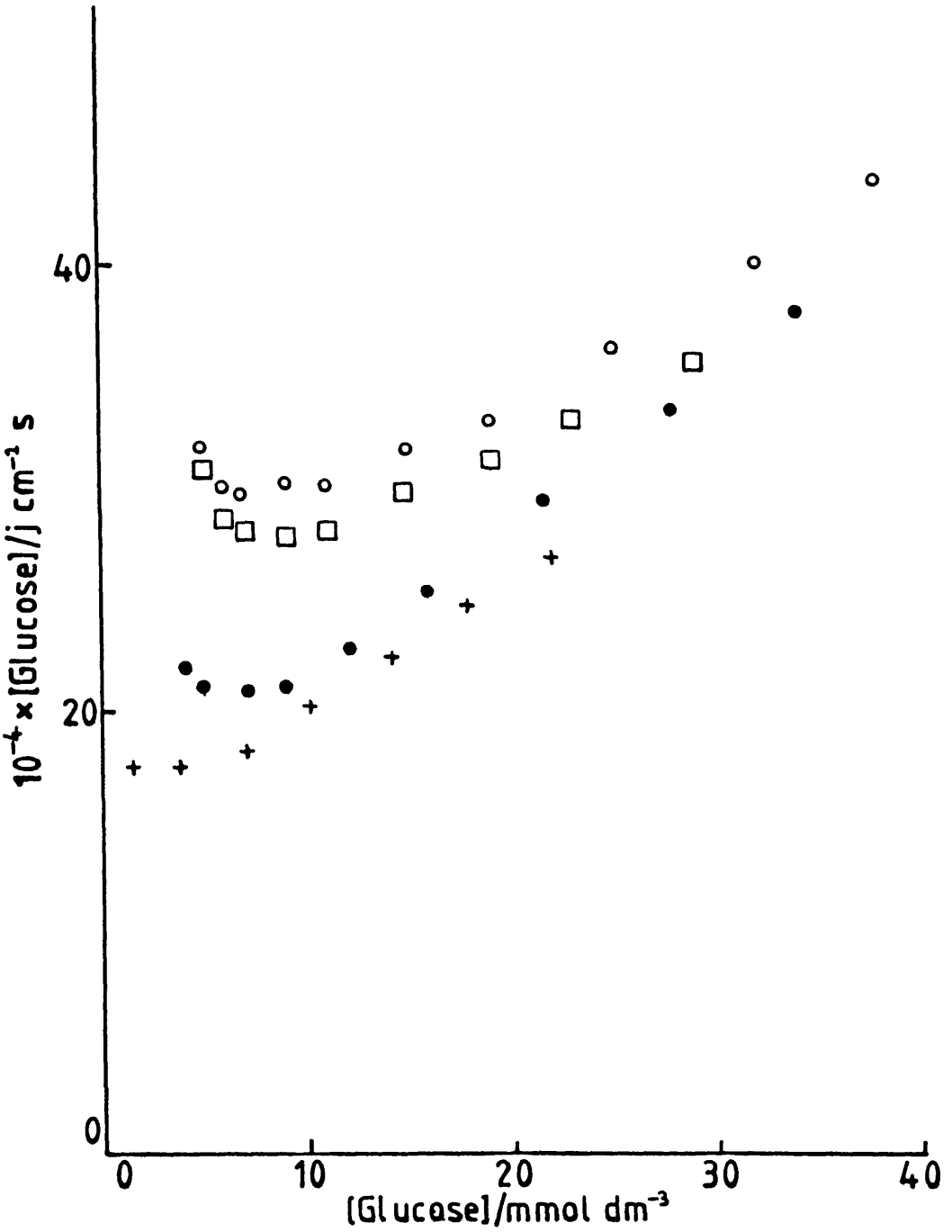

Figure 4.3.5: Hanes plot of the data in figure 4.3.4 for a TTF TCNQ/glucose oxidase membrane electrode after 1 (+), 9 (●), 14 (□) and 28 (o) days of continuous operation.

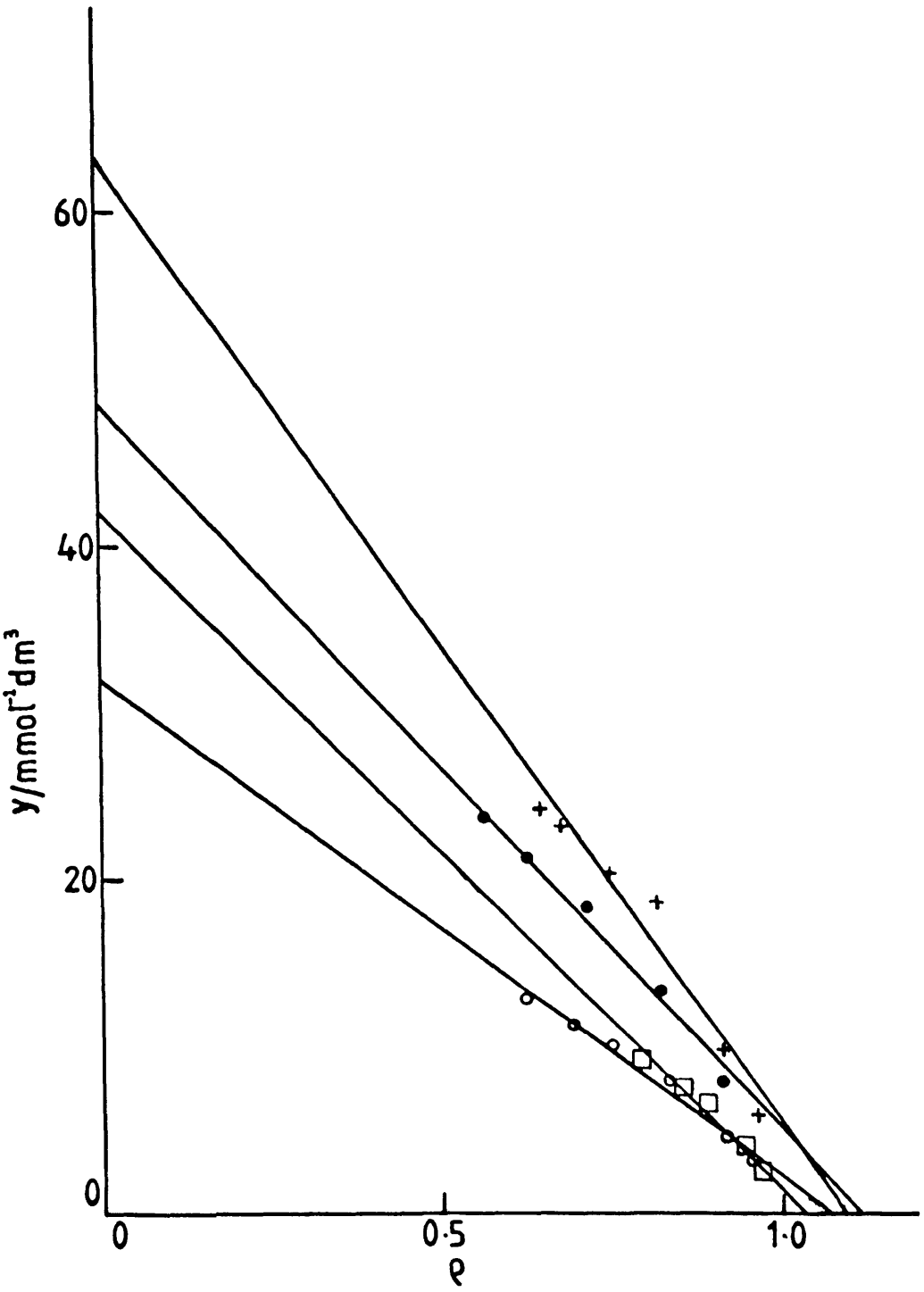

Figure 4.3.6: y versus ϱ plots from the data in figure 4.3.5 for a TTF TCNQ/glucose oxidase membrane electrode after 1 (+), 9 (●), 14 (□) and 28 (o) days of continuous operation.

TABLE 4.3

Rate Constants for TTF TCNQ/Glucose Oxidase Membrane Electrodes After Different Numbers of Days of Continuous Operation

Day	k'_S/cm s^{-1}	K_{ME}/mmol dm^{-3}	k'/cm s^{-1}
1	5.69×10^{-5}	15.9	6.0×10^{-2}
9	4.76×10^{-5}	20.6	6.5×10^{-2}
14	3.58×10^{-5}	23.7	5.6×10^{-2}
28	3.30×10^{-5}	31.1	6.8×10^{-2}

values of the saturated rate constant, $k'_{cat,E}$, which were calculated using equation (3.23). These values of $k'_{cat,E}$ are again interpreted, by the same argument given above, as being equal to the electrochemical rate constant k'. The values of k' remain fairly constant over the 28 day period.

It appears therefore that the electrodes are fairly stable with time, with no decrease in the saturated response, and a 42% decrease in the unsaturated response, being observed after 28 days of continuous use. The drop in the unsaturated response is caused by a deterioration in the membrane.

4.4 Adsorbed Glucose Oxidase

An increase in current on addition of glucose is observed using conducting salt electrodes pretreated by soaking in a solution of phosphate buffer containing glucose oxidase. This shows that glucose oxidase is adsorbed irreversibly onto the surface of conducting salt electrodes, with this adsorbed enzyme able to undergo electron transfer with the electrode. Thus it is possible to make a sensor for the determination of glucose levels, without the need for a membrane.

Figure 4.4.1 shows typical responses of $Q^+(TCNQ)_2^-$, TTF TCNQ and NMP TCNQ adsorbed enzyme electrodes. These results were obtained using cavity electrodes which were soaked for twelve hours in solutions of 810 ($Q^+(TCNQ)_2^-$), 1865 (NMP

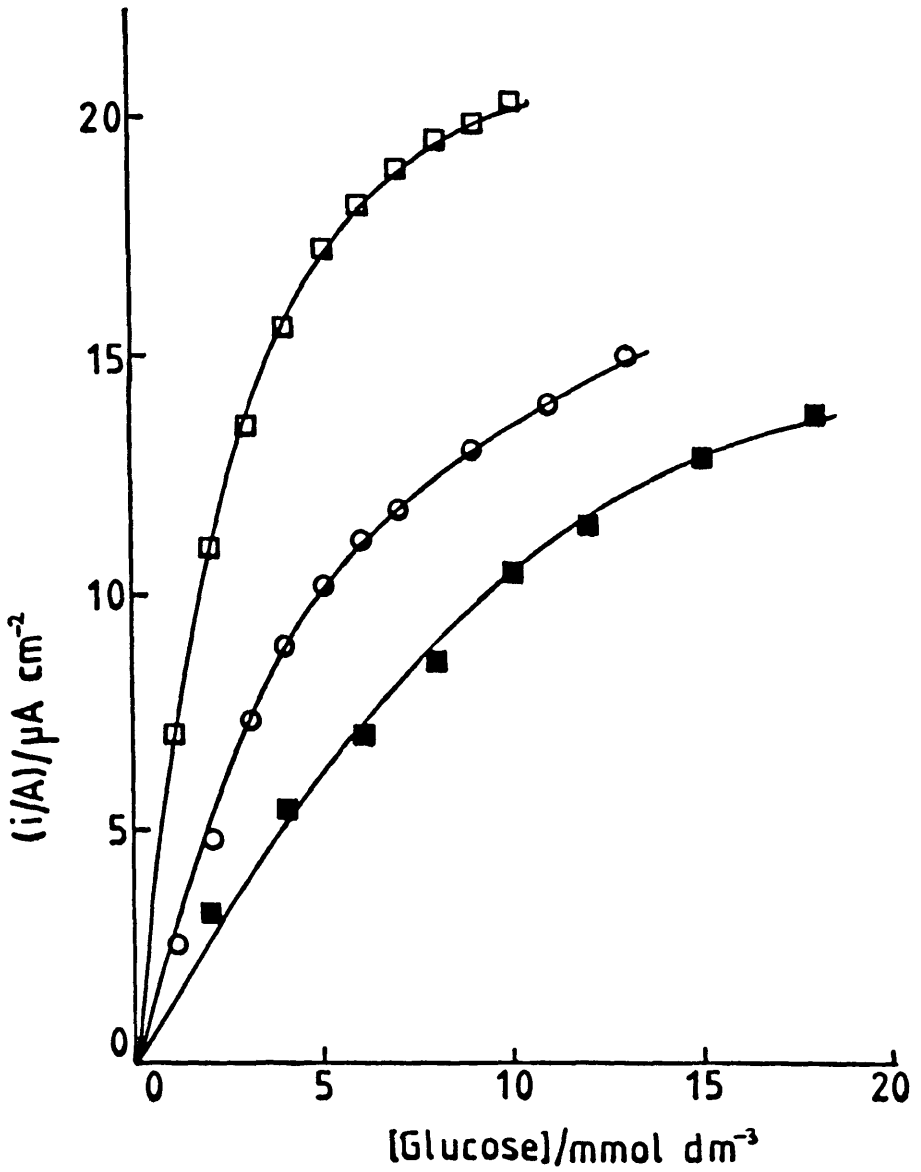

Figure 4.4.1: Current response of adsorbed enzyme electrodes with increasing glucose concentration. The three electrode materials were TTF TCNQ (□), NMP TCNQ (O) and $Q^{+}(TCNQ)_{2}^{-}$ (■).

TCNQ) and 1925 (TTF TCNQ) Units of glucose oxidase per cm^{-3} of buffer. Hanes plots of the data in figure 4.4.1 are linear for all three electrode materials (figure 4.4.2).

The response of the adsorbed enzyme electrodes can be modelled in a very similar way to that of the membrane electrodes (see chapter 3). The seven equations (3.10) to (3.16) still apply, but the physical significance of some of the parameters is different. For example, the terms e, es, e'p and e' now refer to the concentrations in mol cm^{-2} of the various enzyme species on the electrode surface. Consequently in equation (3.15) the electrochemical rate constant has units of s^{-1}. In addition s_0 and p_0 now represent the concentrations of S and P at the electrode. In equations (3.13) and (3.14), k'_s and k'_p describe the diffusion of substrate from the bulk solution into the enzyme layer, and the diffusion of product from the enzyme layer into the bulk respectively. These are given by

$$k'_x = D_x/X_D \qquad (4.3)$$

where x is either s or p, D_x is the diffusion coefficient of x in the solution and X_D is the thickness of the diffusion layer on the surface of the electrode. Also in equations (3.10) to (3.12) the L terms vanish as the reaction is now confined to the electrode surface. Hence if we again assume no product inhibition, equation (3.19) still applies. Linear Hanes plots and horizontal lines for the y versus ϱ plots (figure 4.4.3) show that k'_{ME}/k'_s is approximately zero,

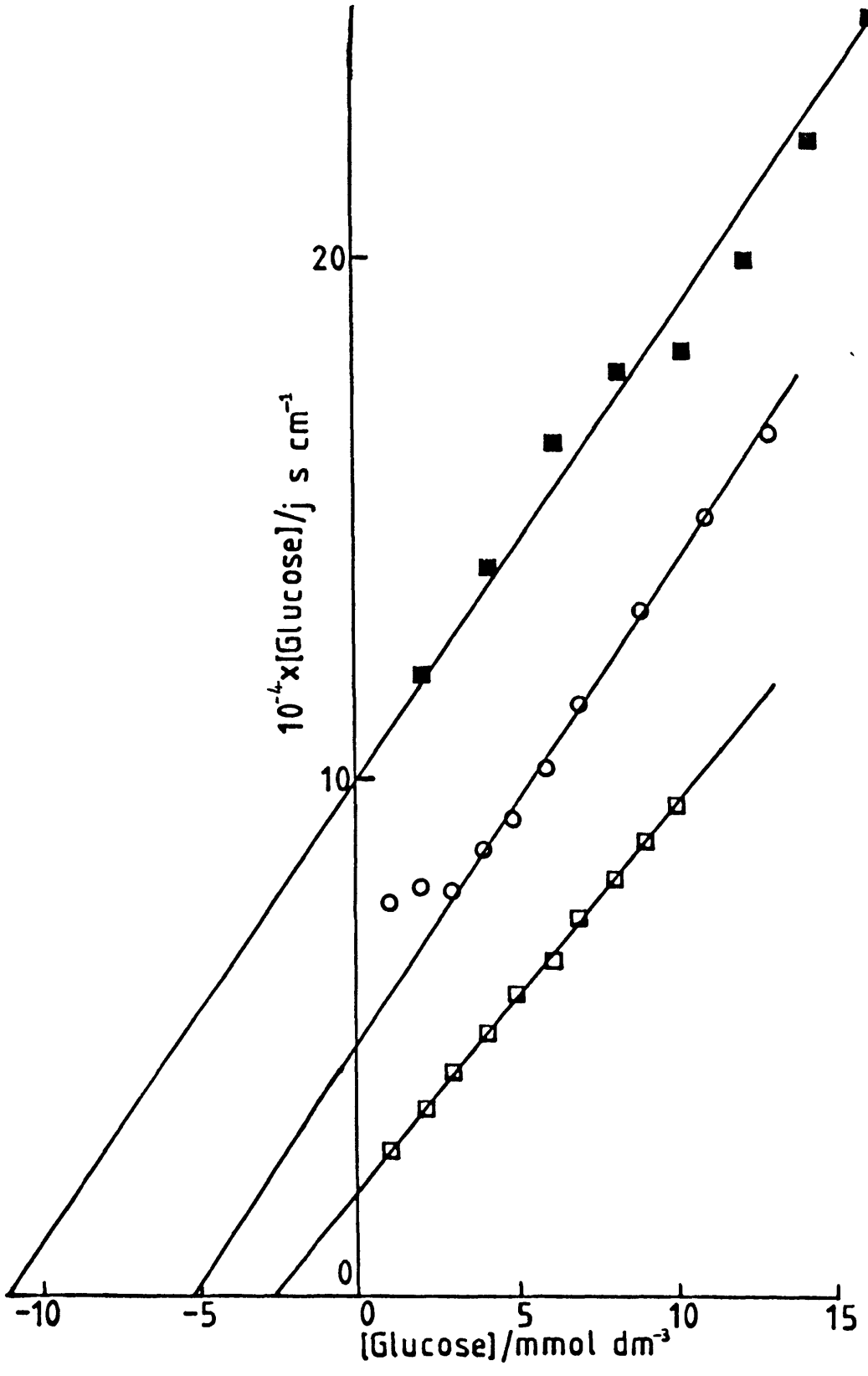

Figure 4.4.2: Hanes plots of the data in figure 4.4.1 for adsorbed enzyme electrodes. The three electrode materials were TTF TCNQ (□), NMP TCNQ (○) and $Q^{+}(TCNQ)_2^{-}$ (■).

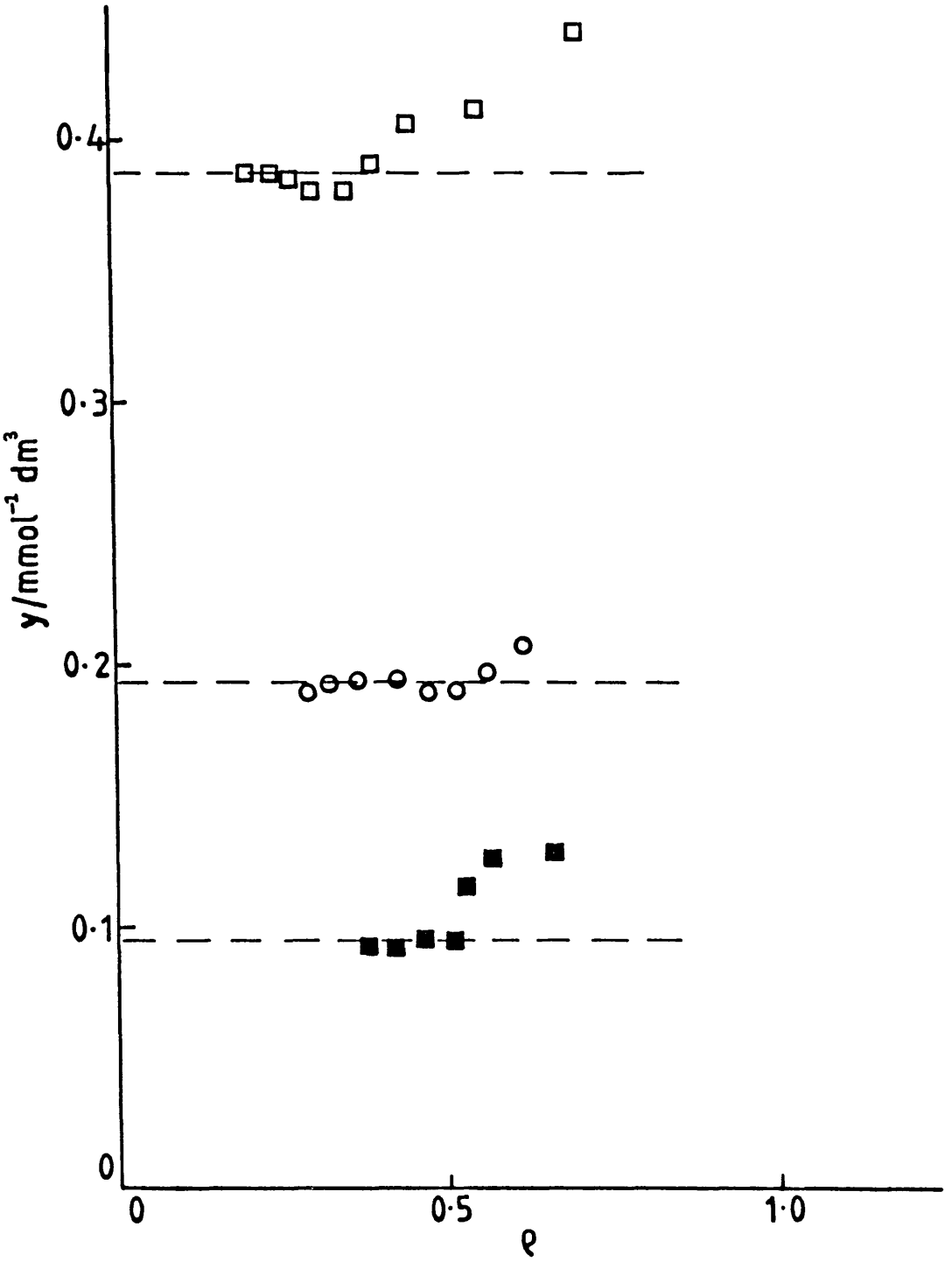

Figure 4.4 3: y versus ϱ plots from the data in figure 4.4.2 for adsorbed enzyme electrodes. The three electrode materials were TTF TCNQ (□), NMP TCNQ (O) and $Q^+(TCNQ)_2^-$ (■).

and so under unsaturated conditions the response is controlled by the enzyme kinetics. Equation (3.19) therefore becomes:-

$$\frac{s_\infty}{j} = \frac{K_M}{e_\Sigma k_{cat}} + \frac{s_\infty}{e_\Sigma}\left\{\frac{1}{k_{cat}} + \frac{1}{k'}\right\} \qquad (4.4)$$

The intercept on the x-axis of the Hanes plot, $-K_{M'}$, is given by

$$K_{M'} = K_M/(1 + k_{cat}/k') \qquad (4.5)$$

and therefore $K_{M'} < K_M$.

Figure 4.4.2 shows that the experimental values of $K_{M'}$ are all within a factor of 3 of the literature value for the free enzyme of K_M of 7 mmol dm^{-3}. If it is assumed that the K_M and the k_{cat} of the adsorbed enzyme are the same as that of the free enzyme, then the electrochemical rate constants for the oxidation of the adsorbed enzyme (k') for the three electrode materials are all of the order of 800 s^{-1}. The maximum flux, J_M, is given by:-

$$J_M = k'_{cat,E} e_\Sigma$$

where

$$(k'_{cat,E})^{-1} = (k')^{-1} + (k_{cat})^{-1}$$

The maximum current obtained, i_M, for each of the adsorbed enzyme electrodes was about 0.6 μA. With a value of n of 2 then $j_M/A = 3 \times 10^{-12}$ mol s^{-1}, where A is the area of the electrode. For a monolayer coverage of enzyme a reasonable estimate for e_Σ is about 10^{-12} mol cm^{-2}, and so taking $k'_{cat,E}$ to be 800 s^{-1}, j_M is approximately 8×10^{-10} mol cm^{-2} s^{-1}. Combining this with the value for j_M/A, we find that A is about 3×10^{-3} cm^2. This is considerably less than the surface area of the electrode, which ignoring roughness is 3×10^{-2} cm^2. Though the K_M and k_{cat} of the adsorbed enzyme are unlikely to be the same as that of the free enzyme, the difference between the areas is such that it is likely that the enzyme occupies less than a monolayer.

The consequence of sub-monolayer coverage of irreversibly adsorbed enzyme is that any free enzyme in the surrounding solution can also come into contact with the electrode surface. Hence in the case of membrane electrodes, the response can be thought of in terms of contributions from both adsorbed and free enzyme. This explains why larger saturation currents are obtained using membrane electrodes than are obtained using adsorbed enzyme

electrodes.

4.5 Other Enzymes

Like glucose oxidase the enzymes xanthine oxidase, D-amino acid oxidase and L-amino acid oxidase contain the prosthetic group FAD, which is reduced during the enzymatic oxidation of the enzyme substrate. In conjunction with Mr Mark Bycroft, experiments were carried out to ascertain whether the reduced forms of these enzymes can be oxidised directly on the surface of a TTF TCNQ electrode, according to the reaction scheme:-

$$SH_2 + E(FAD) \longrightarrow S + E(FADH_2)$$

$$E(FADH_2) \xrightarrow{\text{TTF TCNQ electrode}} E(FAD) + 2H^+ + 2e^-$$

For this purpose membrane electrodes were constructed for each of the three enzymes using packed cavity electrodes and dialysis membrane (Gallenkamp), as described in chapter 2. TTF TCNQ was used as the electrode material as this gives lower background currents than the other conducting salts. Further experiments were also carried out using electrodes which had previously been soaked in a solution of the appropriate enzyme, to find out if the enzyme is both adsorbed on, and able to undergo electron transfer with, the electrode surface.

4.5.1 D-amino acid oxidase

a) Membrane electrodes

Figure 4.5.1 shows the current response of a TTF TCNQ/ D-amino acid oxidase membrane electrode to increasing concentrations of D-alanine. The concentration of enzyme behind the membrane was 70 Units cm^{-3}.

The Hanes plot of this data is shown in figure 4.5.2. As in the case of glucose oxidase a horizontal section is observed at low concentrations of substrate with the intercept on the y axis equal to 3.9×10^{4} cm^{-1} s^{-1}. From equation (3.19) this gives a value of k'_{ME} of 2.6×10^{-5} cm s^{-1}. Figure 4.5.3 shows the y versus ϱ plot of this data according to equation (3.25). This is linear with an intercept on the x-axis (equal to the ratio k'_s/k'_{ME}) of about 1. Thus $k'_{ME} \approx k'_s$ and so the response of the electrode at low concentrations of D-alanine is controlled by the rate of its transport through the membrane. The intercept on the y-axis is equal to 940 $mol^{-1}dm^{-3}$ which gives a value of K_{ME} of 1.1 mmol dm^{-3}.

Taking a value of k_{cat} of 9.8 s^{-1} [35] equation (3.23) gives that $k'_{cat,E} = 2.3 \times 10^{-4}$ cm s^{-1}. This value of $k'_{cat,E}$ can be compared with the much larger value of Lk_{cat} of 9.8×10^{-3} cm s^{-1} (taking L to be 10 μm). Rearrangement of equation (3.22) gives:-

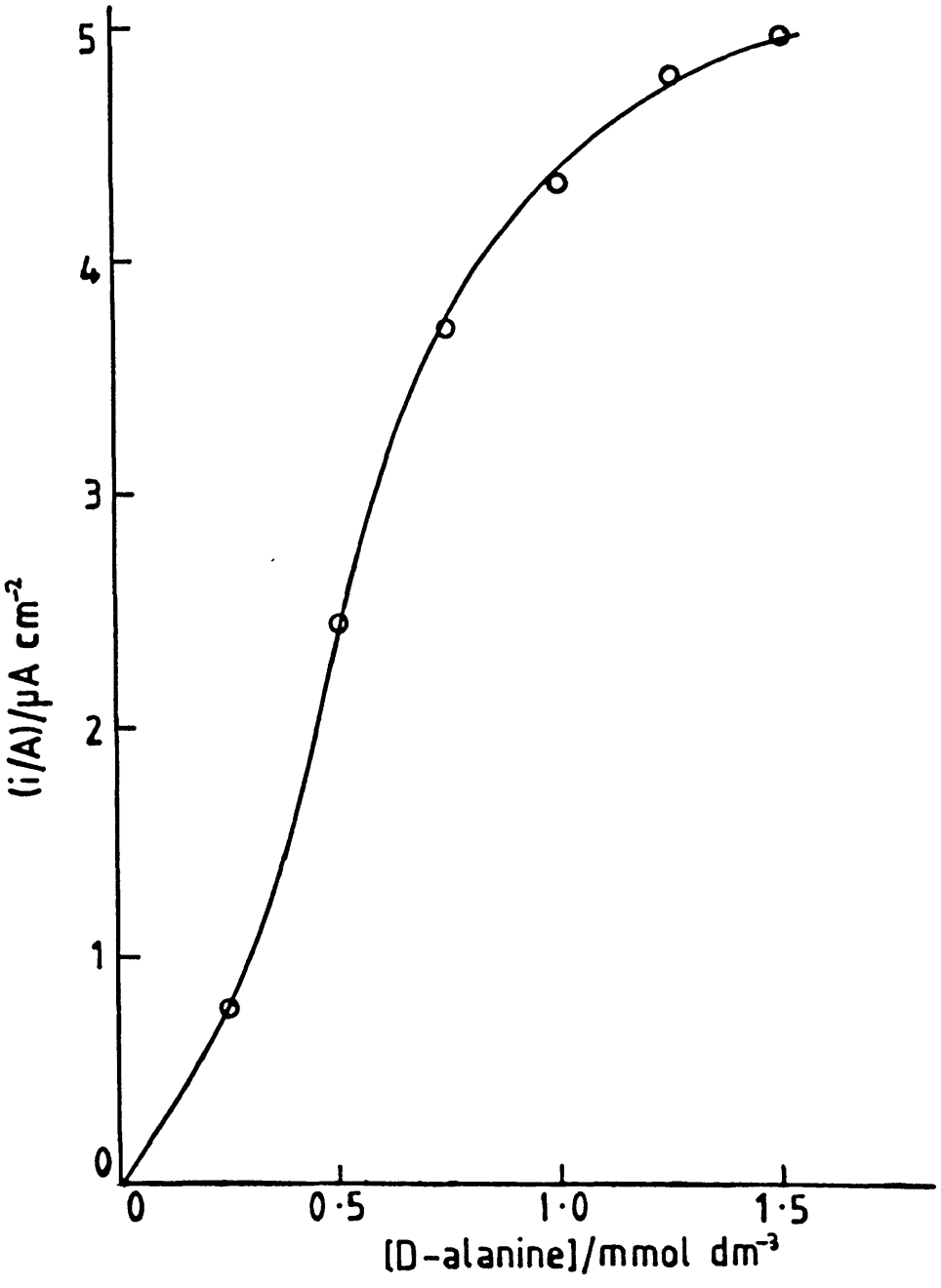

Figure 4.5.1: Current response of a TTF TCNQ/D-amino acid oxidase membrane electrode to increasing concentrations of D-alanine.

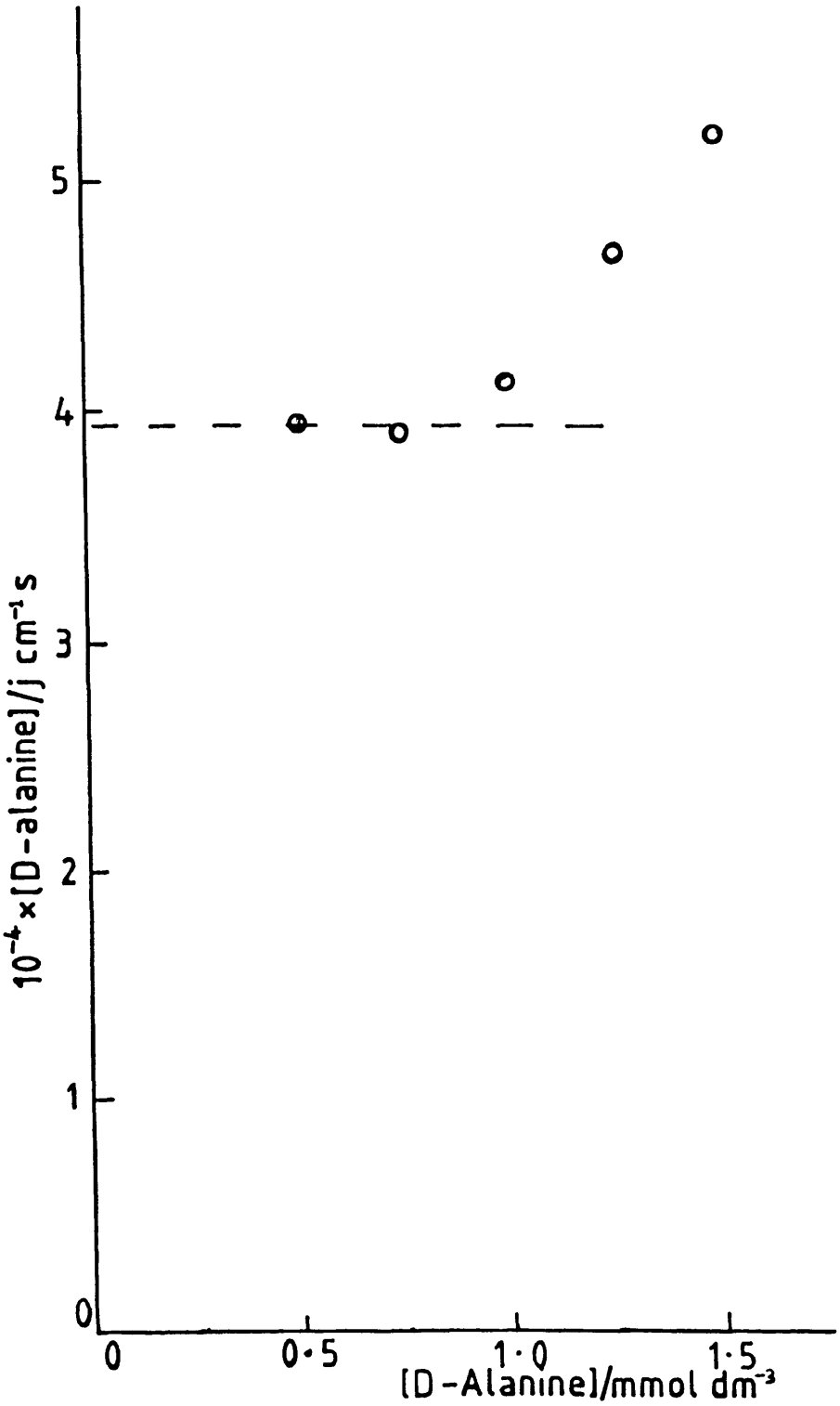

Figure 4.5.2: Hanes plot of the data in figure 4.5.1 for a TTF TCNQ/D-amino acid oxidase membrane electrode.

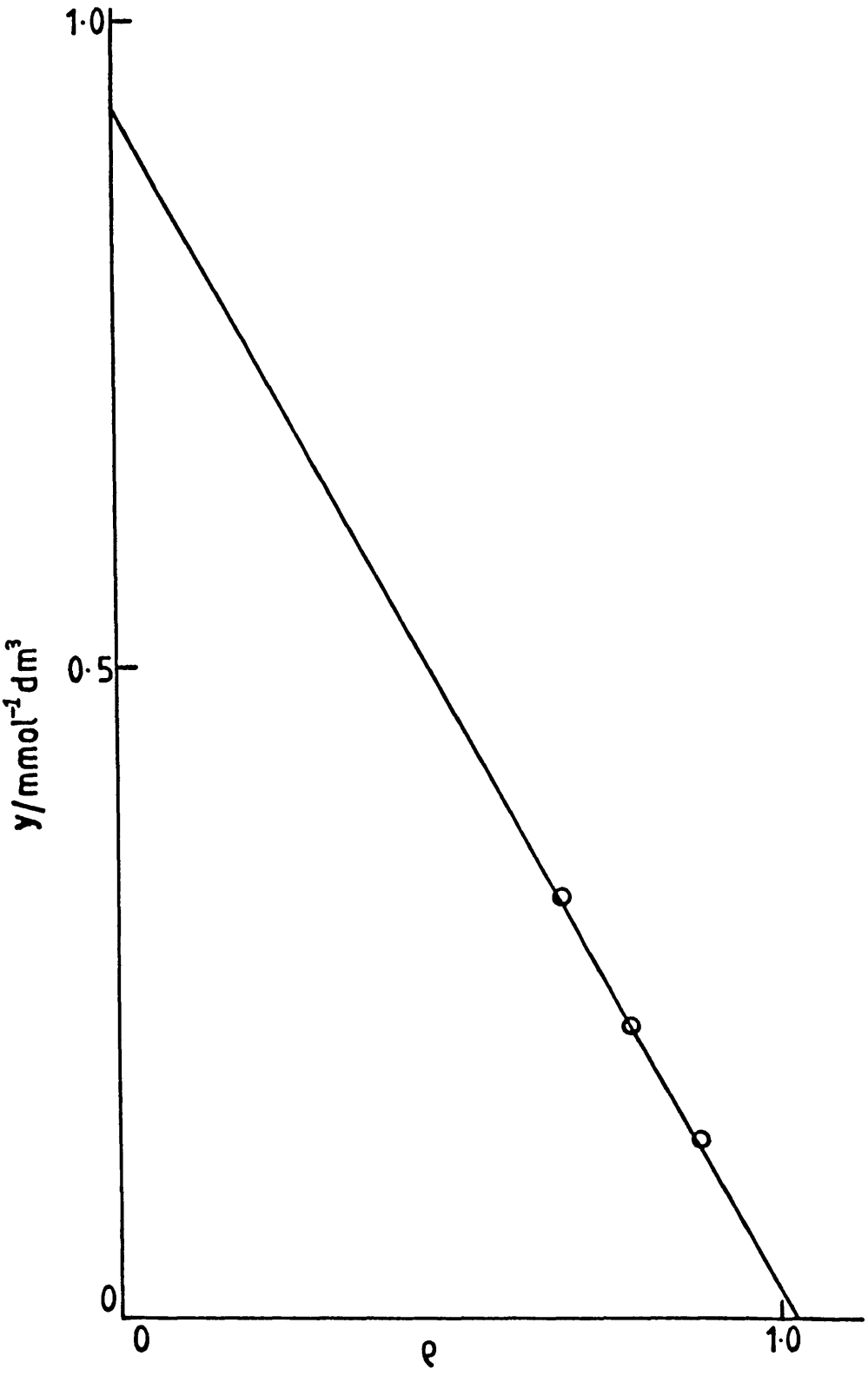

Figure 4.5.3: y versus ρ plot from the data in figure 4.5.2 for a TTF TCNQ/D-amino acid oxidase membrane electrode.

$$\frac{Lk_{cat}}{k'} = \frac{Lk_{cat}}{k'_{cat,E}} - 1$$

Because $Lk_{cat} >> k'_{cat,E}$ means that $Lk_{cat} >> k'$ and so the saturated response of the electrode is controlled by the rate of enzyme turnover on the electrode.

b) Adsorbed enzyme electrodes

A TTF TCNQ electrode left overnight in a solution containing 70 Units cm^{-3} of enzyme also gave a response to increasing concentrations of D-alanine. The current versus concentration and Hanes plots of these data are shown in figures 4.5.4 and 4.5.5 respectively. The intercept on the x-axis, $-K_M'$, is equal to -0.2 mmol dm^{-3} which compares with a literature value for the free enzyme of about 2 mmol dm^{-3} [101]. If it is assumed that the K_M and k_{cat} of the adsorbed enzyme are the same as for the free enzyme, then analysis in the same manner as before (for adsorbed glucose oxidase) gives that the electrochemical rate constant for the oxidation of adsorbed enzyme is approximately 1 s^{-1}. The maximum current obtained was approximately 60 nA giving a value for the electrode area, assuming monolayer coverage of enzyme, of about 0.1 cm^2. The geometric area of the electrode is approximately 0.03 cm^2, but because of the roughness of the surface the actual surface area is somewhere between 50 to 100 times this value (the surface roughness of the electrode is discussed in more detail in chapter 5). This indicates that the surface

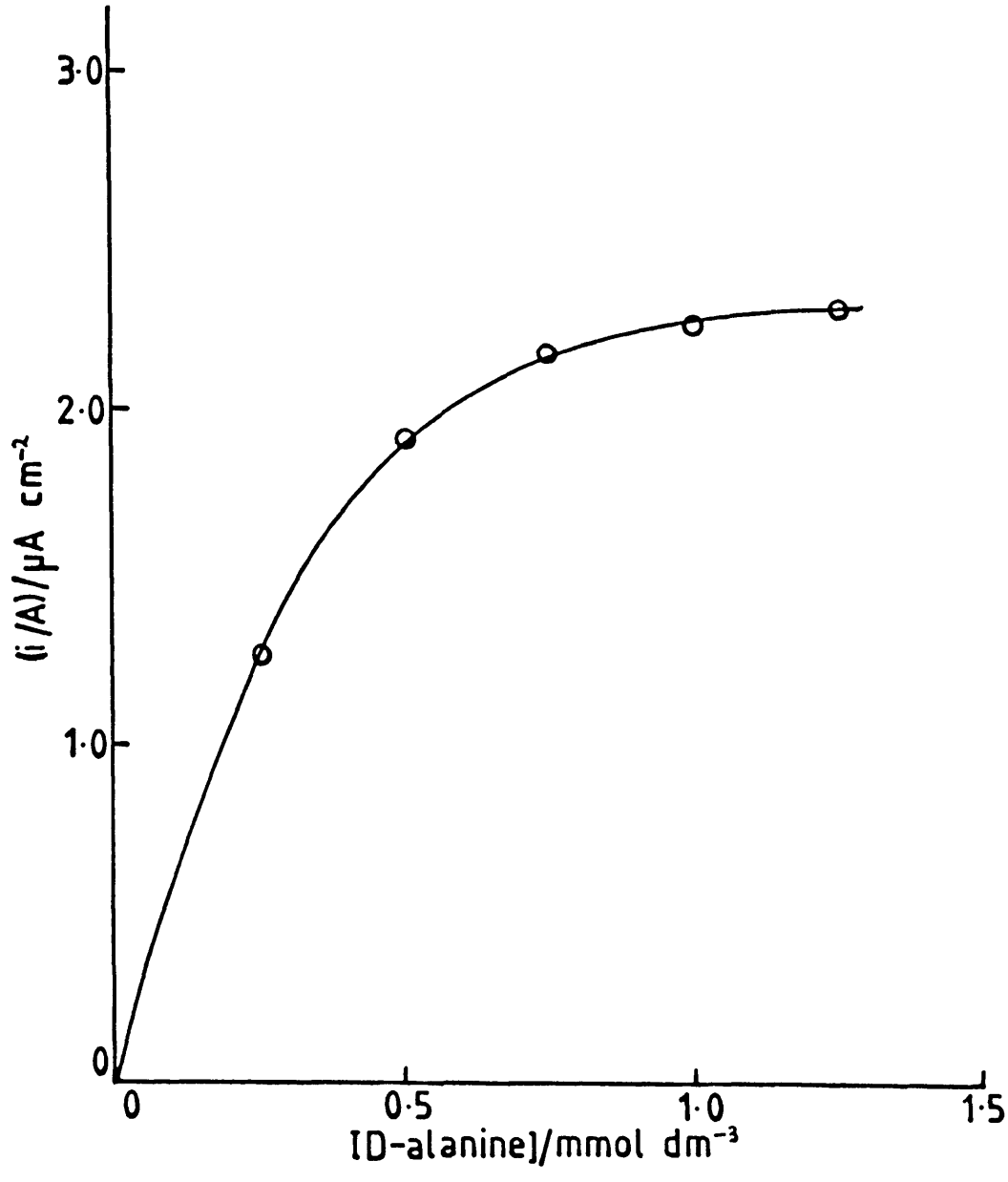

Figure 4 5.4: Current response of a TTF TCNQ/D-amino acid oxidase adsorbed enzyme electrode to increasing concentrations of D-alanine.

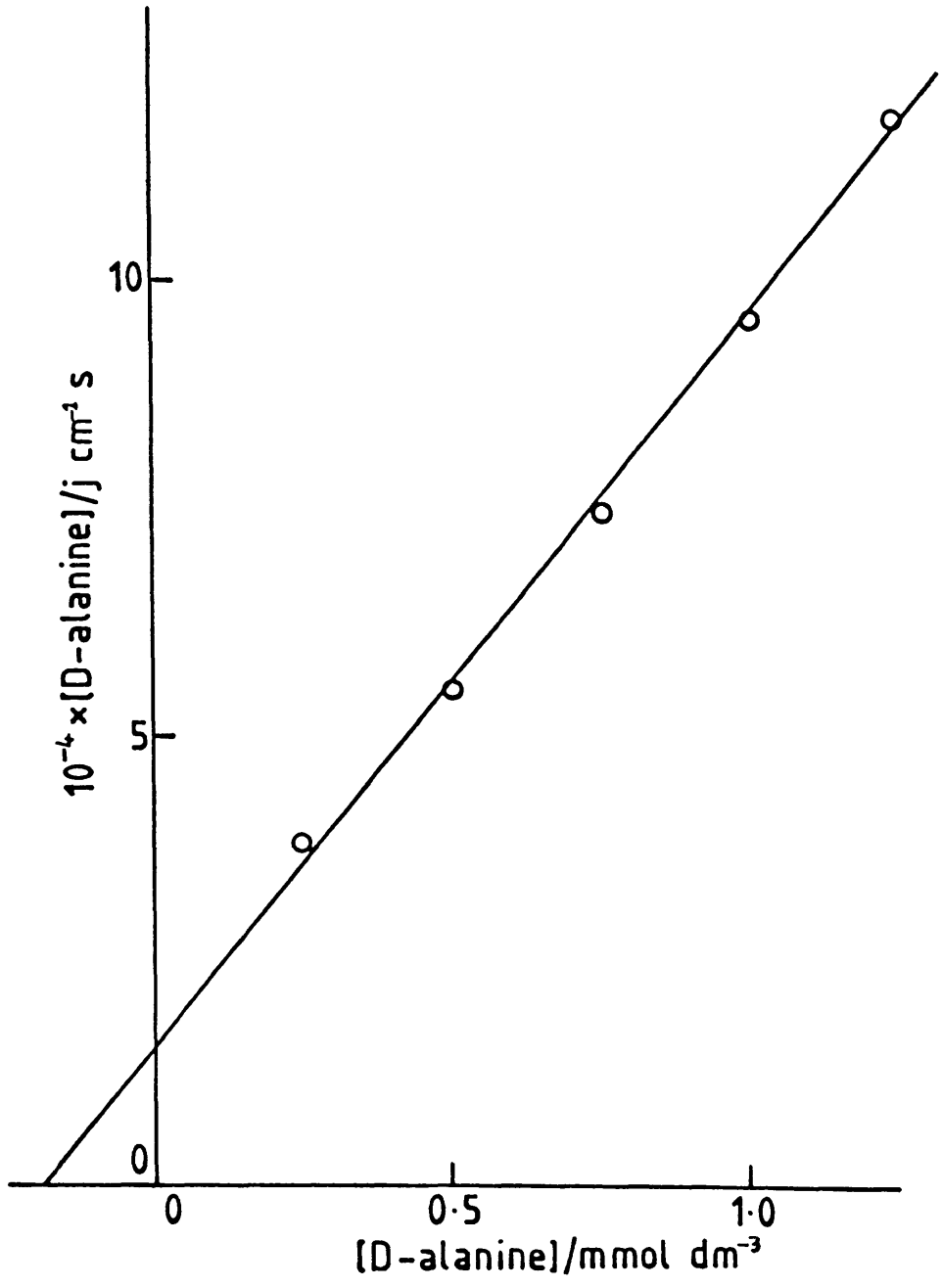

Figure 4.5.5: Hanes plot of the data in figure 4.5.4 for a TTF TCNQ/D-amino acid oxidase adsorbed enzyme electrode.

coverage of the electrode by the enzyme is less than a monolayer. This is what would be expected, as greater currents are obtained using membrane electrodes than with the adsorbed enzyme electrodes.

4.5.2 L-Amino Acid Oxidase

a) Membrane electrodes

An increase in current was observed using an L-amino acid oxidase/TTF TCNQ membrane electrode (the concentration of enzyme behind the membrane was 11 Units cm^{-3}) on addition of L-phenylalanine. Plots of current versus concentration, Hanes and y versus ϱ plots (equation (3.25)) for the data obtained are shown in figures 4.5.6, 4.5.7 and 4.5.8 respectively. Again the Hanes plot shows a horizontal section at low substrate concentrations with an intercept on the y-axis of 3.4×10^{4} cm^{-1} s, giving a value of k'_{ME} of 2.9×10^{-5} cm s^{-1}. The y versus ϱ plot is linear with an x-axis intercept of 1. This implies that under unsaturated conditions the response of the electrode is controlled by the transport properties of L-phenylalanine in the membrane with $k'_{ME} \approx k'_{s}$. From the intercept on the y-axis a value for K_{ME} of 2.6 mmol dm^{-3} is obtained. The concentration of enzyme, e_{Σ}, is given by the number of units of enzyme per cm^{-3} divided by k_{cat}. Rearrangement of equation (3.23) gives:-

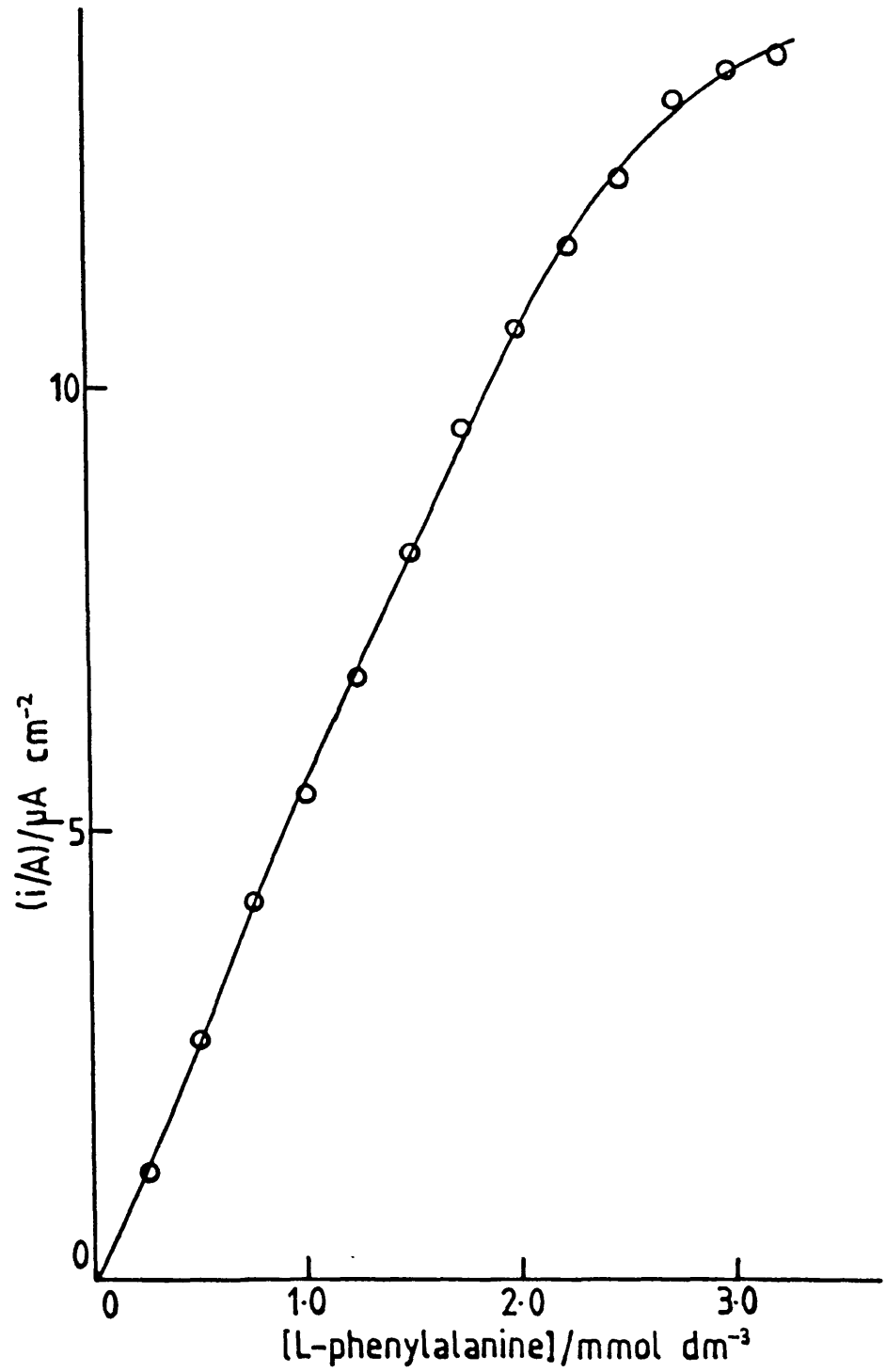

Figure 4.5.6: Current response of a TTF TCNQ/L-amino acid oxidase membrane electrode with increasing concentrations of L-phenylalanine.

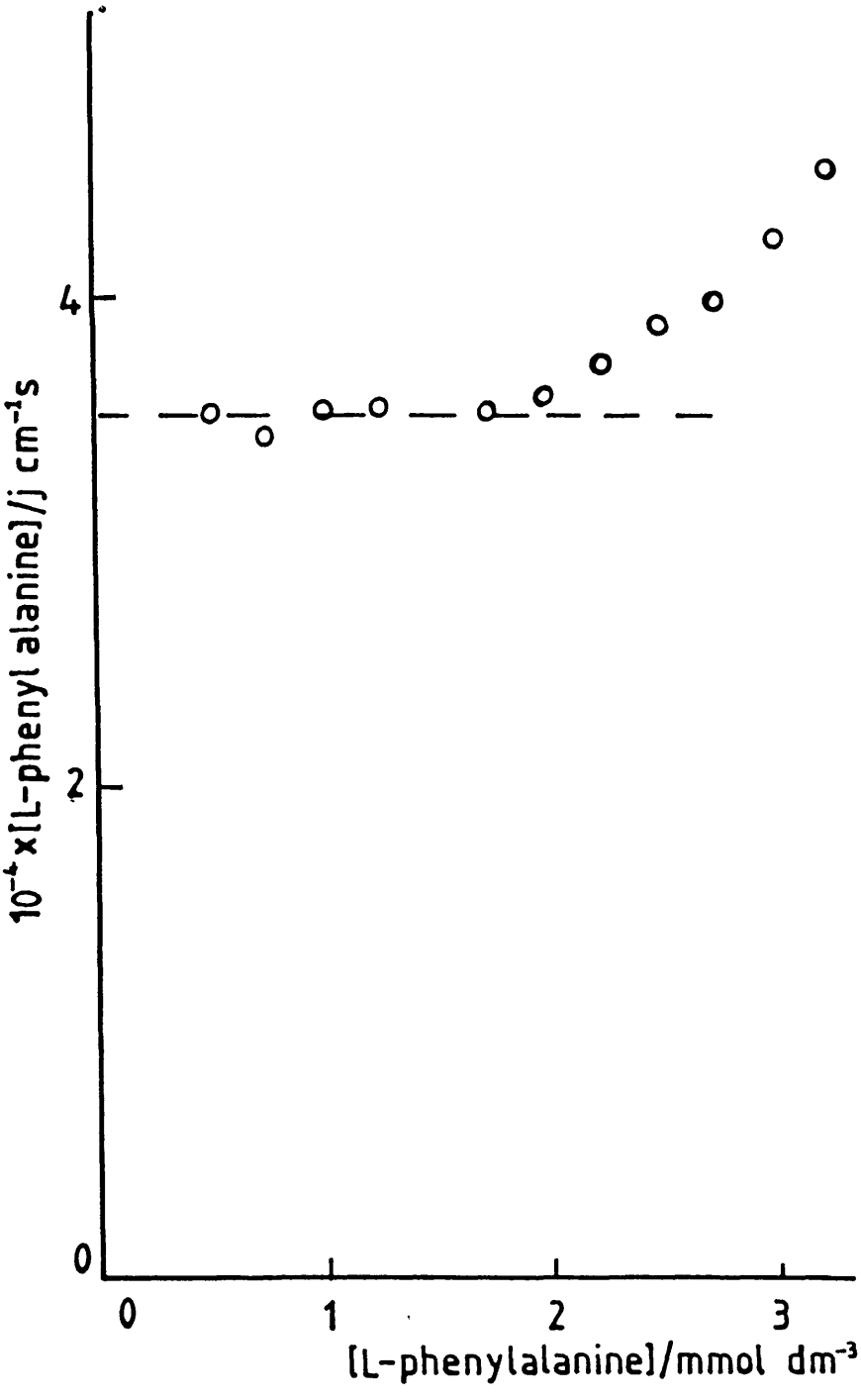

Figure 4 5.7: Hanes plot of the data in figure 4.5.6 for a TTF TCNQ/L-amino acid oxidase membrane electrode.

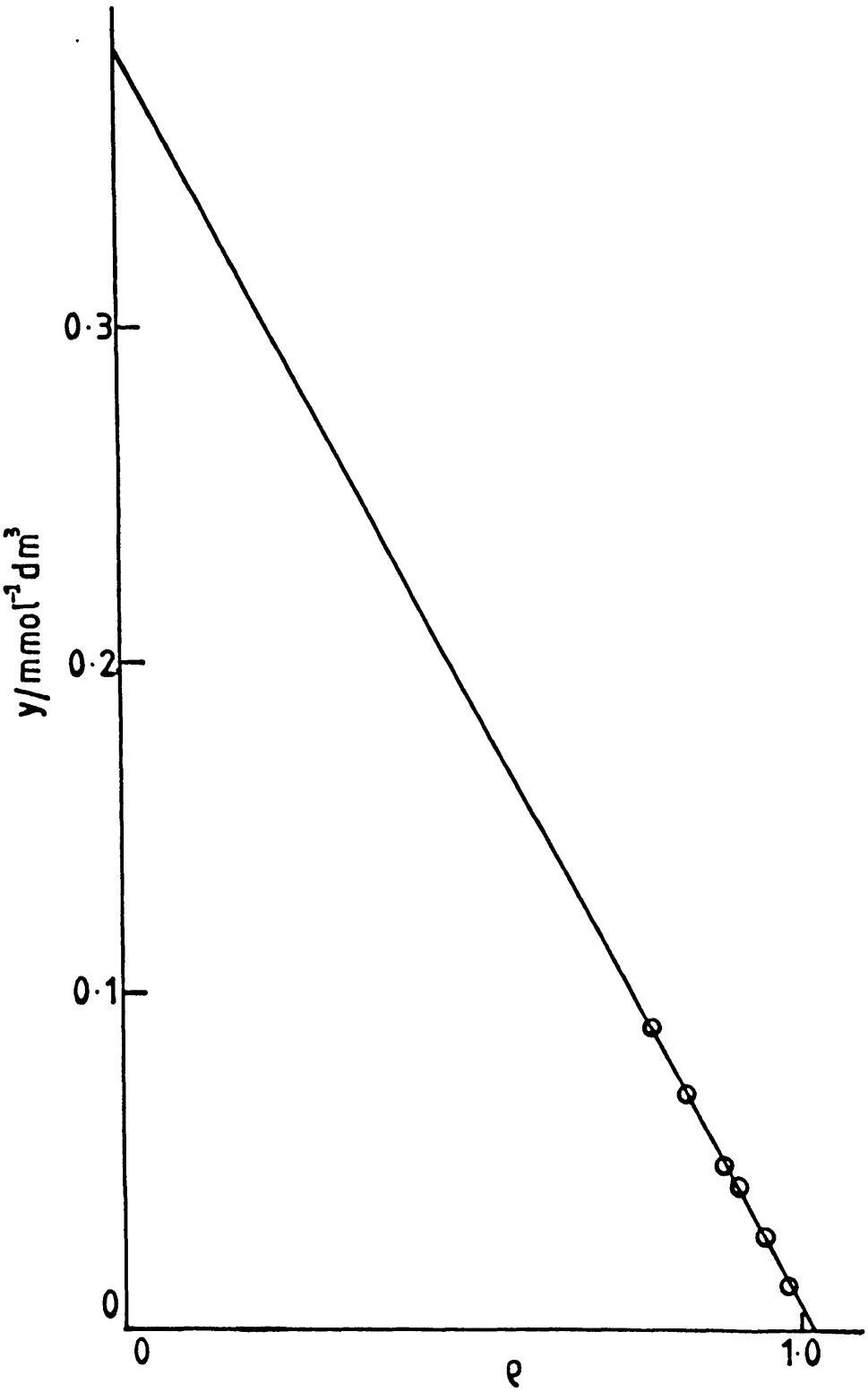

Figure 4.5.8: y versus ρ plot from the data in figure 4.5.7 for a TTF TCNQ/L-amino acid oxidase membrane electrode.

$$\frac{k_{cat}}{k'_{cat,E}} = \frac{\text{units per cm-3}}{K_{ME}k'_{ME}}$$

This leads to a value of $k_{cat}/k'_{cat,E}$ of 2.4×10^{4} cm^{-1}. From equation (3.22)

$$\frac{k_{cat}}{k'_{cat,E}} = \frac{1}{L} + \frac{k_{cat}}{k'} \qquad (4.6)$$

Since L is several tens of microns then $1/L < 10^{3}$ cm^{-1} << $k_{cat}/k'_{cat,E}$, and hence from (4.6) $k'_{cat,E} \approx k'$. It can therefore be concluded that the saturated response of the device is controlled by the rate of enzyme turnover on the electrode.

b) Adsorbed enzyme electrodes

Figures 4.5.9 and 4.5.10 show the current versus concentration and Hanes plots respectively for an L-amino acid oxidase adsorbed enzyme TTF TCNQ electrode, using L-phenylalanine as the substrate. The intercept on the x-axis gives a value for K_M, of 3.6×10^{-4} mol dm^{-3}. Unfortunately no literature value of K_M is available for comparison.

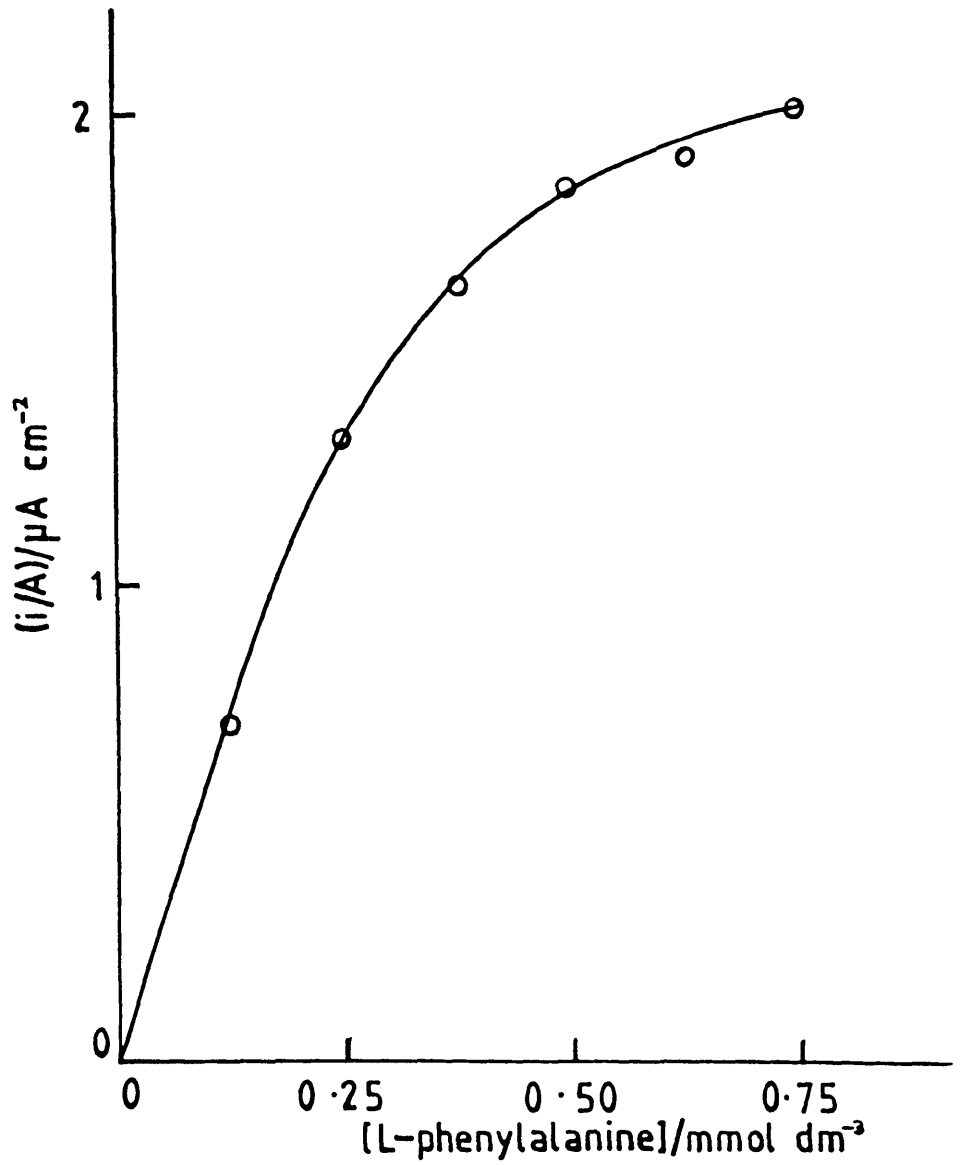

Figure 4.5.9: Current response of a TTF TCNQ/L-amino acid oxidase adsorbed enzyme electrode to increasing concentrations of L-phenylalanine.

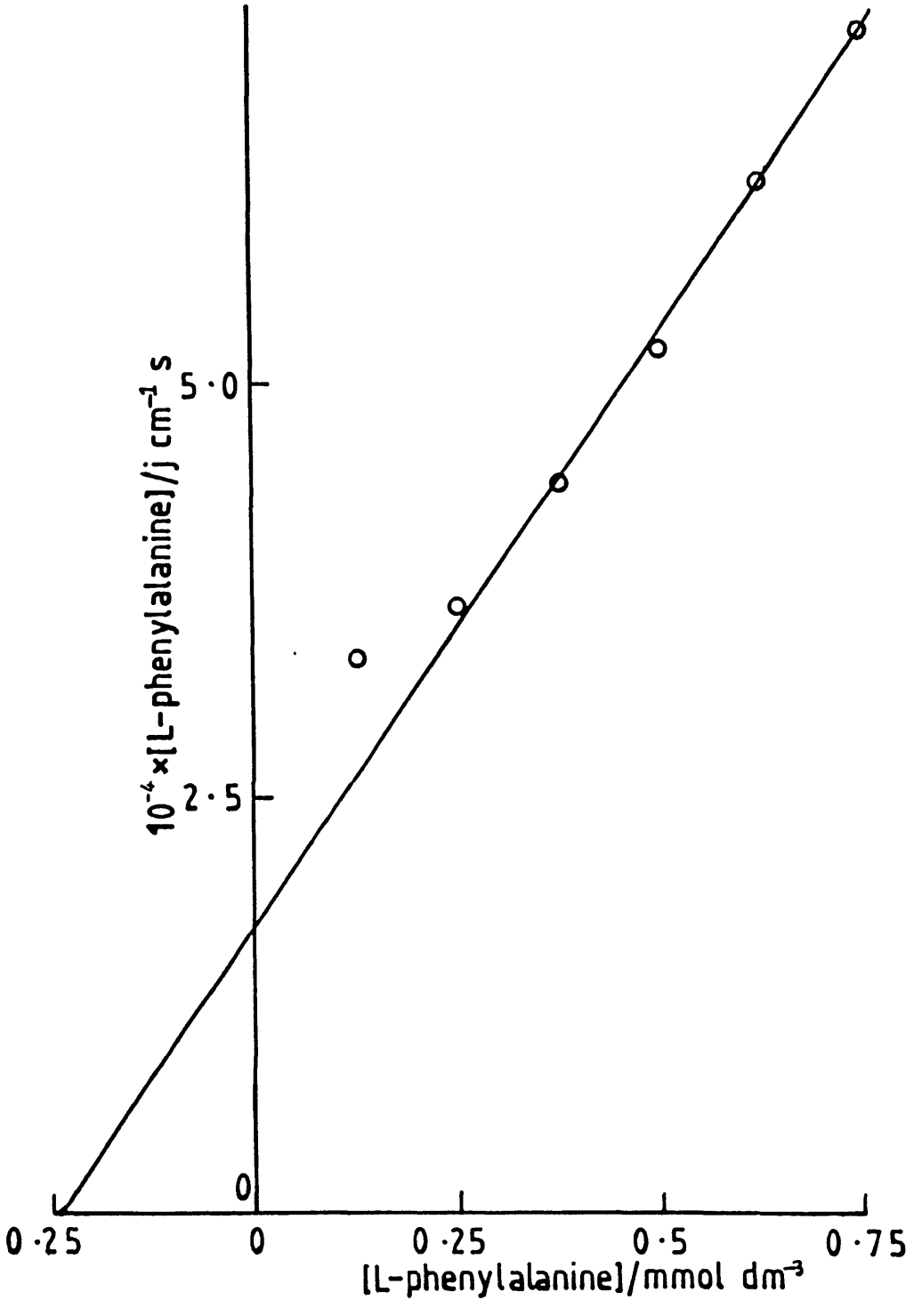

Figure 4.5.10: Hanes plot of the data in figure 4.5.9 for a TTF TCNQ/L-amino acid oxidase adsorbed enzyme electrode.

4.5.3 Xanthine Oxidase

a) Membrane electrodes

Figure 4.5.11 shows the current response obtained using a xanthine oxidase/TTF TCNQ membrane electrode (with an enzyme concentration equal to 30 Units cm^{-3}) with increasing concentration of xanthine. The Hanes plot of these data is shown in figure 4.5.12. Again a horizontal section is observed at low substrate concentrations with the intercept on the y-axis giving a value of k'_{ME} of 1.2×10^{-4} cm s^{-1}. The y versus ρ plot of the data is shown in figure 4.5.13. The intercept on the x-axis is equal to 1, which means that at low concentrations of xanthine, the response of the device is controlled by the transport kinetics of the substrate in the membrane, and hence $k'_{ME} \approx k'_s$. The intercept on the y-axis is equal to 6 $mmol^{-1}$ dm^3 which gives a value of K_{ME} of 0.17 mmol dm^{-3}. Taking k_{cat} for the enzyme substrate reaction as being 18 s^{-1} [102] a value for $k'_{cat,E}$ of 7.1×10^{-4} cm s^{-1} is obtained. This can be compared with the much larger value of Lk_{cat} of approximately 1.8×10^{-2} cm s^{-1} and hence it can again be concluded, as in the case of the amino acid oxidases, that the saturated response of the electrode is controlled by the rate of enzyme turnover on the electrode.

b) Adsorbed enzyme electrodes

Adsorbed xanthine oxidase/TTF TCNQ electrodes also show a small response to increasing concentrations of xanthine, indicating that electron transfer does occur between

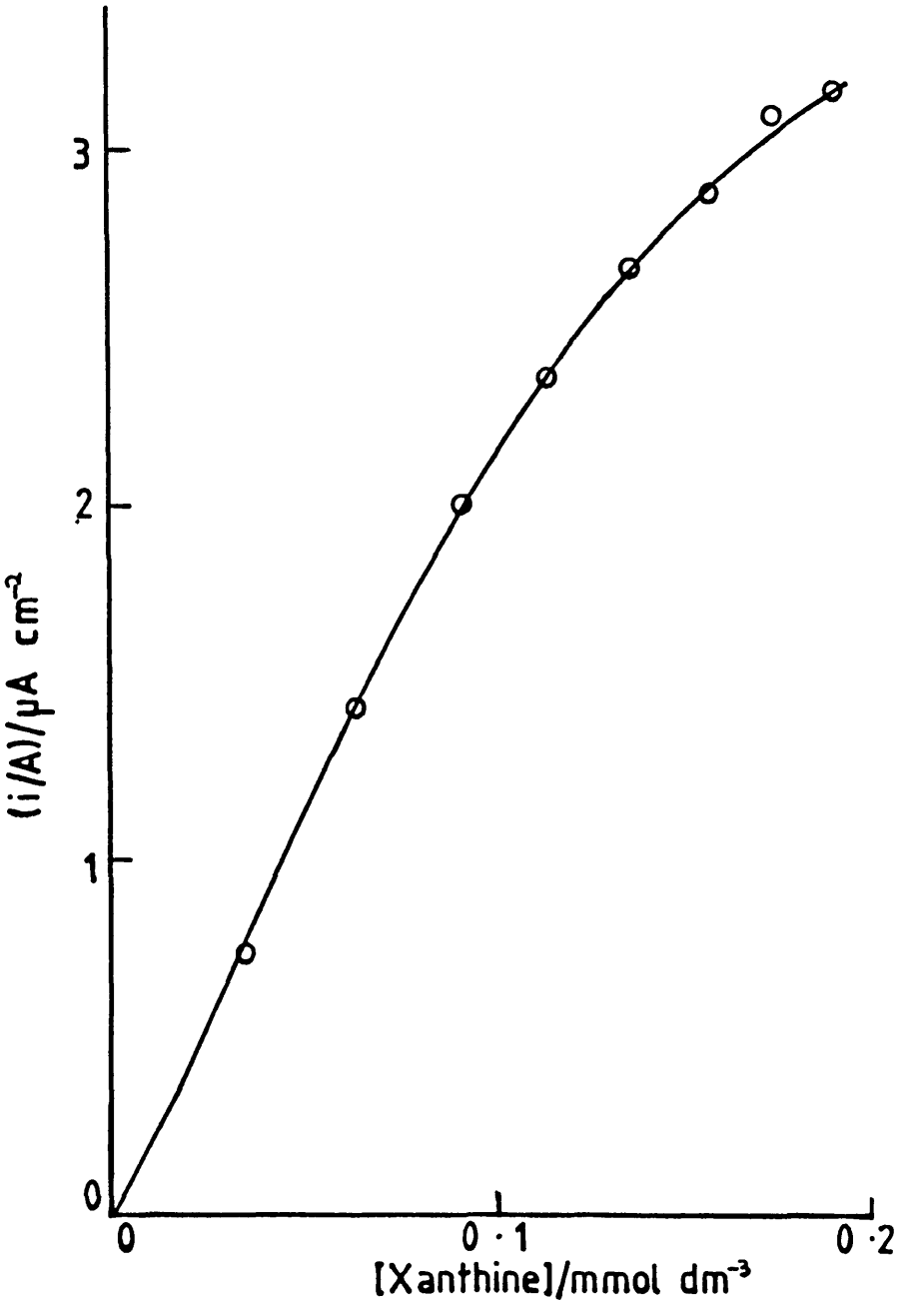

Figure 4.5.11: Current response of a TTF TCNQ/xanthine oxidase membrane electrode to increasing concentrations of xanthine.

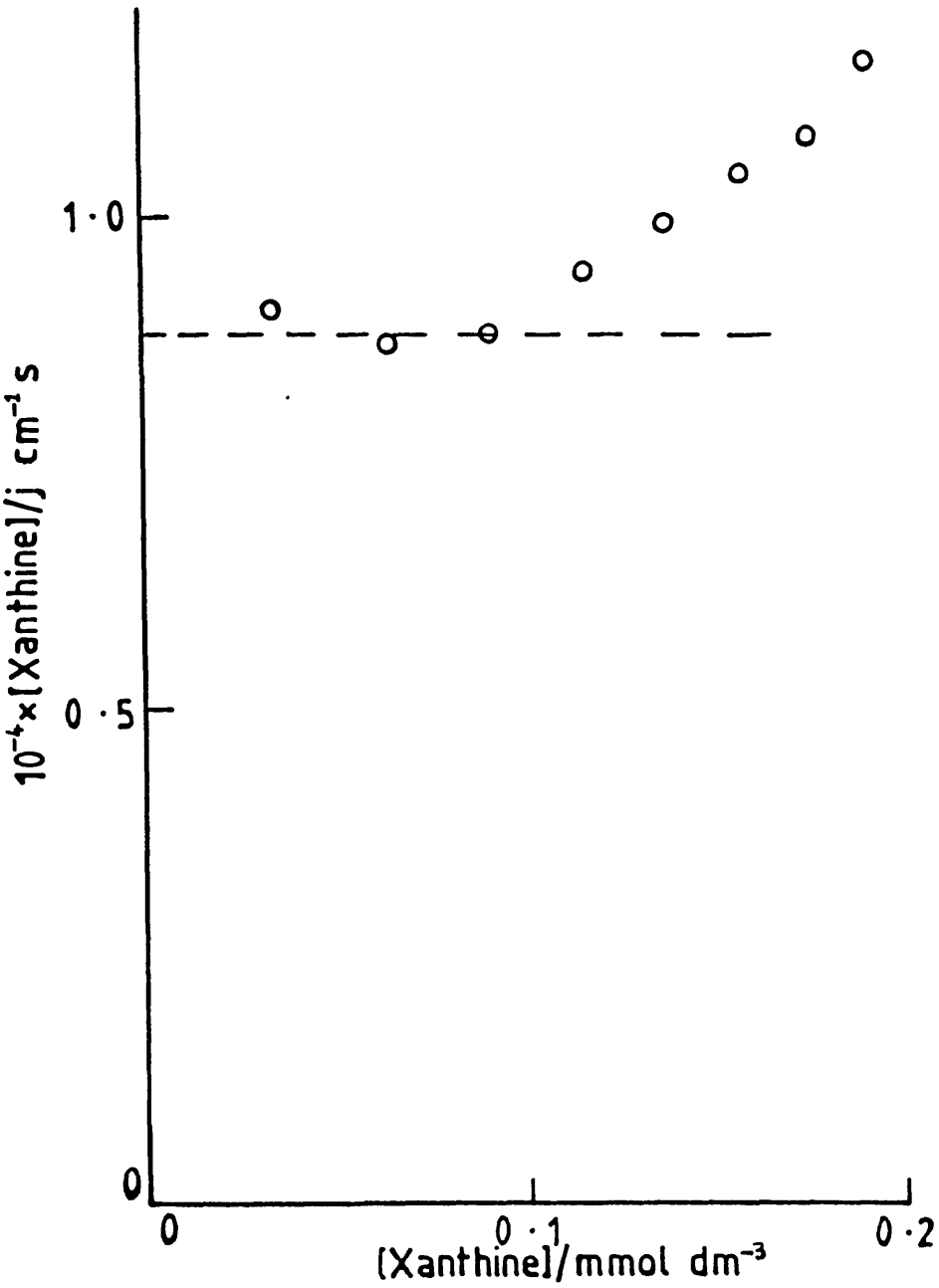

Figure 4.5.12: Hanes plot of the data in figure 4.5.11 for a TTF TCNQ/xanthine oxidase membrane electrode.

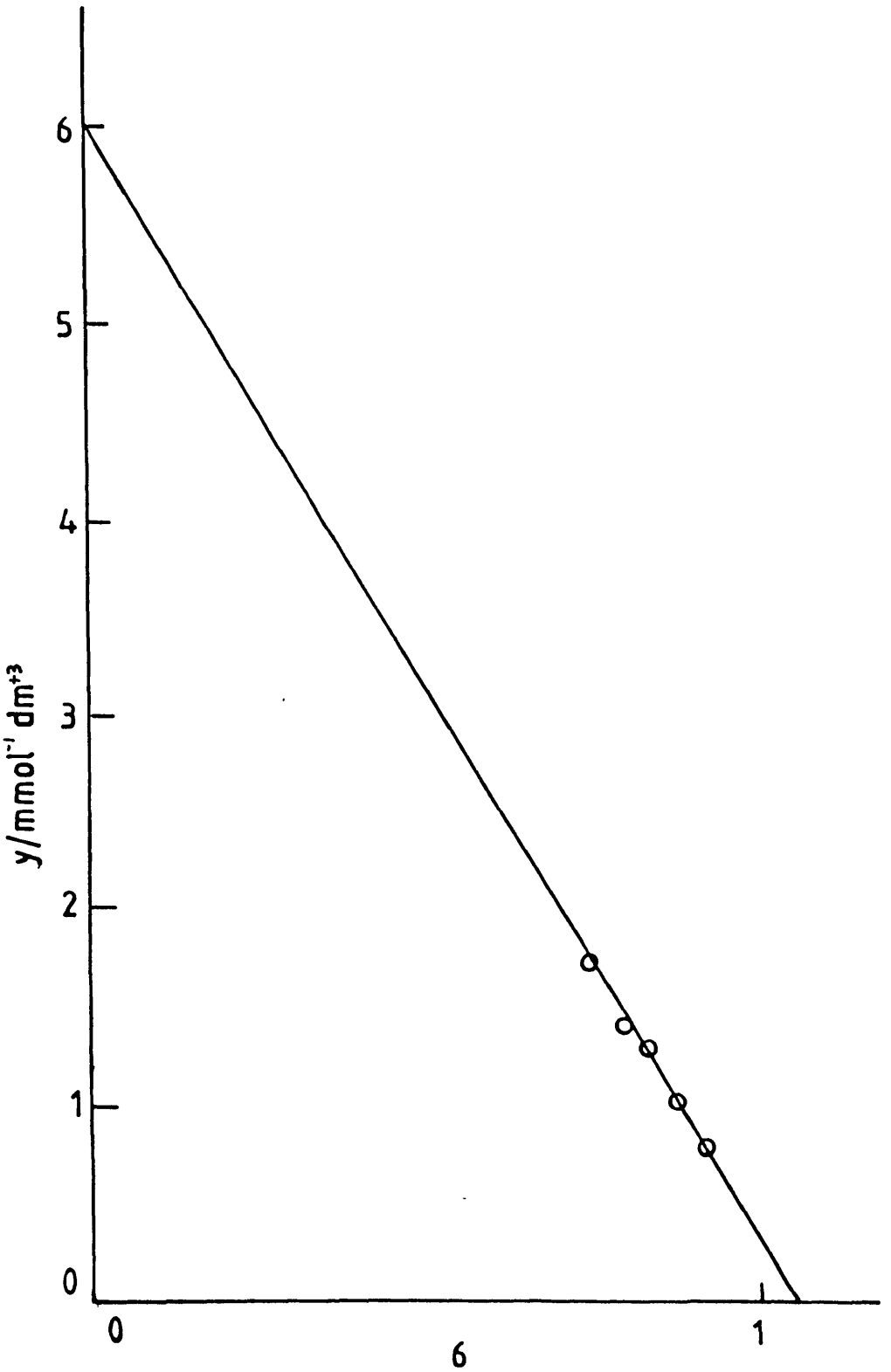

Figure 4.5 13: y versus ϱ plot from the data in figure 4.5.12 for a TTF TCNQ/xanthine oxidase membrane electrode.

adsorbed enzyme and the electrode. Analysis of this data proved difficult due to the small currents obtained.

4.6 Conclusions

The results show that all of the conducting salts tested so far show some electrocatalytic activity for the oxidation of glucose oxidase. The best materials, as far as stability and magnitude of the background current is concerned, are the TCNQ salts of TTF, NMP and Q. TTF TCNQ has also been used successfully as an electrode material for the oxidation of the flavoenzymes D-amino acid oxidase, L-amino acid oxidase and xanthine oxidase.

Results obtained for the four enzymes using TTF TCNQ membrane electrodes have been analysed by the method described in chapter 3. For each of the enzymes the rate limiting step controlling the response of the device under unsaturated conditions is the diffusion of substrate through the membrane. This is the most desirable condition for a reliable sensor, since the enzyme and electrochemical kinetics do not affect the response of the sensor. As long as this condition is maintained any decay in the enzyme or electrode has no effect on the response of the device. The values of the rate constant for the transport of substrate through the membrane (Gallenkamp), k'_s, for each of the enzyme electrodes are summarised in table 4.4. The difference in k'_s values for the four enzymes is a function

TABLE 4.4

Rate Constants for TTF TCNQ Membrane electrodes

	k'_S/cm s^{-1}	K_{ME}/mmol dm^{-3}	k'/cm s^{-1}
Glucose Oxidase	4.7×10^{-5}	20	9.0×10^{-2}
D-Amino Acid Oxidase	2.6×10^{-5}	1.1	2.4×10^{-4}
L-Amino Acid Oxidase	2.8×10^{-5}	2.6	4.6×10^{-2}
Xanthine Oxidase	1.1×10^{-4}	0.2	3.7×10^{-4}

of the difference in the diffusion and partition coefficients of the enzyme substrates in the membrane.

The saturated response of each of the different enzyme electrodes is controlled by the rate of enzyme turnover on the electrode as described by the rate constant k'. Table 4.4 summarises the values of k' for each of the different enzyme electrodes. All of these electrochemical rate constants are greater than 10^{-4} cm s^{-1} indicating that TTF TCNQ is an effective electrocatalyst for the oxidation of these four flavoenzyme oxidases.

The stability of the glucose oxidase electrode is excellent. A membrane electrode was run continuously for 28 days. At the end of this period the sensor had lost 42% of its original activity under unsaturated conditions, but gave the same saturated response. Kinetic analysis showed that transport of the substrate through the membrane was still the rate limiting step under unsaturated conditions, and so the loss of activity must be caused by a deterioration of the membrane.

The enzymes mentioned above can be adsorbed irreversibly onto the surface of TTF TCNQ electrodes. The adsorbed enzymes can also undergo electron transfer with the electrode, so allowing the measurement of substrate concentration without the need for a membrane.

CHAPTER 5

THE OPTIMISATION AND MECHANISM OF THE ELECTROCHEMICAL OXIDATION OF GLUCOSE OXIDASE ON CONDUCTING SALT ELECTRODES

In the previous chapter a device for the electrochemical monitoring of glucose levels, which involves the use of electrodes made from conducting organic salts in conjunction with the enzyme glucose oxidase was described. This device consists of a solution of the enzyme trapped on the surface of the conducting salt electrode using a membrane, and is based on the electrochemical oxidation of the reduced enzyme. Analysis of the current obtained at different concentrations of glucose has identified the rate limiting steps which control the overall response of the device. Under unsaturated conditions this is found to be the rate of transport of glucose through the membrane, and for saturated conditions it is the electrochemical reaction which is rate limiting. This chapter begins with a description of the electrode reaction, its potential dependence and new methods of electrode fabrication. The overall aim of the analysis is the improvement of the consistency and magnitude of the electrode response. Lastly, the mechanism for the electron transfer between the enzyme and the electrode is discussed.

5.1 Electrode Fabrication

5.1.1 Other Electrode Binders

The membrane electrodes described in the last chapter were all constructed using cavity electrodes. These electrodes are made using a slurry of the organic salt and polyvinyl chloride (PVC) in tetrahydrofuran (THF), as described in chapter 2. The PVC is added to act as a binder, thus providing greater mechanical stability. Attempts to pack these electrodes without the use of a binder proved to be impossible because of poor cohesion between separate crystallites of the salt. Polystyrene was also found to be an effective binder for these electrodes. In this case electrodes are constructed using a thick slurry, made by mixing the conducting salt with a solution of dichloromethane containing dissolved polystyrene, with the ratio of salt to binder being 9:1 w/w. This slurry is then packed into a cavity electrode in the same manner as with the PVC/THF mixture.

Glucose oxidase membrane electrodes constructed using TTF TCNQ polystyrene packed cavity electrodes give increased currents in the presence of glucose. Figure 5.1.1 shows the current versus concentration plots of the data obtained using one of these electrodes, with a Spectrapor 2 membrane and an enzyme solution of 813 Units cm^{-3}. The electrode potential was maintained at +50 mV. These results were analysed by the procedure described in chapter 3. The Hanes

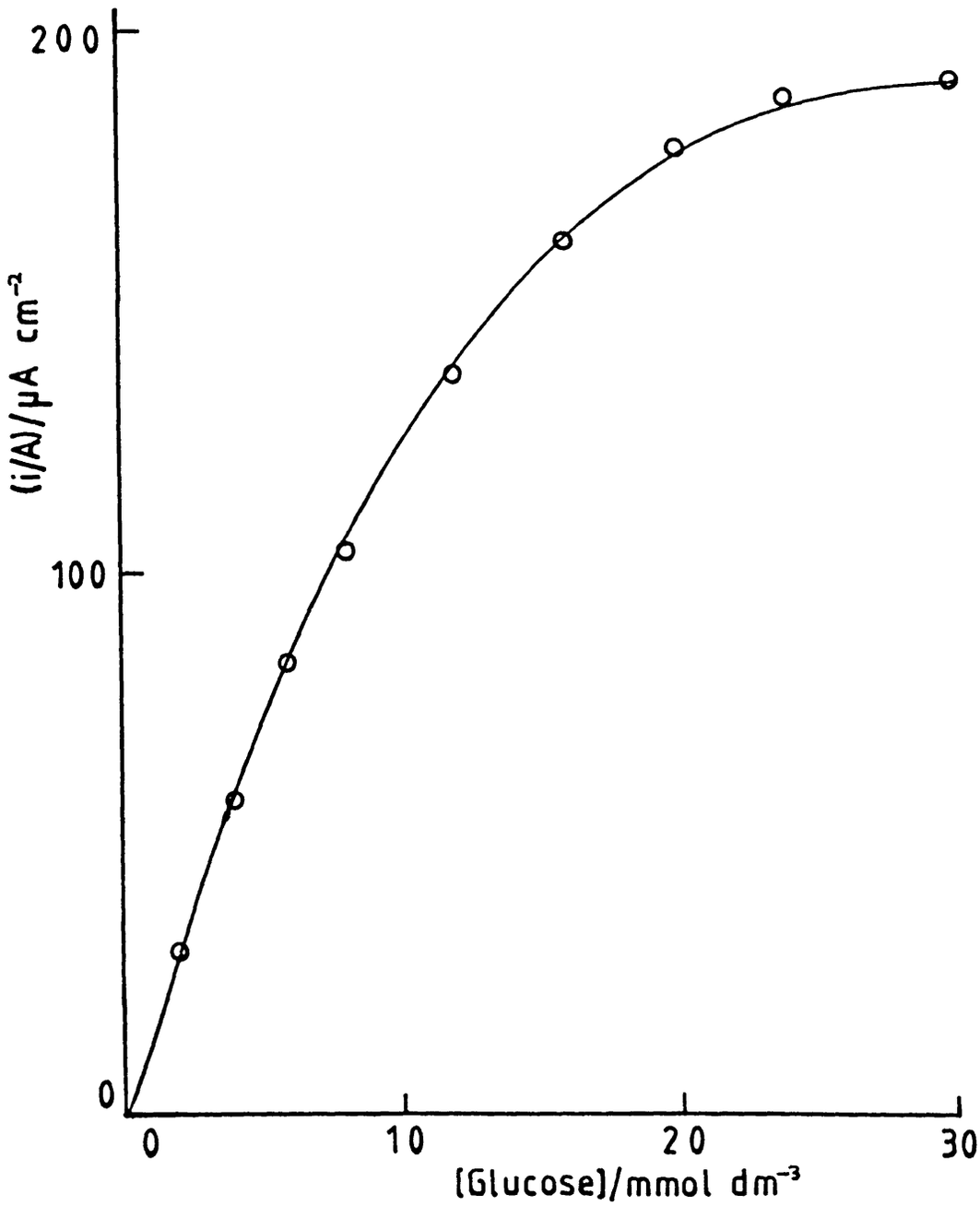

Figure 5.1.1: Plot of the current density versus concentration of glucose for a TTF TCNQ/glucose oxidase membrane electrode. The TTF TCNQ electrode was constructed using polystyrene as a binder.

plot (equation 3.19) and the y versus ϱ plot (equation 3.25) are shown in figures 5.1.2 and 5.1.3 respectively. The intercept on the y-axis of the Hanes plot is equal to 1.3×10^{4} cm^{-1} s which gives a value for k'_{ME} of 7.8×10^{-5} cm s^{-1}. The intecept on the x-axis of the y versus ϱ plot is close to unity which shows that $k'_{ME} \approx k'_{s}$, and hence the the rate limiting step controlling the response of the electrode under unsaturated conditions is the transport of glucose through the membrane. The intercept on the y-axis of this plot gives a value of K_{ME} of 14 mmol dm^{-3}, which using equation (3.23) gives the saturated rate constant for the electrode, $k'_{cat,E}$, as 6.4×10^{-2} cm s^{-1}. By the same argument as was used in 4.3.1, this is interpreted as being equal to the electrochemical rate constant, k'. These values of k'_{s} and k' can be compared with the values obtained using TTF TCNQ/PVC electrodes of 5.9×10^{-5} cm s^{-1} and 2.6×10^{-2} cm s^{-1} respectively. The k'_{s} values are slightly different which is not surprising, since in the above experiment Spectrapor 2 membranes were used, whereas previous results were obtained using Gallenkamp membranes. The electrochemical rate constants also differ, but are of the same order of magnitude thus showing that the response of these electrodes is not greatly affected by the choice of binder.

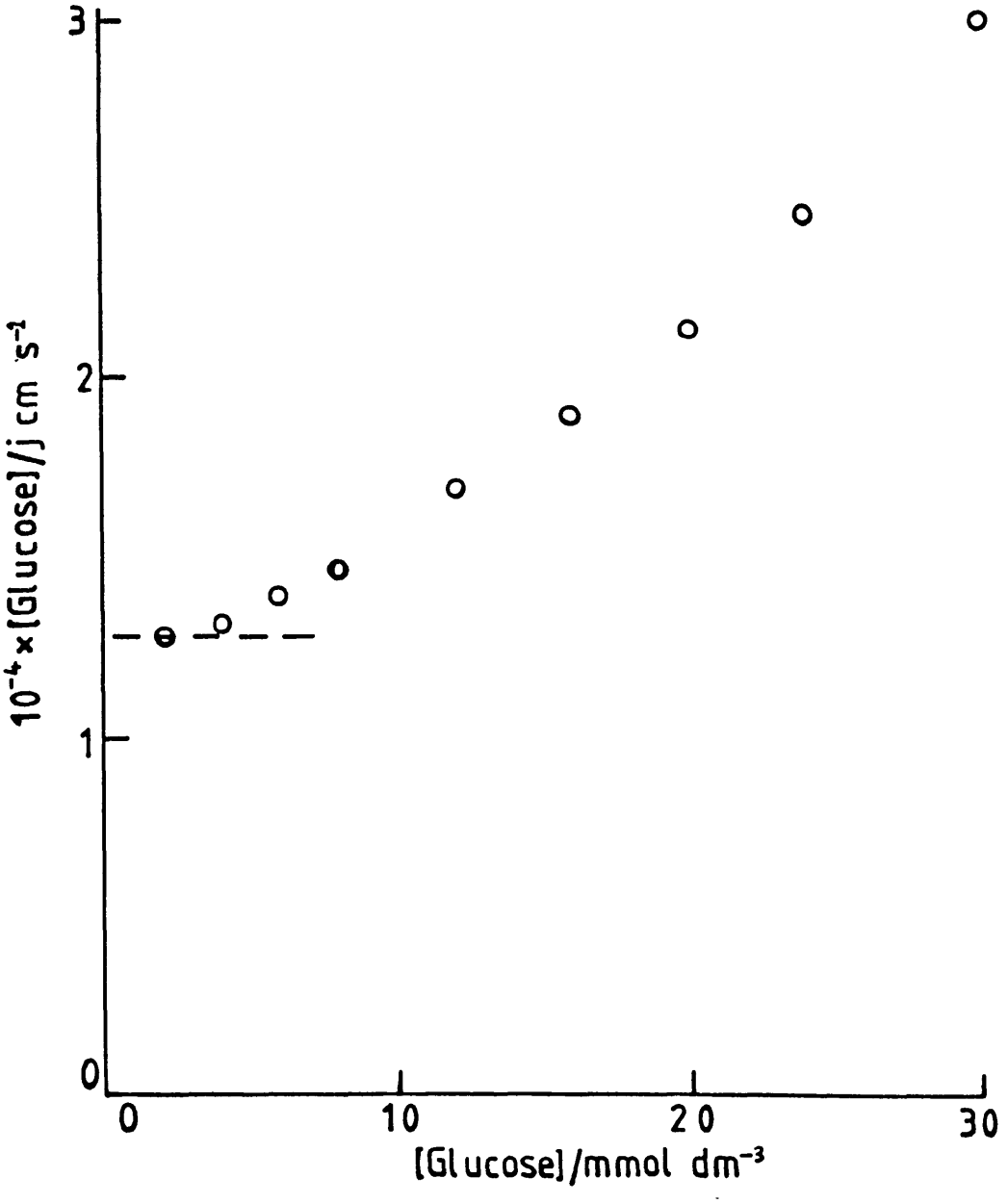

Figure 5.1.2: Hanes plot of the data in figure 5.1.1 for a TTF TCNQ/glucose oxidase membrane electrode. The TTF TCNQ electrode was constructed using polystyrene as a binder.

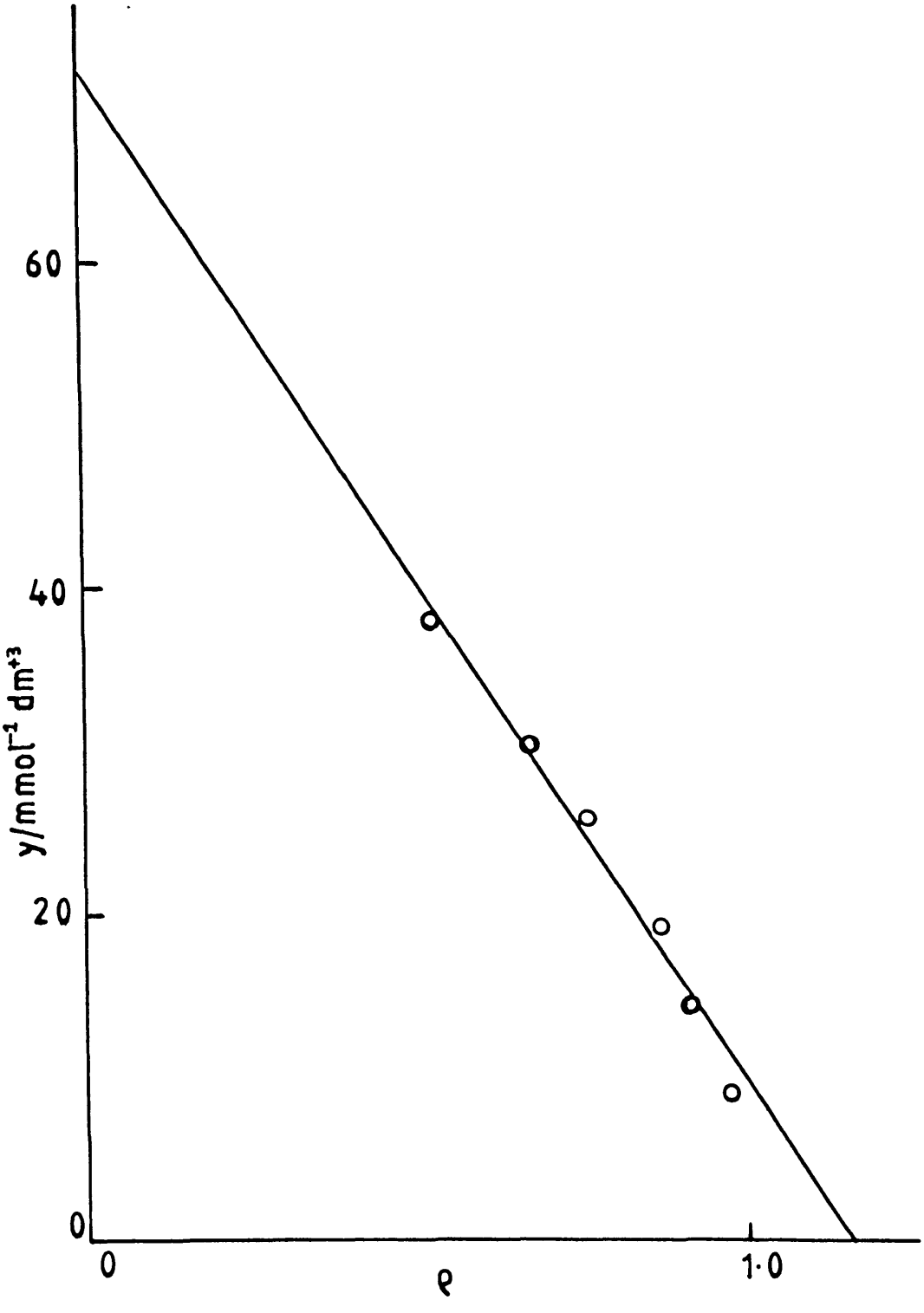

Figure 5.1.3: y versus ϱ plot from the data in figure 5.1.2 for a TTF TCNQ/glucose oxidase membrane electrode. The TTF TCNQ electrode was constructed using polystyrene as a binder.

5.1.2 Electrochemical Coating

In chapter 4 analysis of the saturated response of glucose oxidase/TTF TCNQ membrane electrodes, gave an electrochemical rate constant for the oxidation of the enzyme (at an electrode potential of +50 mV) of between 10^{-2} and 10^{-1} cm s^{-1}. These electrochemical rate constants were calculated using the geometric area of the electrodes, which because of their nature (i.e. rough and porous surface) is much less than the surface area. A far more accurate value of this rate constant can be obtained using pressed pellet electrodes, where the geometric and surface areas are the same. A TTF TCNQ pressed pellet electrode of area 0.2 cm^2 held at a potential of +50 mV, in a solution containing 787 Units cm^{-3} of glucose oxidase, gave a saturation current on addition of excess glucose of 1 μA. This gives an electrochemical rate constant of 1.6×10^{-3} cm s^{-1}, which suggests that the surface roughness of cavity electrodes leads to an increase in the surface area by a factor of about 10-100. Examination of the cavity electrodes under a scanning electron microscope did indeed show the surface to be highly porous [103].

One of the problems associated with using these packed cavity electrodes is that the surface area can vary considerably between different electrodes because of the random way in which they are constructed. For example it was found that the surface areas of electrodes made from a conducting salt/PVC slurry varied depending on whether or

not the THF contained a small amount of water. With water present the surface area of the electrode was larger and hence the saturation current obtained was greater than with electrodes constructed with no water in the THF. To obtain a more defined surface area a better approach would be to coat electrochemically the conducting salt on to a standard electrode substrate, such as glassy carbon or a noble metal. If it is possible to coat electrochemically a rough electrode of known surface area, then the resulting conducting salt modified electrode could be used to construct membrane electrodes, which would give a large and consistent saturated response. Furthermore if the response of this electrode began to deteriorate then the coat could easily be removed, and replaced with a new one with an identical surface area.

Wheland and Gillison have shown that it is possible to grow crystals of TTF TCNQ electrochemically [79]. This was achieved by passing a constant current through an acetonitrile solution saturated in TTF TCNQ and N-methylquinolinium TCNQ, containing 0.06 mol dm^{-3} TTF. This section describes attempts to coat electrochemically glassy carbon electrodes with TTF TCNQ.

a) Electrochemistry of $TCNQ^0$ and TTF^0 in acetonitrile

The cyclic voltammograms of TTF^0 and $TCNQ^0$ in acetonitrile containing 0.1 mol dm^{-3} lithium perchlorate are shown in Figures 5.1.4 & 5.1.5 respectively. These were obtained using a glassy carbon working electrode and a

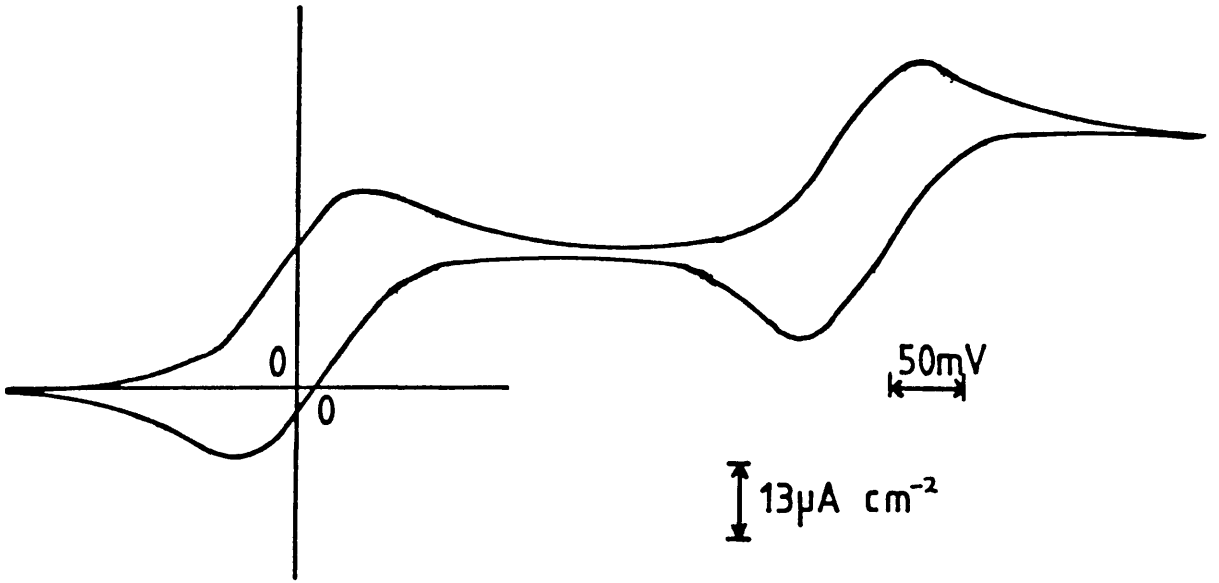

Figure 5.1.4: Cyclic voltammogram of TTF (1 mmol dm^{-3}) in acetonitrile with 0.1 mol dm^{-3} lithium perchlorate at a glassy carbon electrode versus Ag/Ag^{+}. The scan rate was 5 mV/s.

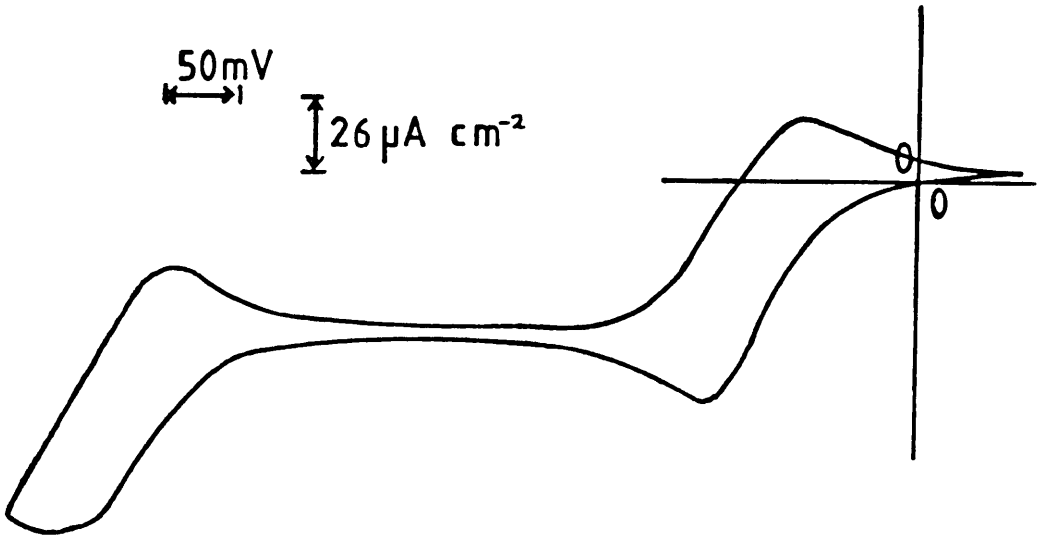

Figure 5.1.5: Cyclic voltammogram of TCNQ (1 mmol dm^{-3}) in acetonitrile with 0.1 mol dm^{-3} lithium perchlorate at a glassy carbon electrode versus Ag/Ag^{+}. The scan rate was 5 mV/s.

Ag/Ag^+ reference electrode. Consider first the cv of TTF. Two sets of peaks are observed corresponding to the TTF^0/TTF^+ and TTF^+/TTF^{2+} redox couples. The standard redox potentials, E^0, with respect to a Ag/Ag^+ reference electrode (as obtained from the cv) are as follows:-

$$TTF^+ + e^- \longrightarrow TTF^0 \qquad 2.5 \pm 5mV$$

$$TTF^{2+} + e^- \longrightarrow TTF^+ \qquad 375 \pm 5mV$$

The separation between the oxidation and reduction peaks are 85 mV and 75 mV for the TTF^+/TTF^0 and TTF^{2+}/TTF^+ redox couples respectively, which suggests that the electrode kinetics of both of these are quasi-reversible. Rotating disc [104] experiments carried out in the same solution gave Levich behaviour [105] up to a rotation speed of 25 Hz, with a diffusion coefficient for TTF^0 of 9.7×10^{-6} cm^2 s^{-1} being obtained. Two sets of peaks are also observed in the TCNQ cyclic voltammogram. These correspond to the $TCNQ^0/TCNQ^-$ and $TCNQ^-/TCNQ^{2-}$ redox couples. The standard redox potentials of these two processes with respect to a Ag/Ag^+ reference electrode are:-

$$TCNQ^0 + e^- \longrightarrow TCNQ^- \qquad -125 \pm 5 \text{ mV}$$

$$TCNQ^- + e^- \longrightarrow TCNQ^{-2} \qquad -530 \pm 5 \text{ mV}$$

For both of these pairs the peak separation is

approximately 80 mV, again suggesting that both couples are quasi-reversible on glassy carbon electrodes. Rotating disc experiments gave Levich behaviour from 1 to 25 Hz, with a diffusion coefficient for $TCNQ^0$ of 2.7×10^{-5} cm^2 s^{-1}.

b) Electrochemical deposition of TTF TCNQ

The electrochemical coating of an electrode with TTF TCNQ was conducted using a procedure similar to that used by Wheland. This involved forcing an oxidation current through a glassy carbon electrode, which was immersed in an acetonitrile solution containing TTF^0 and $TCNQ^-$. The work of Melby and coworkers [65] suggested that the simple 1:1 TCNQ salt of triethylammonium (TEA^+TCNQ^-), would be suitable to use as a background electrolyte and source of $TCNQ^-$. This was supported by solubility measurements using a conductivity meter, which showed that this salt is soluble up to 30 mmol dm^{-3}.

An acetonitrile solution saturated in TEA^+TCNQ^- and containing 10 mmol dm^{-3} was prepared. Into this solution was placed a glassy carbon electrode and a platinum counter electrode. A current density of 52 µA cm^{-2} was passed between these two electrodes for a period of two hours using a galvanostat [94]. The current was passed in such a direction that an oxidation reaction occurred at the glassy carbon electrode. The solution was deoxygenated over the coating period and the glassy carbon electrode rotated at

0.5 Hz to ensure an adequate supply of both TTF^0 and $TCNQ^-$ to the surface. During the experiment the potential of the working electrode was monitored using a Ag/Ag^+ reference electrode. The potential initially +900 mV, fell away rapidly to +400 mV and then gradually decreased reaching -120 mV at the end of two hours. The cyclic voltammograms described above suggest that the electrode process should be;

$$TCNQ^- - e^- \longrightarrow TCNQ^0$$

followed by the solution reaction:-

$$TCNQ^0 + TTF^0 \longrightarrow TTF\ TCNQ$$

At the beginning of the experiment the potential is such, however, that it would appear the electrode reaction would also be possible, where

$$TTF^0 - e^- \longrightarrow TTF^+$$

followed by:-

$$TTF^+ + TCNQ^- \longrightarrow TTF\ TCNQ$$

Because there is an adequate supply of $TCNQ^-$ to the electrode it is unlikely that the latter case occurs, and hence it is assumed that the high potential is due to the iR

drop between the reference and working electrode. This is presumably due to there being an insufficient quantity of ions in the solution to carry the charge. The concentration of background electrolyte should have been sufficient to make the iR drop insignificant. The solution used was made up immediately prior to use, but it is difficult to determine whether all of the background electrolyte added dissolved, because of the high optical density of the solution. If the dissolution of $TEA^{+}TCNQ^{-}$ is slow then at the beginning of the experiment only a small amount of this would be dissolved, resulting in a high solution resistance. As the experiment proceeds more of the salt dissolves and hence the solution resistance decreases. This explains the observed slow fall in potential due to a gradual decrease in the iR drop. At the end of the two hour period the potential has reached a value near to the E^{0} of the $TCNQ^{0}/TCNQ^{-}$ redox couple. This condition would be expected for an iR drop of virtually zero at the current density employed.

Over the two hour period approximately 3.74×10^{-6} mol cm^{-2} of the conducting salt should have been produced, which assuming an even coverage should give about 10^{4} layers of the salt on the electrode. In reality however the coat produced was far from uniform with most of the salt formed at the edge of the electrode and very little material on the centre. This again can be explained by a high solution resistance, which results in an uneven current

distribution over the electrode, with the greatest current being passed at the edge. This effect has been described by Newman [106,107], and is due to a lower solution resistance at the edge of the electrode than at the centre.

Cyclic voltammograms of this electrochemically prepared TTF TCNQ modified electrode, taken in phosphate buffer, showed identical electrochemical behaviour to that described previously (4.1) for pressed pellet and packed cavity electrodes. The electrode also gave electrocatalytic currents in the presence of glucose and glucose oxidase.

A more even distribution of the material would most likely have been obtained if the plating solution had been left for long enough to allow all of the $TEA^{+}TCNQ^{-}$ to dissolve. The problem is that $TCNQ^{-}$ solutions are generally fairly unstable in the presence of dissolved oxygen and light. So rather than leaving the solution for several hours before use, it was decided to use an alternative approach to obtaining a more even coating involving reducing the field at the electrode edge. Because the current flow reaches the electrode edge, not just from directly below the electrode but also from outside it, the field here is greater than over the rest of the surface. For this purpose a special cylindrical teflon sleeve was made, which when placed over the electrode effectively turns it into a cavity electrode (figure 5.1.6). Using this and the same plating solution as before, several attempts were made to coat the surface of glassy carbon and platinum electrodes. These again involved galvanostatically passing a current through

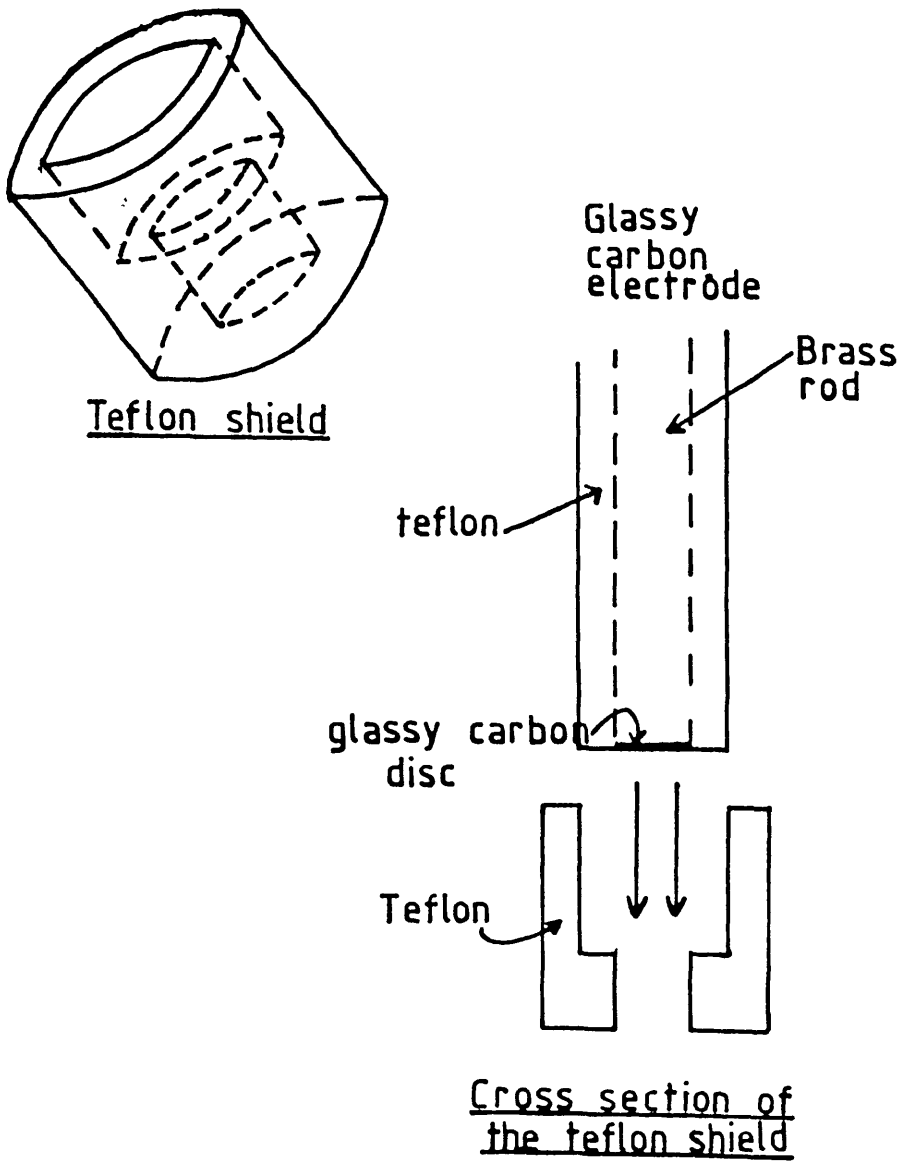

Figure 5.1.6: Schematic representation of the teflon shield which was used to reduce the field at the electrode edge.

the solution for a certain period of time. A variety of different current densities and plating times were attempted. In every case a sufficient number of coulombs were passed to give at least 1000 monolayers of salt on the electrode surface.

It was found that the use of the sleeve did considerably reduce the amount of material formed on the edges of the electrode, but unfortunately all the coats formed were patchy and non uniform. There are several possible explanations for this observation. Firstly the salt does not adhere strongly to the electrode surface hence, as subsequent layers of the material begin to build up some fragments will simply fall off. Some precipitate is in fact observed in the solution at the end of the coating period. Secondly the rate of the reaction between $TCNQ^0$ and TTF^0 might not be sufficiently rapid to prevent the $TCNQ^0$ formed on the electrode diffusing out into solution before reacting to form the salt. Thirdly, the overpotential for the oxidation of $TCNQ^-$ may be smaller on the conducting salt than on the base electrode. This means that after an initial nucleation period forming surface TTF TCNQ sites, growth will occur preferentially on these areas resulting in an uneven coat. Lastly is the possibility that because of depletion of $TCNQ^-$ and TTF^0 at the electrode surface, any crystals growing out into the bulk solution will receive a greater supply of these, and hence grow more rapidly than the rest of the coat. This is less likely than the other

explanations as the experimental conditions were always chosen to avoid significant depletion of these two species at the electrode surface.

All of the electrochemically modified TTF TCNQ electrodes were found to be electrocatalysts for the oxidation of the reduced form of glucose oxidase. Although these are preliminary results, they do show that if the plating procedure could be modified to produce even coats, the resulting electrodes could be used effectively for sensor applications. Further work is presently being carried out in this area with a view to obtaining better coats. Possible improvements in the coating procedure may be to make fewer layers of the material or to find a more "sticky" substrate to coat the material onto, in order to prevent lumps of the salt falling off the electrode. Other approaches to electrochemically forming the salt may also prove fruitful. For example, two step methods are possible, where the electrode is first coated with either TTF^{0} or $TCNQ^{0}$ and this then either reduced in the presence of TTF^{+} or oxidised in the presence of $TCNQ^{-}$ respectively. This procedure would have the advantage of carrying out both steps in aqueous solution, with enough background electrolyte to make the solution resistance unimportant.

5.2 Potential Dependence

As described previously (4.3.1) the maximum current obtainable using a TTF TCNQ/glucose oxidase membrane electrode, at a potential of +50 mV, is controlled by the rate of oxidation of the enzyme on the electrode. Cyclic voltammetry carried out on these electrodes in a phosphate buffer solution, containing sufficient glucose to saturate the electrode, shows that the rate of the electrode process is potential dependent. However, because of the high capacitance associated with these conducting salt electrodes, it is impossible to accurately determine the current, linked with the enzyme oxidation, at different potentials by this technique.

To measure the potential dependence of the enzyme oxidation a special electrode was used. This comprised of a triangular array of three cavity electrodes, each of approximately 1.5 mm diameter, separated from each other by 1 to 2 mm. Each of these electrodes was packed using a conducting salt/PVC slurry, as described in chapter 2. An enzyme electrode was made by trapping a solution of glucose oxidase over all three using a membrane held in place by an "o" ring. By poising each of these electrodes at different potentials it is possible to obtain values for the electrochemical rate constant, k', at three potentials simultaneously, while keeping all of the other variables constant (i.e. enzyme concentration and thickness of the

electrolyte layer).

A triple cavity membrane electrode was constructed, as described above, using a buffer solution containing 312 Units cm^{-3} of glucose oxidase and a Spectrapor 2 membrane. Initially all of these electrodes were held at +50 mV, and the current of each monitored with increasing concentrations of glucose. The current versus concentration profiles thus obtained are shown in figure 5.2.1. The slight differences in the saturated responses of these electrodes can be attributed to differences in their surface areas. The ratios of the saturated currents of the different electrodes was therefore used as a normalization factor to compensate for the different electrode areas. The same device was then placed in a fresh solution of buffer with the potential of each of the three electrodes set to different values. The saturation currents of these electrodes were then obtained by injecting sufficient glucose to give a concentration of 200 mmol dm^{-3}. Further additions of glucose gave no increase in current. The same procedure was repeated once more with the electrodes again poised at three different potentials. Values of the normalized saturation currents, i_{sat}, at different electrode potentials, are given in table 5.1, along with the corresponding values of the electrochemical rate constant, k', given by the equation:-

$$k' = i_{sat}/(e_{\Sigma}nFA)$$

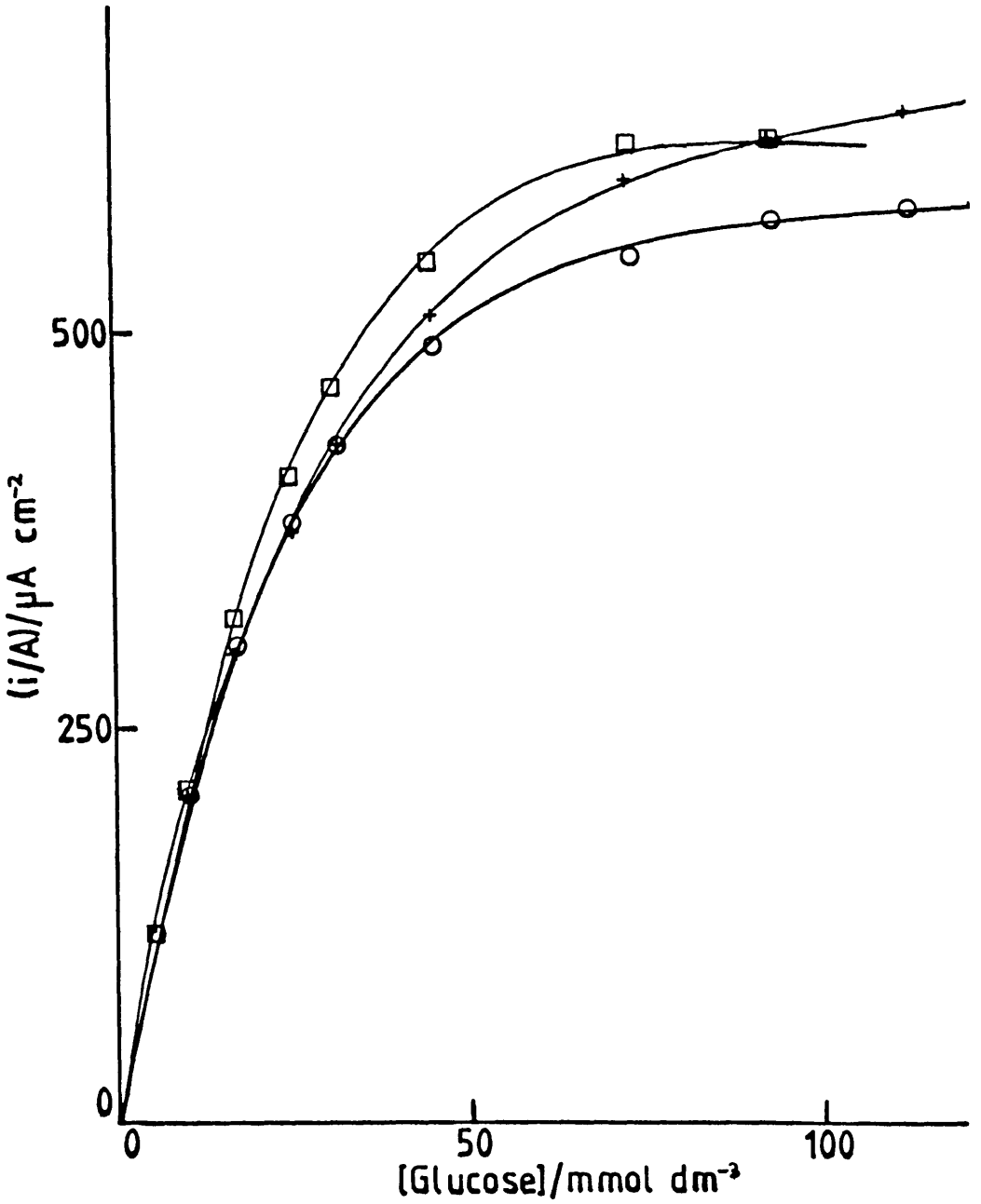

Figure 5.2.1: Plots of current versus concentration of glucose for the triple cavity/glucose oxidase membrane electrode. The potential of each of the cavity electrodes was 50 mV.

TABLE 5.1

Values of the Saturation Currents and Electrochemical Rate Constants of TTF TCNQ Membrane Electrodes at different Potentials

Potential/mV	i_{sat}/μA	k'/cm s^{-1}
-50	4.40	0.19
0	5.69	0.24
+50	6.56	0.28
+100	9.99	0.43
+150	15.91	0.68
+200	20.73	0.89
+250	14.57	0.62

All potentials are with respect to a standard calomel electrode.

As can be seen these values of k' are larger than those previously observed, suggesting that the electrodes have a very high surface area.

Figure 5.2.2 shows a plot of ln(k') versus potential as given by the Tafel equation [108]. A straight line can be obtained showing a fair degree of scatter. This scatter probably arises due to the difficulties involved in measuring the saturation current, which drifted considerably with time. The electrochemical rate constant can be given by:-

$$k' = k_0 \exp(\alpha F/RT(E - E^0))$$

Where k_0 is the standard heterogeneous rate constant [108], α is the transfer coefficient for the oxidation [108], T is the temperature (in Kelvin), R is the gas constant (8.314 J mol^{-1} K^{-1}), E^0 is the standard redox potential for the process, and E is the applied potential. This means that the slope of the Tafel plot is equal to $\alpha F/RT$. The gradient of the straight line Tafel plot is 6.45 V^{-1} which leads to a value for α of 0.17. The interpretation of this value of α will be discussed in the next section, which describes the possible mechanism for the electrode process. It is sufficient to note at this stage that it is a very low value of α. This indicates that the process is not very potential dependent between -50 and +200 mV, with only a five fold increase in the value of k' being observed over this range.

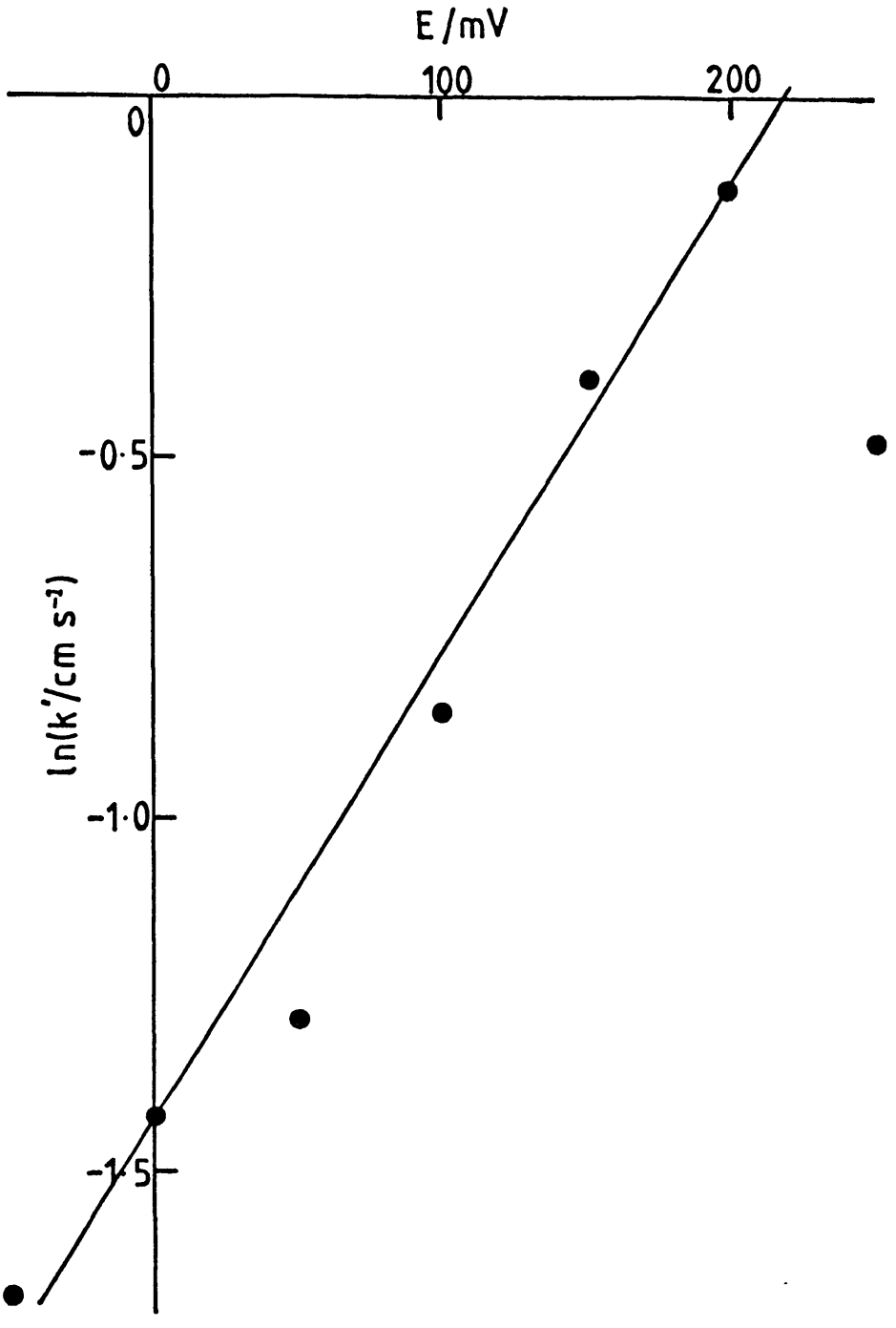

Figure 5.2.2: Tafel plot for the oxidation of glucose oxidase on a TTF TCNQ electrode.

5.3 The Mechanism of the Electron Transfer Process

5.3.1 Homogeneous mediation

Kulys and coworkers were the first to utilise conducting salts as electrode materials for the oxidation of the reduced forms of glucose oxidase and xanthine oxidase [59,60]. The two organic conductors that they have used are the TCNQ salts of NMP and N-methylacridinium (NMA). The mechanism which they have proposed [62,109,110] for the electron transfer, involves dissolved mediators from the electrode acting as shuttles carrying electrons from the enzyme to the electrode. Thus in the case of NMP TCNQ the possible mediators are NMP^+, $TCNQ^0$ and $TCNQ^-$ with the homogeneous reactions with the enzyme being:-

$$NMP^+ + GOD(FADH_2) \longrightarrow NMPH + GOD(FAD) + H^+$$

$$2TCNQ^0 + GOD(FADH_2) \longrightarrow 2TCNQ^- + GOD(FAD) + 2H^+$$

$$2TCNQ^- + GOD(FADH_2) \longrightarrow 2TCNQ^{2-} + GOD(FAD) + 2H^+$$

The reduced forms of the mediators formed by the above reactions are then oxidised on the conducting salt electrodes.

The evidence which Kulys et al. put forward to support this mechanism is as follows:-

1) All of the three species mentioned above are known to act as mediators for the oxidation of the reduced form of glucose oxidase [62]. The rate constants for the homogeneous reactions, k_{ox}, were found to be:-

$TCNQ^0$ $\quad k_{0x} = 3 \times 10^6$ mol dm^{-3} s^{-1}

$TCNQ^-$ $\quad k_{ox} = 6.6 \times 10^4$ mol dm^{-3} s^{-1}

NMP^+ $\quad k_{ox} = 9 \times 10^4$ mol dm^{-3} s^{-1}

2) The concentration of NMA^+ and NMP^+ observed fluorimetrically, when NMA TCNQ or NMP TCNQ are left in potassium buffer and allowed to equilibrate, are 9 and 13-18 μmol dm^{-3} respectively. It is therefore assumed that the concentration of $TCNQ^-$ is also this value. A value for the concentration of $TCNQ^0$ of 10-40 μmol dm^{-3} is observed spectrophotometrically in a lithium phosphate buffer solution containing 2% acetonitrile [62]. These concentrations combined with the above rate constants are sufficient to explain the currents obtained, in the presence of glucose and glucose oxidase, using NMA TCNQ and NMP TCNQ electrodes. Higher currents are obtained using NMP TCNQ than using NMA TCNQ electrodes because NMP^+ is a mediator for the oxidation of the enzyme, whereas NMA^+ is not. Potassium TCNQ (K^+TCNQ^-) modified electrodes are also found to be electrocatalysts for the oxidation of glucose oxidase [62], with again the rate constant and the solubility sufficient to explain the observed currents. Increases in

current are also obtained using $TCNQ^0$ modified electrodes when glucose and glucose oxidase are present [62].

For membrane electrodes if the electron transfer occurs by way of solution mediators, then the system can be described mathematically using Fick's law of diffusion, giving

$$D\frac{\partial m^2}{\partial x^2} - k_{ox}e_{\Sigma}m = 0$$

and

$$D\frac{\partial p^2}{\partial x^2} + k_{ox}e_{\Sigma}m = 0$$

where e_{Σ}, m and p are the concentrations of the reduced enzyme, oxidised mediator and reduced mediator respectively; and D is the diffusion coefficient of both forms of the mediator (taken to be the same). Solving these two equations with the boundary conditions $m = m_s$, $p = 0$ at $x = 0$, and $m = p = 0$ at $x \geq d$, where d is the thickness of the enzyme layer behind the membrane, gives that the electrode current is equal to

$$i = nFAD(\partial p/\partial x) = nFAD(\beta\coth(\beta d) - d^{-1})m_s$$

where $\beta^2 = k_{ox}e_{\Sigma}/D$ and A is the area of the electrode.

When $\beta d < 1$ then this equation reduces to:-

$$i = 0.33\ nFAdk_{ox}e_{\Sigma}m_s \qquad (5.1)$$

This gives that the current is directly proportional to the concentration of enzyme. The assumption that $\beta d < 1$ holds is when the thickness of the enzyme layer is less than that of the reaction layer, given by β^{-1}. This means that the mediator can diffuse out into the bulk solution without undergoing reaction with the enzyme. If the reaction layer is less than d then $\beta d >> 1$ then the current will be given by:-

$$i = nFA(De_{\Sigma}k_{ox})^{1/2}m_s \qquad (5.2)$$

This is half order in enzyme and corresponds to the case where none of the mediator escapes into the bulk solution.

For the $TCNQ^0$ modified electrodes, Kulys found that the current obtained using membrane electrodes was directly proportional to the concentration of enzyme. Equation (5.1) therefore applies and gives a value for m_s of 13.7 μmol dm^{-3}. This surface concentration is claimed to be feasible, since the dissolution of $TCNQ^0$ is larger than this. It is also claimed that because of the surface roughness, a concentration of $TCNQ^0$ as low as 1.3 μmol dm^{-3} would be sufficient to explain the observed fluxes.

3) A current is only observed if the applied potential is positive of the standard redox potentials of the mediators

(i.e. a current is only observed at potentials where the reoxidation of the reduced mediator can be effected).

4) The current obtained is inhibited by oxygen at low substrate concentrations.

In the following sections new experimental results concerning the mechanism of the electron transfer between the enzyme and the conducting salt electrodes are presented. As a concequence of this the arguments described above require fresh consideration.

5.3.2 Solubility of the Conducting Salts

To measure the dissolution of species from the surface of the conducting salts NMP TCNQ and TTF TCNQ rotating ring disc electrodes were employed. Here dissolved species at the surface of the conducting salt disc electrode will diffuse out into the bulk solution, with a proportion of these, given by the collection efficiency [111] of the electrode, being swept to the platinum ring electrode. At the ring electrode dissolved species can be reduced or oxidised electrochemically. The current thus obtained at the ring can then be used to obtain the flux of species away from the disc electrode, and hence the surface concentration of the possible mediators can be found.

a) NMP TCNQ

In the case of NMP TCNQ a cavity disc platinum ring electrode was used, with the disc being packed with a NMP TCNQ/PVC mixture as previously described (chapter 2). The collection efficiency of this electrode varied with rotation speed between 0.15 (1Hz) and 0.1 (16Hz). This variation in collection efficiency is probably caused by the roughness of the disc surface. To obtain the surface concentration of dissolved mediators the electrode was rotated at 9 Hz (collection efficiency = 0.12) in a solution of 0.1 mol dm^{-3} lithium chloride, and the potential of the disc electrode cycled between the limits of the stable range of the salt. The ring electrode was held at various potentials between -500 and +500 mV with respect to a standard calomel electrode, but no current was observed. This shows that the surface concentration of the various mediators are less than 10^{-7} mol dm^{-3} when the applied potential is within the stable range of the electrode. When the disc potential was taken beyond the stable range of the salt then a ring current was observed.

b) TTF TCNQ

To obtain the solubility of TTF TCNQ a pressed pellet disc (area 0.07 cm^2) platinum ring electrode was used. This was rotated at 16 Hz in a solution of phosphate buffer (pH = 7.4) with the ring potential being varied between -500 and +800 mV, and its current monitored with changes in the disc potential. In the disc potential range of 0 to 100 mV

no current was observed on the ring, but at higher and lower potentials than these small amounts of current were obtained. At a ring potential of -500 mV all of the possible mediator species from the salt i.e. $TCNQ^0$, $TCNQ^-$, TTF^+ and TTF^{2+}, can be reduced (the latter of these was unlikely to be formed at the disc potentials used, which were between +250 and -150 mV). At this potential the maximum current observed was 10 nA, this being obtained when the disc was held at +250 mV. With the collection efficiency of the electrode being 0.22, this gives a disc flux of 2.44×10^{-2} mol cm^{-2} s^{-1} and hence a surface concentration of mediators of about 1.6×10^{-6} mol dm^{-3}. However with the disc potential in the vicinity of +50 mV no current is observed and hence the surface concentration of mediator is again less than 10^{-7} mol dm^{-3}.

c) Comparison of the observed and theoretical electrode fluxes

For NMP TCNQ/glucose oxidase membrane electrodes the electrochemical rate constant (chapter 4) was found to be 8×10^{-2} cm s^{-1}. Taking this and a typical value for the enzyme concentration of 10^{-5} mol dm^{-3} gives a flux for the saturated electrode of 8×10^{-10} mol cm^{-2} s^{-1}. The surface concentration of the mediators is less than 10^{-7} mol dm^{-3}. Using this concentration of mediator, the same concentration of enzyme as above, a k_{ox} of 3×10^6 mol^{-1} dm^3 s^{-1}, and a value for the diffusion coefficient of the mediator of 5×10^{-6} cm^2 s^{-1}, then it is found from equation (5.2) that

the flux that would be obtained (ignoring surface roughness) is approximately 1 x 10^{-12} mol cm^2 sec^{-1}. This is the flux if the electron transfer occurred via dissolved mediators, and as can be seen its value is about a factor of 10^3 less than the observed flux.

From section 5.1.2 a pressed pellet TTF TCNQ electrode of area 0.2 cm^2 held at a potential of +50 mV gave a saturation current of about 1μA in a solution containing 787 Units cm^{-3} glucose oxidase and excess glucose. Equation (5.2) applies for the mediated process in the absence of a membrane. If the maximum rate for the mediator reaction (that for $TCNQ^0$) is 3 x 10^6 mol^{-1} dm^3 s^{-1} and D is 5 x 10^{-6} cm^2 s^{-1} then the current is less than 0.07 μA. This is a factor of more than ten less than the observed current.

Table 5.2 summarises the values of the observed fluxes and the corresponding theoretical fluxes, for both NMP TCNQ and TTF TCNQ electrodes. It can be seen that these theoretical values are in both cases much smaller than the observed values. It appears therefore that the dissolution of mediator from the surface of these electrode is insufficiently rapid to explain the observed fluxes.

5.3.3 Surface Area Effects

As described previously (5.1.2) the surface roughness results in an increase in the saturation response of the electrode by a factor of 10 to 100. For the mediated mechanism surface roughness will only be important when the

TABLE 5.2

Comparison of the Theoretical and Observed Fluxes for NMP TCNQ and TTF TCNQ Electrodes in the Presence of the Reduced Form of Glucose Oxidase

Salt	Theoretical flux/mol cm^{-2} s^{-1}	Observed flux/mol cm^{-2} s^{-1}
NMP TCNQ	1×10^{-12}	8×10^{-10}
TTF TCNQ	1×10^{-12}	8×10^{-12}

enzyme mediator reaction layer, given by

$$\beta^{-1} = (D/k_{ox}e_{\Sigma})^{1/2}$$

is much less than the distance between the crystallites that make up the porous electrode. Using the value of k_{ox} for $TCNQ^{0}$, a typical value for the concentration of enzyme of 1×10^{-5} mol dm^{-3}, and a value for the diffusion coefficient of the mediator of 5×10^{-6} cm^{2} s^{-1} gives a reaction layer of 4 μm. Observation of the surface of TTF TCNQ packed cavity electrodes using a scanning electron microscope [103] shows that the spacing between the crystals is less than 10 μm. This means that the reaction layer from one of crystallite would overlap that of its nearest neighbour, and hence it is unlikely that the increase in current of about 100 would be observed in going from pressed pellet to packed cavity electrode.

Furthermore changing the size of the reaction layer from 10 μm (where there is a large degree of the overlap between the reaction layers of the seperate crystals) to 2 μm (where there is little encroachment of the reaction layers) should result in a vast increase in the saturation current. Such a change would be seen by increasing the concentration of the enzyme from about 2×10^{-6} mol dm^{-3} to 4×10^{-5} mol dm^{-3}. When this is done no such change in current is observed. It can therefore be concluded that the mediator mechanism is not consistent with the observed

current dependence on electrode roughness.

5.3.4 Current Dependence on the Concentration of the Enzyme

For a homogeneous mediated process the current obtained in an unstirred solution in the absence of a membrane is given by equation (5.2). This means that the current obtained is proportional to the square root of the concentration of the enzyme. For a direct electron transfer with the electrode the response varies linearly with enzyme concentration, so that:-

$$i = nFAke_{\Gamma}$$

where k is given either by the electrochemical rate constant k', or by $(Dk_{cat})^{1/2}$, and D is the diffusion coefficient of the enzyme.

Recently the work of Dr P. N. Bartlett, at the University of Warwick, showed that the current obtained at single crystal TTF TCNQ electrodes is proportional to the square root of the enzyme concentration [103]. This therefore rules out the possibility that the electron transfer occurs directly on the electrode surface. Although the square root dependence is consistent with the mediated mechanism, the solubility and surface area affects described above suggest that this is also unlikely.

5.3.5 Heterogeneous Redox Catalysis

Another possible mechanism is one in which the electron transfer occurs via species adsorbed on the surface of the conducting salt. These surface species are formed as a result of the equilibrium dissociation of the salt, with the overall scheme being as follows:-

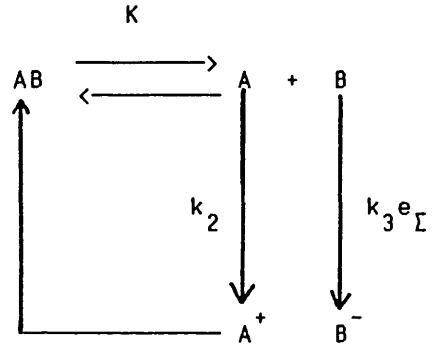

Here AB is the conducting salt and A and B are its dissociation products; at least one of which must be mobile on the surface in order to obtain second order kinetics. For the situation where the conducting salt AB is TTF TCNQ, A can be either TTF^0 or $TCNQ^-$ and hence B is correspondingly either $TCNQ^0$ or TTF^+. Which of these is the case will depend on the relative free energies of the zero and charged species on the electrode surface.

For the above scheme the following relationships apply:-

$$K = [A][B]$$

$$J = k_2[A]$$

$$j = k_3 e_\Sigma [B]$$

therefore

$$j^2 = k_2 k_3 e_\Sigma [A][B] = k_2 k_3 e_\Sigma K$$

and hence

$$j = (k_2 k_3 e_\Sigma K)^{1/2}$$

This means that this mechanism is consistent with the observed square root dependence of the flux on the concentration of the enzyme.

Since k_2 represents the electrochemical rate constant for the oxidation of A, this will tend to zero at potentials below the E^0 for the adsorbed A/A^+ redox couple. This explains the observation made by Kulys (5.3.1 (3)), that no current is observed until a potential large enough to oxidise the reduced mediator is applied. If either k_2 or k_3 have a normal value for the transfer coefficient α of 0.5 then the square root will mean that the observed value of α will be about 0.25. This then agrees with the low value of α of 0.17 as obtained experimentally (section 5.2).

Finally we can ignore the fact that the current obtained using glucose oxidase, at low substrate concentrations, is inhibited by oxygen in any discussion of the mechanism. This oxygen effect merely shows that the rate constant for the reoxidation of the enzyme by oxygen, is of the same order of magnitude (or higher) than the rate of the electrode process. This could be the case for any of

the mechanisms discussed.

It therefore appears that this latter mechanism gives the best agreement with the observed experimental results.

5.4 Conclusions

This chapter has been concerned with the electrochemical oxidation of the reduced form of glucose oxidase, on electrodes made from the conducting organic salts TTF TCNQ and NMP TCNQ. It is the rate of this process which has been found to control the saturated response of a glucose sensor. What has emerged is that the electrode response can be increased in two different ways. Firstly the larger the surface area of the electrode the greater the response. Secondly, this electrode process is potential dependent with the rate constant increasing with a corresponding increase in the electrode potential.

The mechanism of the electrode process is still not entirely understood. It is known that it is unlikely to occur by way of a homogeneous reaction, between dissolved species from the salt and the enzyme, as the dissolution of the salt is insufficiently rapid to explain the observed fluxes. It is also clear that this oxidation process does not occur by a direct electron exchange between the enzyme and the electrode. What seems most likely, is that the electron transfer occurs via a heterogeneous reaction, between the enzyme and species from the salt adsorbed onto the electrode surface.

CHAPTER 6

CONCLUSIONS

6.1 The Use of Conducting Organic Salt Electrodes in Enzyme Electrochemistry

This research project has been concerned with the development of enzyme electrodes based on the use of conducting organic salts as electrode materials. These have been found to show considerable promise in the range of their possible applications. In this thesis systems have been described which involve electrodes made from the conducting salt TTF TCNQ in conjunction with a flavoenzyme, either glucose oxidase, xanthine oxidase, D-amino acid oxidase or L-amino acid oxidase. These devices can be used not only as sensors for the particular enzyme substrate, but also for other species, such as sucrose [112] or phosphate [113], by coupling with other enzymes.

There are many other possible uses of these conducting salt electrodes in the area of enzyme electrochemistry. Firstly there are a number of other flavoenzyme oxidases, and the electrochemistry of the reduced forms of some of these on conducting salt electrodes is presently being investigated. The results obtained so far look encouraging and should allow the development of sensors for a number of other biological molecules. It has also been found that

electrodes constructed from the conducting organic salts NMP TCNQ [109,114] and TTF TCNQ [115] can be used to oxidise the biological cofactor NADH. There are several hundred enzymes that use NAD^+ (or $NADP^+$) as a cofactor to oxidise their substrate, with the resulting formation of NADH (NADPH). By monitoring the production of NADH, it is then possible to develop sensors for a large number of different species [115,116].

Another attractive feature concerning the use of conducting salts in enzyme electrodes is the simplicity of the resulting device. The enzyme (and cofactor in the case of the NAD^+ dependent enzymes) can simply be trapped onto the electrode surface using a membrane, with no need for the addition of any mediators. The sensors can be made by simply dipping the electrode into a solution containing the enzyme in the case of the flavoenzyme oxidases, which have been found to adsorb strongly onto the surface of these salts.

6.2 The Importance of the Determination of the Rate Limiting Step

For the enzyme electrodes developed in this research project much emphasis has been placed on the determination of the rate limiting step at different concentrations of substrate. It is this step which controls the response of the device, and it is only through a knowledge of this that the sensor can be adapted to suit different possible applications. For example in the case of the glucose

oxidase membrane electrodes described in chapter 4, it was found that the rate limiting step controlling the saturated response of the device was the diffusion of glucose through the membrane. If low levels of glucose (less than 1 mmol dm^{-3}) were to be determined, then the sensitivity of the electrode can be increased by changing the membrane to one which is more permeable to glucose. Conversely for high concentrations (greater than 30 mmol dm^{-3}), with sensitivity being less of a problem, a thicker or less permeable membrane can be used to increase the concentration range over which the response is linear.

6.3 Problem Areas

At present there are several areas which require further investigation. These include:

1. The development of new sensors based on the use of a conducting salt electrode in conjunction with one or more enzymes.
2. The improvement in the consistency of the electrode response. The packed cavity electrodes used in this study are difficult to reproduce in a manner such that they will always give a large response. Work is required on new methods of electrode fabrication to find a way of easily obtaining electrodes with a high surface area. Electrochemically coating these salts onto the surface of a standard electrode substrate shows some signs of success, and it is hoped that developments

along this line may prove useful.

3. The mechanism of the oxidation of flavoenzymes on these conducting salt electrodes is not as yet fully understood. Further work in this area is currently being carried out, and it is hoped that the use of spectroscopic techniques coupled with further information on the solubility of the salts, the potential dependence of the enzyme oxidation, and the relationship of surface roughness to electrode response will lead to a clearer understanding of the electrode process.

REFERENCES

1. Carr, P. W., & Bowers, L. D., In: "Immobilized Enzymes in Analytical and Clinical Chemistry, Fundamentals and Application", ed. Elving, P. J., & Winefordner, J. D., John Wiley & Son: New York, ch. 5, p 197 (1980).
2. Guilbault, G. G., Appl. Biochem. Biotech., 7, 85 (1982).
3. Scheller, F. W., Schubert, F., Renneberg, R., Muller, H.-G., Junchen, M., & Weise, H., Biosesors, 1, 135 (1985).
4. Guilbault, G. G., In: "Medical and Biological Applications of Electrochemical Devices", Ed. Koryta, J., John Wiley & Son, New York, p. 289 (1980).
5. Koryta, J., Electrochimica Acta, 31, 515 (1986).
6. Mosback, K., (Ed.), Methods in Enzymology, Vol. 44, Academic Press, (1976).
7. Chibata, I., (Ed.), Immobilised Enzyme, John Wiley & Son, New York, (1978).
8. Clark, L., & Lyons, C., Ann. New York Acad. Sci., 102, 29 (1962).
9. Hicks, G.P., & Updike, S.J., Anal. Chem., 38, 726 (1966).
10. Mascini, M., Iannello, M., & Palleschi, G., Anal. Chim. Acta, 146, 135 (1983).
11. Zaborski, O. R., In: "Methods in Enzymology", Vol. 44, Ed. Mosbach, Academic Press, p. 326 (1976).

12. Goldstein, L., In: "Methods in Enzymology", Vol. 44, Ed. Mosbach, Academic Press, p. 397 (1976).

13. Goldstein, L., Levin, Y., & Katchalski, E., Biochemistry, 3, 1913 (1964).

14. Buck, R. P., Anal. Chem., 38, 726 (1966).

15. Bates, R. G., "Determination of pH, Theory and Practice", John Wiley and Son, Ch. 10, p. 290 (1964).

16. Eagan, M. L., & Dubois, L., Anal. Chim. Acta, 70, 157 (1974).

17. Toth, K., & Pungor, E., Anal. Chim. Acta, 54, 189 (1971).

18. Guilbault, G. G., & Montalvo, J. G., J. Am. Chem. Soc., 91, 2164 (1969).

19. Nilsson, H., Acherlund, A., & Mosbach, K., Biochem. Biophys. Acta, 320, 529 (1973).

20. Llenado, R., & Rechnitz, G., Anal. Chem., 43, 1457 (1971).

21. Davis, G., Biosensors, 1, 161 (1985).

22. Clark, L., BRD Patent, K1 421 3/04 Nr 1598 285 (Feb. 4, 1971).

23. Hemmerich, P., Massey, V., Michel, H., & Schug, C., In: "Structure and bonding" Vol. 48, Springer Verlag, p 93 (1982).

24. Elving, J. P., & Janik, B., Chem. Rev., 68, 297 (1968).

25. Ksenzhek, O. S., & Petrova, S. A., Bioelectrochem. Bioenerg., 11, 105 (1983).

26. Swoboda, B. E. P., & Massey, V., J. Biol. Chem., 240,

2209 (1965).

27. Swoboda, B. E. P., Biochim. Biophys. Acta, 175, 365 (1965).

28. Weibel, M. K., & Bright, H. J., J. Biol. Chem., 246, 2734 (1971).

29. Gibson, Q. H., Swoboda, B. E. P., & Massey, V., J. Biol. Chem., 239, 3927 (1964).

30. Nakamura, T., & Ogura, Y., J. Biochem. (Tokyo), 52, 214 (1962).

31. Bright, H. J., & Appleby, M., J. Biol. Chem., 244, 3625 (1969).

32. Massey, V., Ganther, H., Brumby, P. E., & Curti, B., In: "Oxidases & Related Redox Systems", Vol 1, ed. King, T. E., Mason, H. S., & Morrison, M., John Wiley & Son, New York, p 335 (1964).

33. Dixon, M., & Kleppe, K., Biochim. Biophys. Acta, 96, 357 (1965).

34. Koster, J. F., & Veeger, C., Biochim. Biopys. Acta, 151, 11 (1968).

35. Porter, D. J. T., Voet, J. G., & Bright, H. J., J. Biol. Chem., 252, 4464 (1977).

36. Meister, A., & Wellner, D., The Enzymes, 7, 661 (1963).

37. Massey, V., & Curti, B., J. Biol. Chem., 242, 1259 (1966).

38. Page, D. S., & Van Etten, R. L., Biochim. Biophys. Acta, 191, 38 (1969).

39. Barman, T. E., In: "Enzyme Handbook", Vol 1, Springer Verlag, p. 147 (1969).

40. Olson, J. S., Ballou, D. P., Palmer, G., & Massey, V., J. Biol. Chem., 249, 4363 (1974).

41. Lerner, H., Giner, J., Soeldner J. S., & Colton, C. K., J. Electrochem. Soc., 126, 237 (1979).

42. Vassilev, Y. B., Khazova, O. A., & Nikolaeva, N. N., J. Electroanal. Chem., 196, 105 (1986).

43. Chou, T. -C., Chen, W. -J., Jow, J. -J., & Nonaka, T., Electrochim. Acta, 30, 1665 (1985).

44. Updike, S. J., & Hicks, G. P., Nature, 214, 986 (1967).

45. Lubrano, G. J., & Guilbault, G. G., Anal. Chim. Acta, 97, 229 (1978).

46. Thevenot, D. R., Sternberg, R., Coulet, P. R., Laurent, J., & Gautheron, D. C., Anal. Chem., 51, 96 (1979).

47. Kamin, R., & Wilson, G. S., Anal. Chem., 52, 1198 (1980).

48. Fultz, M. L., & Durst, A. R., Anal. Chim. Acta, 140, 1 (1982).

49. Williams, D., Doig, A., & Korosi, A., Anal. Chem., 42, 118 (1970).

50. Mindt, W., Racine, P., & Schlaepfer, P., Ber. Busenges. Phys. Chem., 77, 804 (1973).

51. Cass, A. E. G., Davis, G., Francis, G. D., Hill, H. A. O., Aston, W. J., Higgins, J., Plotkin, E. V., Scott, L. D. L., & Turner, A. P. F., Anal. Chem., 56, 668 (1984).

52. Jonsson, G., & Gorton, L., Biosensors, 1, 355 (1985).

53. Scheller, F., Strnad, G., Neumann, B., Khun, M., &

Ostrowski, W., J. Electroanal. Chem., 104, 117 (1979).

54. Durlait, H., & Comtat, M., Anal. Chem., 56, 148 (1984).

55. Duke, P. R., Kust, R. N., & King, L. A., J. Electrochem. Soc., 116, 32 (1969).

56. Ianniello, R. M., Lindsay, T. J., & Yacynych, A. M., Anal. Chem., 54, 1098 (1982).

57. Ianniello, R. M., Lindsay, T. J., & Yacynych, A. M., Anal Chim. Acta., 141, 23 (1982).

58. Bourdillon, C., Bourgeois, J. P., & Thomas D., J. Am. Chem. Soc., 102, 4231 (1980).

59. Kulys, J. J., Samalius, A. S., & Svirmickas, G. -J. S., FEBS Letters, 114, 7 (1980).

60. Kulys, J. J., Cenas, N. K., Svirmickas, G. -J. S., & Svirmickiene, V. P., Anal. Chim. Acta, 138, 19 (1982).

61. Melby, L. R., Can. J. Chem., 43, 1448 (1965).

62. Kulys, J. J., & Cenas, N. K., Bioelectrochem. Bioenerg., 8, 103 (1981).

63. Akamatu, H., Inokuchi, H., & Matsunga, Y., Nature Lond., 173, 168 (1954).

64. Acker, D. S., Harder, R. J., Hertler, W. R., Mabiler, W., Melby, L. R., Benson, R. E., & Mochel, W. E., J. Am. Chem. Soc., 82, 6408 (1960).

65. Melby, L. R., Harder, R. J., Hertler, W. R., Mahler, W., Benson, R. E., & Mochel, W. E., J. Am. Chem. Soc., 84, 3374 (1962).

66. Ferrais, J., Cowan, D. O., Walatka, V., & Perlstein, J. H., J. Am. Chem. Soc., 95, 948 (1973).

67. Jerome, D., & Schultz, H. J., Advances in Physics, 31, 299 (1982).

68. Torrance, J. B., Acc. Chem. Res., 12, 79 (1979).

69. Garito, A. F., & Heegar, A. J., Acc. Chem. Res., 7, 232 (1974).

70. Scott, B. A., La Placa, S. J., Torrance, J. B., Silverman, B. D., & Welber, B., J. Am. Chem. Soc., 99, 6631 (1977).

71. Comes, R., In: "Chemistry and Physics of 1-Dimensional Metals", Ed. Keller, H. J., Nato Advanced Series, B-Physics, 25, Plenum, New York, p 315 (1977).

72. Ukei, K., & Shirotani, I., Commun. Phys., 2, 159 (1977).

73. Kistenmacher, T. J., Phillips, T. E., & Cowan, D. O., Acta Crystallogr.B, 30, 763 (1974).

74. La Placa, S. J., Cornfield, P. W. R., Thomas, R., & Scott, B. A., Solid. St. Commun., 17, 635 (1975).

75. Morosin, Phys. Lett.A, 53, 455 (1976).

76. Sandman, D. J., Mol. Cryst. Liq. Cryst., 50, 235 (1979).

77. Wegner, G., Agnew. Chem. Int. Ed. Engl., 20, 361 (1981).

78. Torrance, J. B., Scott, B. A., & Kaufman, F. B., Solid St. Commun., 17, 1369 (1975).

79. Wheland, R. C., & Gillson, J. L., J. Am. Chem. Soc., 98, 3916 (1976).

80. Peierls, R. E., In: "Quantum Theory of Solids", Oxford University Press, London, p 108 (1955).

81. Perlstein, J. H., Agnew Chem. Int. Ed. Engl., 16, 519 (1977).

82. Jaeger, C. D., & Bard, A. J., J. Am. Chem. Soc., 101, 1690 (1979).

83. Jaeger, C. D., & Bard, A. J., J. Am. Chem. Soc., 102, 5435 (1980).

84. Chambers, J. Q., Green, D. C., Kaufman, F. B., Engler, E. M., Scott, B. A., & Schumaker, R. R., Anal. Chem., 49, 802 (1977).

85. Lamanche, M., Menet, H. J., & Wely, C., J. Electroanal. Chem., 149, 267 (1983).

86. Lamanche, M., Menet, H. J., & Moradpour, A., J. Am. Chem. Soc., 104, 4520 (1982).

87. Sharp, M., & Johansson, G., Anal. Chim. Acta, 54, 13 (1971).

88. Sharp, M., Anal. Chim. Acta, 85, 17 (1976).

89. Sharp, M., Anal. Chim. Acta, 59, 137 (1972).

90. Lehninger, A. L., In " Biochemistry", Worth publishers Co., Ch. 10, p. 252 (1975).

91. Massey, V., Brumby, P. E., Hirochika, K., & Palmer, G., J. Biol. Chem., 244, 1682 (1968).

92. Hillman, A. R., Ph.D Thesis, Imperial College, (1979).

93. Bard, A. J., & Faulkner, L. R., In: "Electrochemical Methods, Fundamentals and Application", John Wiley and Son, ch. 13, p 553 (1980).

94. Albery, W. J., In: "Electrode Kinetics", Clarendon Press, Oxford, p 58 (1975).

95. Albery, W. J., & Bartlett, P. N., J. Electroanal. Chem., 194, 211 (1985).

96. Albery, W. J., & Knowles, J. R., Biochemistry, 17, 5631 (1976).

97. Hanes, C. S., Biochem. J., 26, 1406 (1932).

98. Bard, A. J., & Faulkner, L. R., In: "Electrochemical Methods, Fundamentals and Application", John Wiley and Son, ch. 6, p 213 (1980).

99. Cardosi, M. F., Ph.D Thesis, Imperial College, (1984).

100. Gough, D. A., & Leypoldt, J. D., J. Electrochem. Soc., 127, 1278 (1980).

101. Barman, T. E., In: "Enzyme Handbook", Vol 1, Springer Verlag, p. 179 (1969).

102. Palmer, T. E., & Olsen, J. S., In: "Molybdenum & Molybdenum Containing Enzymes", Ed. Coughlan, P., Pergammon Press, New York, (1980).

103. Albery, W. J., Bartlett, P. N., & Cass, A. E. G., Phil. Trans. Royal. Soc., to be published.

104. Albery, W. J., In: "Electrode Kinetics", Clarendon Press, Oxford, ch. 3, p. 47 (1975).

105. Bard, A. J., & Faulkner, L. R., In: "Electrochemical Methods, Fundamentals and Application", John Wiley and Son, p 288 (1980).

106. Newman, J., J. Electrochem. Soc., 113, 501 (1966).

107. Newman, J., J. Electrochem. Soc., 113, 1235 (1966).

108. Albery, W. J., In "Electrode Kinetics", Clarendon Press, Ch. 4, p. 92 (1975).

109. Kulys, J. J., Enzyme Microb. Technol., 3, 344 (1981).

110. Kulys, J. J., Biosensors, 2, 3 (1986).

111. Albery, W. J., & Hitchman, M. L., In "Ring-Disc Electrodes", Ch. 3, p. 17 (1971).

112. Bertrand, C., Coulet, P. R., & Gautheron, D. C., Anal. Chim. Acta, 126, 23 (1981).

113. Schubert, F., Renneberg, R., Scheller, F., & Kirstein, D., Anal. Chem., 59, 1677 (1984).

114. Albery, W. J., & Bartlett, P. N., J. Chem. Soc. Chem. Commun., 234 (1984).

115. Sim, K. W., Ph.D. Thesis, Imperial College, (1986).

116. Kulys, J. J., & Razumas, V. J., Mokslas, Vilnius, USSR, (1983).